

**UNIVERSIDADE FEDERAL DE ITAJUBÁ - UNIFEI
PROGRAMA DE PÓS-GRADUAÇÃO EM
ENGENHARIA ELÉTRICA**

Estimation of the Remaining Useful Life of
Hydro Generators.

José Vitor Bernardes Junior

Itajubá, May 20, 2021

**UNIVERSIDADE FEDERAL DE ITAJUBÁ - UNIFEI
PROGRAMA DE PÓS-GRADUAÇÃO EM
ENGENHARIA ELÉTRICA**

José Vitor Bernardes Junior

**Estimation of the Remaining Useful Life of
Hydro Generators.**

Tese submetida ao Programa de Pós-Graduação em Engenharia Elétrica como parte dos requisitos para obtenção do Título de Doutor em Ciências em Engenharia Elétrica.

Área de Concentração: Sistemas Elétricos de Potência

Supervisor: Prof. Dr. Edson da Costa Bortoni

May 20, 2021

Itajubá

UNIVERSIDADE FEDERAL DE ITAJUBÁ - UNIFEI
PROGRAMA DE PÓS-GRADUAÇÃO EM
ENGENHARIA ELÉTRICA

Estimation of the Remaining Useful Life of Hydro Generators.

José Vitor Bernardes Junior

Tese aprovada por banca examinadora em 22 de
Fevereiro de 2021, conferindo ao autor o título de
Doutor em Ciências em Engenharia Elétrica.

Banca Examinadora:

Prof. Dr. Germano Lambert-Torres
Prof. Dr. José Feliciano Adami
Prof. Dr. Eduardo Crestana Guardia
Prof. Dr. Credson Salles

**Itajubá
2021**

José Vitor Bernardes Junior

Estimation of the Remaining Useful Life of Hydro Generators

Tese submetida ao Programa de Pós-Graduação em Engenharia Elétrica como parte dos requisitos para obtenção do Título de Doutor em Ciências em Engenharia Elétrica.

Trabalho aprovado. Itajubá, 22 de Fevereiro de 2021:

Prof. Dr. Edson da Costa Bortoni
Orientador

Prof. Dr. Elias Strangas

Prof. Dr. Germano Lambert-Torres

Prof. Dr. José Feliciano Adami

Prof. Dr. Eduardo Crestana Guardia

Prof. Dr. Credson Salles

Itajubá
May 20, 2021

Acknowledgements

I want to thank god first. Many thanks to my advisor and friend Edson da Costa Bortoni for all the support and encouragement. I appreciate professor Elias Strangas for all the support and guidance during my internship at Michigan State University. I express my gratitude to all UNIFEI teachers who collaborated with my training. I special thanks to my parents, José Vitor Bernardes and Maria Célia Chaib de Sousa Bernardes, for their unconditional support. I also appreciate my brothers, Pedro, João Vitor, and Gustavo, for their friendship during this period. A special thanks to Marianna, my girlfriend. I also express gratitude to my friends Mateus, Guilherme, José Renato, Credson, and Gerson for their help with laboratory tests. Many thanks to my EXCEN co-workers. I cannot pass up the opportunity to specifically acknowledge my great friend Victor Faria.

Abstract

O monitoramento da condição dos geradores é muito desejável para uma operação confiável de uma usina hidrelétrica. As atividades de manutenção podem ser programadas para evitar falhas inesperadas que podem levar a meses ou anos de máquinas paradas sem geração. Estudos indicam que o isolamento do estator é a principal causa de falha do gerador. Nesse sentido, a base da metodologia proposta é o monitoramento do estado atual do sistema de isolamento do estator de hidrogeradores. Testes de descarga parcial nos enrolamentos do estator são aplicados para acessar a condição de isolamento. Um algoritmo para estimar a vida útil remanescente é a principal contribuição deste trabalho. Esta estimativa é baseada em avaliações estatísticas de hidro-geradores e na condição real do sistema de isolamento do estator. Testes de envelhecimento acelerado em amostras de estator com ampla aquisição de variáveis são realizados para entender o processo de envelhecimento. O algoritmo proposto é testado em casos simulados e em dados reais de um ensaio de ciclo térmico, no qual foi observado a ruptura do isolamento.

Palavras-chaves: Hidrogeradores. Sistema de isolamento. Vida útil remanescente.

Abstract

The monitoring of generators' condition is very desirable for a reliable operation of a hydropower plant. Maintenance activities can be scheduled to avoid unexpected failures that can lead to months or years of machines stopped without generation. Studies indicate that stator insulation is the leading cause of generator failure. In this sense, the proposal methodology's base is the monitorization of the actual health stage of the stator insulation system of hydro generators. Partial discharge tests in stator windings are applied to access the insulation condition. An algorithm to estimate the remaining useful life is the main contribution of this work. This estimation is based on both statistical evaluations of hydro generators and the stator insulation system's actual condition. Accelerated aging tests in stator specimens with wide variables acquisition are performed to understand the aging process. The proposed algorithm is tested in simulated cases and real data from a thermal cycle test, which observed an insulation breakdown.

Key-words: Hydrogenerators. Insulation system. Remaining useful life.

List of Figures

Figure 1 – Statistical Survey of CEMIG Generators	17
Figure 2 – Statistical Survey of Generators [1]	18
Figure 3 – Physical and Electrical Model for PD phenomenon [2]	23
Figure 4 – Partial Discharges Generation - Voltage through Time	25
Figure 5 – Physical and Electrical Model of the Radial External Partial Discharge Phenomenon - Corona	26
Figure 6 – Region Formation Phenomenon - Dry and wet Band - Formation of External Partial Discharges	28
Figure 7 – Life curves [3]	30
Figure 8 – Bath Tube For Failure rate [4]	33
Figure 9 – Failure Rate For Normal Probability Density Function [4]	33
Figure 10 – Failure Rate For Weibull Function [4]	34
Figure 11 – Markov model(discrete-time) with deterioration stages	36
Figure 12 – Markov model with two maintenance categories. [5]	36
Figure 13 – Average life time - New Transformer [4]	37
Figure 14 – Remaining life time - Used Transformer [4]	38
Figure 15 – Overview of maintenance Policy [6]	39
Figure 16 – State Space [6] a) Random Failure b) Deterioration	42
Figure 17 – State Space Considering Maintenance [6] a) Random Failure b) Three states for Deterioration	43
Figure 18 – Root Cause of Failure in Rotating Machines [7]	44
Figure 19 – Electrical trees [1]	45
Figure 20 – Breakdown, Degradation and Aging [8]	46
Figure 21 – Aging Factors [1]	47
Figure 22 – Model for interaction between different stresses during aging [9]	49
Figure 23 – Model for interaction between different stresses during aging [10]	50
Figure 24 – Sequence of the test procedure. [11]	51
Figure 25 – Schematic Flowchart for Life Time Estimation of Stator Windings [12]	52
Figure 26 – Formed electrical ageing curves vs. electric field stress for various stator winding insulation systems [12]	53
Figure 27 – Formation of Electric Micro fractures from 50 to 20 μm [13]	54
Figure 28 – Condition Evaluation [14]	55
Figure 29 – Evaluation Criteria for mica Resin Insulated stator windings [9]	56
Figure 30 – Isolation System Evolution Over Time [15]	56
Figure 31 – Insulation resistance as a function of Measurement and Drying Time [16]	65
Figure 32 – Insulation resistance over time for insulation Class B [16]	66

Figure 33 – Models for dielectric losses : a) Parallel model b) Series model [17] . . .	68
Figure 34 – Typical correlation between insulation Power Factor and applied Voltage	69
Figure 35 – End-winding Region [18]	79
Figure 36 – Detection method using differential time of two-way signals [18]	85
Figure 37 – Detection method for off-line partial discharges measures	86
Figure 38 – Equivalent circuit to Detection for off-line partial discharges measures .	86
Figure 39 – PMA graphic extracted from an off-line partial discharge test at LAT- UNIFEI	88
Figure 40 – PPA graphic extracted from an off-line partial discharge test at LAT- UNIFEI	89
Figure 41 – Partial Discharges Quantity Calculation	91
Figure 42 – PPA graphic extracted from an off-line partial discharge test at LAT- UNIFEI	95
Figure 43 – PPA graphic extracted from the Hydro power plant Volta Grande CEMIG	95
Figure 44 – PPA graphic-Typical pattern for surface tracking [19].	96
Figure 45 – PPA graphic-Typical pattern for corona discharge[19].	97
Figure 46 – PPA graphic-Typical pattern for discharge between phases [19].	97
Figure 47 – PPA graphic - Typical pattern for PD between the ground wall and the copper conductors [19].	98
Figure 48 – Schematic of the PI System Levels [20]	99
Figure 49 – schematic of the proposed methodology	101
Figure 50 – Maintenance strategy scheme	103
Figure 51 – Statistical Analysis Results	109
Figure 52 – Voltage Applied - Test Configuration	111
Figure 53 – Voltage Applied - Overview of the Test Configuration	112
Figure 54 – 1pu voltage test - Partial discharges intensity (Q_m)	112
Figure 55 – 1pu voltage test - Trend analysis by moving average (Q_{m+})	113
Figure 56 – 1pu voltage test - Trend analysis by moving average (Q_{m-})	113
Figure 57 – 2pu voltage test - Trend analysis by moving average (Q_{m+})	114
Figure 58 – 2pu voltage test - Trend analysis by moving average (Q_{m+})	114
Figure 59 – 2pu voltage test - Trend analysis by moving average (Q_{m-})	115
Figure 60 – Circuit with Inductors and Insulated Cable	116
Figure 61 – The Cooling System	117
Figure 62 – Overview of the Test Bench	117
Figure 63 – Thermal cycle test 1 - PD intensity (moving average window = 25) . .	118
Figure 64 – Thermal cycle test 1 - Upper Limit = 140 C	119
Figure 65 – Thermal cycle test 1- Coil Condition after failure	119
Figure 66 – Thermal cycle test 2 - Insulation breakdown	120

Figure 67 – Thermal cycle test 2 -Half cycle events analysis (Thermal Cycle experiment with 10 kV) - Duration in minutes (dashed lines are averages), Room Temperature and applied current.	121
Figure 68 – Thermal cycle test 2 - Q_m on Temperature Levels over cycles	121
Figure 69 – Thermal cycle test 2 - Half-cycle events analysis - PD intensity averages in nC (Dashed lines are averages).	122
Figure 70 – scale=2.0	127
Figure 71 – scale=2.0	128
Figure 72 – Partial Discharges Trends [21]	131
Figure 73 – Simulation 1 - Q_m over Time	135
Figure 74 – Simulation 1 - RUL over Time	135
Figure 75 – Simulation 1 - RUL versus Time (zoom)	136
Figure 76 – Simulation 1 - State Variables over Time	136
Figure 77 – Simulation 2 - Q_m over Time	137
Figure 78 – Simula 2 - RUL over Time	137
Figure 79 – Simulation 2 - RUL over time (zoom)	138
Figure 80 – Simulation 2 - State variables over Time	138
Figure 81 – Simulation 03 - Q_m over time	139
Figure 82 – Simulation 03 - Tendency Change Simulation	139
Figure 83 – Simulation 03 - State Variables over Time	140
Figure 84 – Simulation 04 - Q_m x time	141
Figure 85 – Simulation 04 - RUL over Time	141
Figure 86 – Simulation 04 - RUL over Time (zoom)	142
Figure 87 – Simulation 04 - State Variables over Time	142
Figure 88 – Thermal Cycle Test 2 - Q_m over Cycle	143
Figure 89 – Thermal Cycle Test 2 - RUL over Cycles	143
Figure 90 – Thermal Cycle Test 2 - RUL over Cycles	144
Figure 91 – Thermal Cycle Test 2 - State Variable (Q_m) over Cycles	144
Figure 92 – Thermal Cycle Test 2 - State Variable (a) over Cycles	145

List of Tables

Table 3 – The breakdown, degradation and aging characteristics [8]	47
Table 4 – Test Voltages for voltage-endurance test	59
Table 5 – Temperatures limits to Thermal Cycle Test	60
Table 6 – Thermal class	62
Table 7 – Thermal Classification of the insulation system for rotating machines . .	63
Table 8 – polarization Index	66
Table 9 – Statistical Overview of Cemig Database (History update date - 01/01/2018)	104
Table 10 – Failure rate and Life expectancy for exponential model	106
Table 11 – Statistical result for useful life	108
Table 12 – Statistical result for the Aging Phase	109
Table 13 – Hydrogenerators with coupling capacitor 80 pF - Qm values (mV) . . .	129
Table 14 – Simulation 1	133
Table 15 – Simulation 1 - Parameters	133
Table 16 – Simulation 2	133
Table 17 – Simulation 2 - Parameters	134
Table 18 – Simulation 3	134
Table 19 – Simulation 4	139
Table 20 – Simulation 4 - Parameters	140
Table 21 – Data Base Cemig 1	150
Table 22 – Caption	151
Table 23 – Useful information Data base Cemig 1	152
Table 24 – Useful information Data base Cemig 2	153

List of abbreviations and acronyms

AC	<i>Alternate Current</i>	23
CEMIG	<i>Companhia Energética de Minas Gerais</i>	17
DC	<i>Direct Current</i>	23
EKF	<i>Extended Kalman Filter</i>	102
IEEE PES	<i>IEEE Power Engineering Society</i>	29
KF	<i>Kalman Filter</i>	102
MTTF	<i>Mean Time to Failure</i>	18
PD	<i>Partial Discharges</i>	19
PDA	<i>Partial Discharge Analysis</i>	84
PI	<i>PI system</i>	20
PMA	<i>Pulse Magnitude Analysis</i>	88
PPA	<i>Phase Pulse Analysis</i>	88
RCM	<i>Reliability Centered Maintenance</i>	38
TC	<i>Thermal cycle</i>	22
TEAM	<i>Thermal, Electrical, Ambient, and Mechanical</i>	57
VET	<i>Voltage Endurance Test</i>	49

List of symbols

A	Constant	62
A_1	Constant	68
B	Constant	62
C_1	Capacitance that models the void	23
C_2	Capacitance connected in series with the void	23
C_3	Capacitance equals the dielectric arrangement	23
C_{ins}	Insulation Capacitance	87
E	Electric field	73
E_t	Life expectancy	105
F	Spark gap	23
FS	Maximum magnitude window in millivolts at unity gain.	91
F_{mag}	Magnetic induced force	75
G	Gain of the partial discharge detector	91
I	Electric Current	75
I_t	Average discharge current	92
K	Constant	64
L	Life time	62
L_1	Voltage endurance lifetime for frequency 1	60
L_2	Voltage endurance lifetime for frequency 2	60
N	Number of magnitude windows i ,	91
NQN	Normalized Quantity Number	90
N_F	Number of failures observed	105
P_i	Number of pulses per second in magnitude window i ,	91
Q	Apparent Charge	24
Q_m	Largest repeatedly occurring PD magnitude.	91
R_{40}	Resistance at 40°C	64
T	Period of the voltage signal	93
T_0	Life Extension for no maintenance Policy	30
T_1	Life Extension for maintenance Policy 1	30
T_2	Life Extension for maintenance Policy 2	30
T_{L1}	Time transit by L1	89
T_{L2}	Time transit by L2	89
T_{Ot}	Total operation time	105
T_k	Temperature in kelvin	62
U	Voltage	24

U_0	Ionization Onset voltage	68
U_{1-0}	Open-circuit Voltage	24
U_D	Breakdown Voltage	23
U_{ON}	Onset Voltage	24
U_p	Voltage Value where partial discharges start manifest	24
V	Applied Voltage	87
ΔQ	Discharge	87
ΔV	Voltage pulse	87
λ	Phase angle	105
ϕ	Phase angle	92
d	Width of the stator slot	75
f	Frequency	68
f_1	Frequency 1	60
f_2	Frequency 2	60
kV	Rated voltage in kV	64
k_c	quadratic term coefficient	108
n	Number of discharges pulses per cycle	25
t	time	24
t_{max}	Maximum life with 99% of probability	108

Contents

1	INTRODUCTION	17
1.1	Objectives	19
1.2	Organization of work	20
2	BIBLIOGRAPHY REVIEW	21
2.1	Insulation Aging mechanics and failure process	21
2.1.1	Thermal Mechanics	22
2.1.2	Dielectric Solicitation	23
2.1.2.1	Partial Discharges	23
2.1.2.2	Electrical Tracking and Moisture Absorption	27
2.1.2.3	Transient Voltages	28
2.1.2.4	Mechanical Solicitations and Aging	28
2.1.2.5	Environmental Solicitations and Aging	29
2.2	Useful life of electrical equipment	29
2.3	Aging, life time and reliability	31
2.3.0.1	Aging in equipment	31
2.3.0.2	Life Time Concepts	31
2.3.0.3	Estimation of the Average Lifetime	32
2.3.0.4	End-of-life Failure Calculation	32
2.3.0.5	Evaluation of the Remaining Life of insulation of Rotating Machines	34
2.3.0.6	Evaluation the remaining useful life of the insulation system for transformers	37
2.3.0.7	Aging and Maintenance	37
2.4	Predictive Maintenance	38
2.4.0.1	Reliability Centered maintenance	38
2.4.0.2	Mathematical Models	41
2.5	Aging factors	43
2.6	Accelerated Aging and Diagnostic tests	55
2.6.1	Accelerated Aging test	55
2.7	Thermal aging tests	61
2.7.1	Diagnostic test	63
3	THEORETICAL BASIS OF THE METHODOLOGY	71
3.1	Aging Stress	71
3.1.1	Thermal Stress	72
3.1.2	Electrical Stress	73
3.1.3	Ambient Stress	73

3.1.4	Mechanics Stress	74
3.1.5	Multiple Stress	76
3.2	Stator Failure Mechanism	76
3.3	Diagnostic Test	83
3.3.1	PD Measurements Systems	83
3.4	Data Storage and Management	98
4	METHODOLOGY	100
4.1	Statistical Analysis of the Remaining Useful Life of Hydro Generators	104
4.1.1	Overview of CEMIG Database	104
4.1.2	Adjusted Model	106
4.2	Accelerated Aging Tests	110
4.2.1	Tests	110
5	STATE ESTIMATION	123
5.1	Kalman Filter	123
5.2	Extended Kalman Filter	125
5.3	State Estimators Apply to Partial Discharges Measurements	126
5.3.1	Algorithm for Hydrogenerators	126
5.3.2	Partial Discharges Levels	127
5.3.3	Degradation model	128
5.3.3.1	Test results Simulation	130
5.4	Algorithm application in Thermal Cycle Test 2	135
6	CONCLUSION	146
	ANNEX	148
	ANNEX A – DATA BASE CEMIG	149
	BIBLIOGRAPHY	154

1 Introduction

Hydropower generation is the primary source of electricity in Brazil, responsible for 70% of total energy generated. For this reason, the generators' condition in hydropower plants is very important for the reliability of the electric power system in Brazil. It plays an essential role in the hydro generators of companies' assets.

An unpredicted stop of a given generator leads to problems in the operation and stability of the electrical power systems. Moreover, the company may suffer financial loss for an extended period without power generation and with the high costs of emergency maintenance.

The equipment failure rates increase with aging. However, many generators are in operation for more than 50 years, as shown in figure 1 representing a statistical survey with CEMIG (*Companhia Energética de Minas Gerais*) generators..

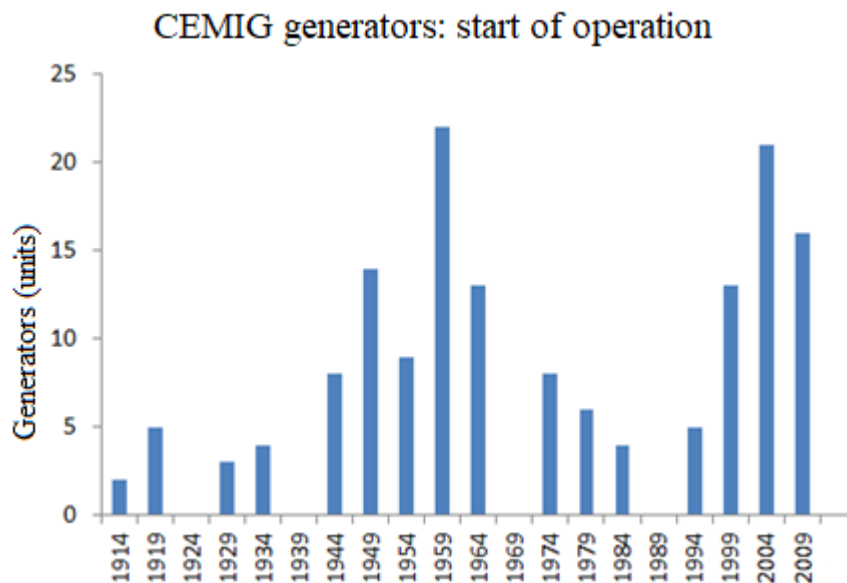


Figure 1 – Statistical Survey of CEMIG Generators

According to figure 1, the useful life of hydro generators is quite extensive. For example, two generators started the operation in 1914 and are still in service, which is more than 100 years in operation. On the other hand, there are examples of generators that have failures in less than ten years of operation, as depicted in annex A.

Thus, just a descriptive statistical analysis of generators' service time is not reliable for predicting useful life. Technical features such as operation condition, maintenance strategy, machine manufacture process, insulation material, among others, are essential to perform an appropriate prognostic of the remaining useful life.

The useful life of any machine consists of the time from the operation's starts to non-repairable failure. There is much discussion about this topic, and a prevision of the remaining useful life of hydro generation is still desired.

The generators useful life is extremely difficult to estimate. The failures in some electrical machines such as transformers and reactors are due to insulation degradation, and it is characterized by insulation breakdown. On the other hand, hydro generators are affected by several problems, as depicted in figure 2. This fact makes the prognostic in hydro generators even more difficult.

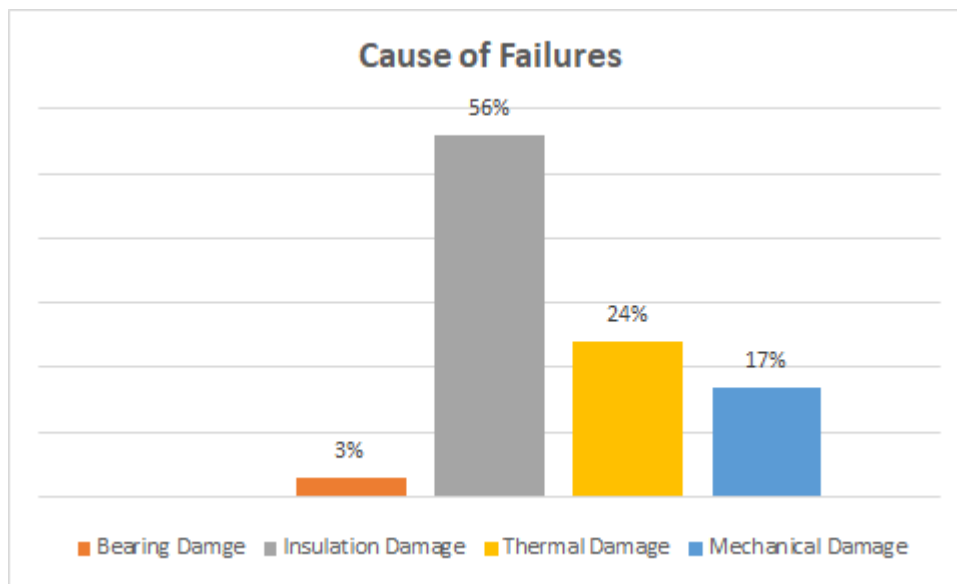


Figure 2 – Statistical Survey of Generators [1]

The leading cause of generators' failure is due to problems in the stator insulation system. Figure 2 shows that 56% of the failures occur due to insulation damage.

Indeed, the stator insulation system is the weakest part of a synchronous machine. For example, hydropower companies generally perform a generator rewind in aging generators. That is the replacement of the stator windings. Such a strategy makes the generator capable of operating for many years, almost like a new one.

Hence, develop a study to estimate the remaining useful life of hydro generators based in stator insulation system conditions is an accurate and trustworthy evaluation. It simplifies the complexity of a hydro generator prognostic, excluding some minor problems. Moreover, since insulation is the weakest part of the generator, the *MTTF (Mean Time to Failure)* of insulation and generator will likely be the same. The results of this study can also be applied to develop and improve the predictive maintenance of generators insulation system.

Predictive maintenance is responsible for extending the useful life of Equipment. For generators, the maintenance of the insulation system could slow down or avoid dete-

rioration problems that lead to intense degradation.

Indeed, predictive maintenance can be very favorable to extend generators' useful life. However, it is essential to evaluate the economic part. Sophisticate's maintenance strategy leads to an increase in the economic spending. On the other hand, it has a cost of operation, and it is necessary to take into account determining the strategy, which leads to the best economic benefit for the company.

Considering what was exposed about the insulation system in hydro generators, the base of predictive maintenance of hydro generators can be accessing the actual health condition of the insulation system. It is achieved by performing diagnostic tests in the windings.

There are many types of diagnostic tests for stator insulation system of generators, such as *PD (Partial Discharges)*, delta tangent, tip-up, visual inspection, among others. These tests play an essential role in both diagnostic deterioration's problems and prognostic of remaining useful life.

The most relevant diagnostic test for the stator isolation condition is the PD test. The test provides diagnostic information for most deterioration processes. The insulation condition has continuous access by partial discharges monitoring, especially when partial discharges measures are made from the start of generator operation. Finally, it is not an invasive test, causing no damage in insulation, and can be performed even with the machine in service, as with the online partial-discharges test.

1.1 Objectives

The main objective of this research is to make the prognostic of the remaining useful life of hydro generators taking into account the condition of the isolation system.

Propose the improvement of maintenance strategies based on monitoring the insulation condition is also an essential goal of the thesis.

Others secondary objectives are the following:

- Identification of pre-failure modes, tendency, and critical values for partial discharges;
- Development of accelerated aging test schemes with the combination of aging stress and continuous monitoring of partial discharge;
- Statistical evaluation of machine useful life;
- Online monitoring of a real hydropower plant;
- Online monitoring of the accelerated aging tests;

1.2 Organization of work

This Ph.D. thesis was written in order to introduce a reliable mathematical model for estimating the remaining useful life of hydro generators. This tool is vital to improve maintenance efficiency, as well as for better management of the company's assets.

The work is composed of 6 chapters, being the present chapter the introduction, where an overview of the subject and the main objectives are present.

Chapter 2 is a vast bibliographic review about the main topics treated in this thesis, such as the aging mechanism, degradation process in the stator insulation of generators, diagnostic tests for stator windings, among other topics.

Chapter 3 presents the theoretical bases of the methodology proposed to estimate the remaining useful life. It is present in detail the principal aging stress, all the stator failures mechanisms, partial discharge test, and the *PI (PI system)*.

Chapter 4 introduces the proposed methodology to estimate the remaining useful life of hydro generators. In the sequence, the static analysis is present, as well as the accelerated aging tests and their results.

Chapter 5, the Kalman filter and extended Kalman filter are used to estimating the remaining useful life of the stator insulation system, using partial discharge values. For this purpose, simulation and real case data are used to validate the prognostic algorithm.

Chapter 6 represents the work's conclusion, where at first the most relevant contributions are emphasized. Accelerated aging test conclusions and possible future works are also present in this chapter.

2 Bibliography Review

The main objective of the Bibliography Review is to introduce a summary of works done about the estimation of the remaining useful life of hydro generators. After that, a valid and unedited contribution in this field, fulfilling the requirements of a doctoral thesis, is better positioned and understood.

The chapter introduces a considerable review of the theory necessary for a good comprehension of this work. It includes reviewing the primary aging mechanisms inherent in generator operation, and the agings test are usually applied to emulate these aging mechanisms in the laboratory. In the sequence, the available diagnostic tests used to measure the isolation condition. Concepts of maintenance and useful life are also treated.

2.1 Insulation Aging mechanics and failure process

The insulation failures have a significant impact on the rotating machine failures. The industry report that one-third of crashes in these machines are associated with loss of the dielectric properties of the stator insulation. It is essential to point out that the final step of a failure, observed by data inspection, is often attributed to insulation rupture. However, in general, a fault has mechanical, thermal, electrical, ambient, or a combination of these phenomenons as a root cause. Thus, the first step is to discuss the initial stress/efforts that influence the stator insulation performance of rotating machines, pointing out the design, operation, and maintenance contribution for the expected machine's useful life.

The stator insulation of a rotating machine during operation is under high temperatures, voltages, vibration, mechanical forces, and adverse environmental conditions. These operation stress act individually or combined, imposing deterioration and degradation of insulating properties. The thermal aging under high temperatures acting in the insulation is deeply studied. In general, this aging mechanics is treated as a chemical reaction, and can be model by an equation that includes oxidation, depolarization, and other effects.

Moreover, electrical stress can also impose insulation degradation by PD, for example. Eventually, these solicitations lead the insulation to a terminal health condition, and an insulation puncture is characterized, which is a final dielectric failure. However, this failure has as a root cause other phenomenons not associated with the electric field. It is also important to point out that the insulation aging rate increases with aging mechanisms acting in the insulation.

Thus, in this section, the general characteristics of each one of these aging mechanisms are presented concisely. It is essential to point out that the intensity of each mechanism depends on the type and machine conditions under study.

2.1.1 Thermal Mechanics

In general, the trigger to the aging process by thermal effect is high temperatures in which degradation and changes in the insulation electrical and mechanical properties have present. A machine under TC (*Thermal cycle*) request also can impose mechanical solicitation that might result in degradation, as loss of adhesion between conductor and ground wall insulation. It could happen even in low amplitude thermal cycles. For this problem, the coefficients of linear and volumetric expansion of the conductors and the ground wall insulation are contributed to this phenomenon.

The temperature under regular operation for inorganic insulating materials, such as glass and porcelain, is limited under temperatures that cause changes in insulation proprieties such as conduction, loss factor, dielectric withstanding, or fracture problems caused by the thermal gradients. For these insulation materials, the system is first sensitive to its electrical proprieties variations. On the other hand, for organic insulation materials, such as cellulose, the operation temperature is determined by entering the plastic region of the material, being this change irreversible. In general, the temperature limits that result in considerable levels of aging for stator windings of rotating machines are considerably lower than the temperatures that cause changes in the electrical and mechanical proprieties. Except in cases when the variation imposed under service has as characteristic a short duration. Results of short duration phenomenons are:

- Contraction;
- Stiffening;
- Fracture;
- Decrease in the electrical and mechanical supportability;
- Weakening;
- Discoloration,
- Shaped distortions;
- In extreme cases, carbonization.

Theses process are following by:

- Weight loss result of losses of volatile substances;

- Oxidation or pyrolysis to form volatile substances and gases like CO, CO₂ water and hydrocarbons;

2.1.2 Dielectric Solicitation

Dielectric aging occurred when dielectric solicitations applied to the insulation result in deterioration of its properties. Although the solicitations associated with DC (*Direct Current*) voltage also cause damage, the phenomenons resulting from AC (*Alternate Current*) voltage applications are more severe. It is essential to point out that, in general, the dielectric materials used in rotating machines operate under conditions much lower than their breakdown voltage. Hence, the phenomenons related to electrical aging are associated with the presence of weak parts, where there are structural failures; for example, air voids in the insulation resulting from imperfections in the impregnation processes, where partial discharges manifest.

2.1.2.1 Partial Discharges

In general, PD takes place in the insulation parts containing voids generated during the manufacturing process or by thermal and electrical aging; for example, delamination. In general, the occurrence of discharges in the voids results in material surface decomposition.

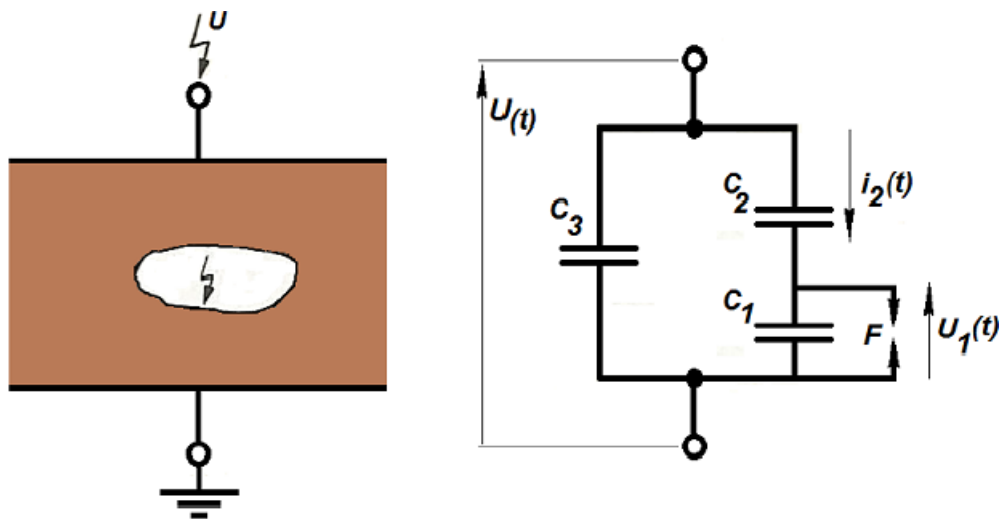


Figure 3 – Physical and Electrical Model for PD phenomenon [2]

Figure 3 shows the process and the internal electric circuit model for a partial discharge. The composition of the electric circuit model proposed by *A. Gemant and W.V. Philippoff* contains: The capacitance C_1 , which models the void. This capacitance is entirely discharged by the spark gap F when the void is under the breakdown voltage U_D . The capacitance C_2 , connected in series with this void, and the capacitance C_3 , equals the equivalent capacitance of the dielectric arrangement in parallel with the void region.

For a sinusoidal voltage source, the open-circuit voltage U_{1-0} applied in the void, that is, in the capacitance C_1 , is represented by 2.1.

$$U_{1-0}(t) = \frac{C_2}{C_1 + C_2} U(t) = \frac{C_2}{C_1 + C_2} U \sin(\omega t) \quad (2.1)$$

The amplitude of open-circuit voltage $U(t) - U_p$, when the voltage reaches the value where the partial discharges started manifest in the voids, as well known as the onset voltage - U_{ON} , is determined by equation 2.2.

$$U_p(t) = \frac{C_1 + C_2}{C_2} U_{ON} \quad (2.2)$$

In this case, the charge associated with the discharge in the void (related to the capacitance C_1) is given by equation 2.3.

$$Q_1 = C_1 U_{ON} \quad (2.3)$$

Since the capacitance values for C_1 and C_2 are generally unknown, it is not possible to determine the exact value for the associated charge due to the electric discharge in the void.

However, the "apparent total charge" (Q) is possible to be measured by an external mode to insulation and associated with the capacitance C_1 and C_2 in series, given by equation 2.4.

$$Q_S = (C_1 + C_2) U_{ON} \quad (2.4)$$

or, also represented by equation 2.5

$$Q_S = C U_{ON} \quad (2.5)$$

where:

$$C = C_2 \gg C_1$$

ergo, according to equation 2.6

$$Q_S \neq Q_1 \quad (2.6)$$

Thereby, in terms of PD, it is recorded equivalent values of charge.

Figure 4 graphically shows the PD process, where it is possible to observe the discharge pulses location near to the region of zero voltage. This is an important feature

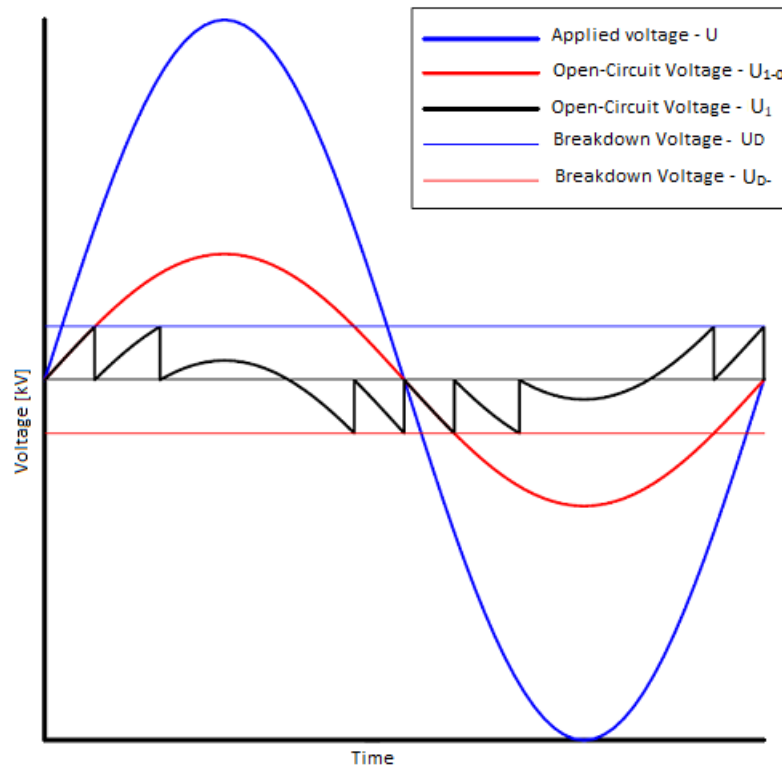


Figure 4 – Partial Discharges Generation - Voltage through Time

that can be used in the detection process and differentiate internal partial discharges from external partial discharges (corona).

The number of discharges pulses per cycle(n) is given by equation 2.7

$$n = 4 \frac{(U - U_{ON})}{U_{ON}} \quad (2.7)$$

For the case of figure 4, where $U = 2,85 U_{ON}$, the calculation by equation 2.7 gives a number of pulses per cycle equal to 8. The calculation $(U - U_{ON})$ must be rounded to its whole upper number.

The breakdown voltage magnitude controls the magnitude of the charges associated with the partial discharges. Therefore, small voids from the manufacturing process appear like a cloud of low magnitude pulses. This intrinsic knowledge is what allows evaluate the PD formation phenomena giving them a possible origin. It is also essential to observe the importance of sync with voltage since it is responsible for the phase definition. The phase is useful to different internal partial discharges from external partial discharges, such as Corona. In general, the automatic systems work with severity maps that take into account charge, current magnitude, phase, among other parameters that have to be well defined.

On the other hand, the equivalent circuit for external partial discharges is present in figure 5. Typically external partial discharges are related to the processes of forming

wet and dry bands. The model is also proposed by *A.Gemant and W.V. Phillippoff*. According to this model, for excitation with sine shape, the open-circuit voltage (U_{1-0}) developed at the capacitance C_1 is given by equation 2.8. The capacitance C_1 models the stored charge responsible for the electric arc.

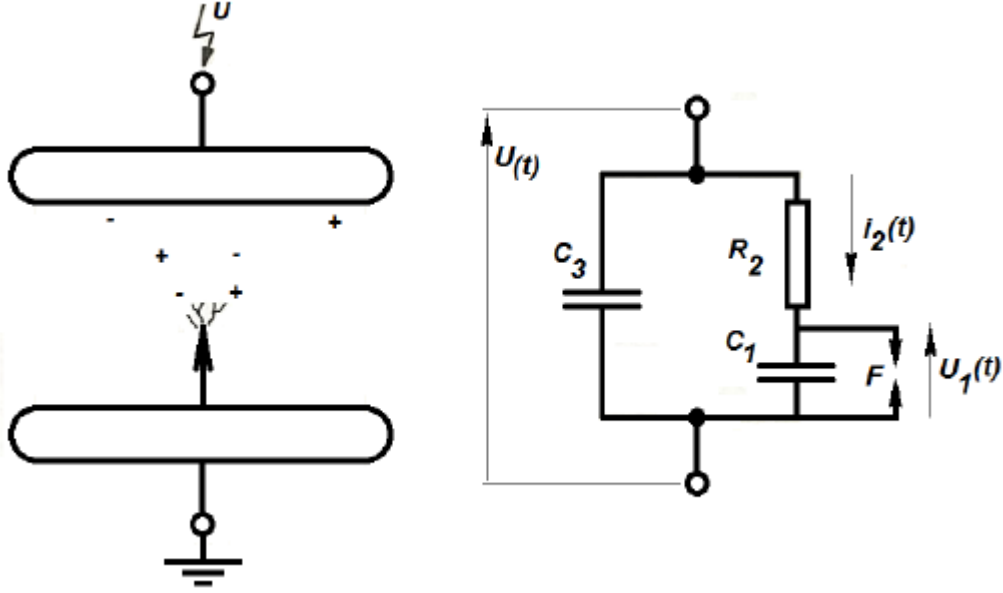


Figure 5 – Physical and Electrical Model of the Radial External Partial Discharge Phenomenon - Corona

$$U_{1-0} = \frac{U \sin(\omega t - \pi/2)}{\omega R_2 C_1} \quad (2.8)$$

The model has the following assumption:

$$R_2 \gg \frac{1}{\omega C_1} \quad (2.9)$$

Therefore:

$$i_2 \approx \frac{U(t)}{R_2} \quad (2.10)$$

Equation 2.11 determines the value for open-circuit voltage ($U(t) - U_p$), where it begins the partial discharges on the insulation surface, also known as onset Voltage (U_{ON}).

$$U_p = \omega \cdot C_1 \cdot R_2 \cdot U_{ON} \quad (2.11)$$

In this case, equation 2.12 determines the charge associated with the electrical discharge.

$$Q_1 = C_1 U_{ON} = \frac{U_p}{\omega R_2} \quad (2.12)$$

Today's systems for partial discharges detection have maps that correlate charge in terms of severity and position in the time. These are useful to evaluate the type and severity of the observed phenomena.

2.1.2.2 Electrical Tracking and Moisture Absorption

Electrical surface tracking is the formation of electrically conductive paths on the insulation surface, mainly at the end winding region. This phenomenon enables currents to flow over the insulation surface as a consequence of the solicitation applied by the electrical field.

Insulation surface can be contaminated by dust and moisture during operation. As a result, the insulation surface becomes conductive. If the currents on the insulation surface become very high, they can overcome the effects of capacitive currents, which are responsible for voltage distribution on clean surfaces. Thus, the voltage distribution depends on the way the conductivity varies along the insulation surface. Usually, the contamination along the surface is not uniform. In this way, the effect of current circulation results in irregular dry processes, which cause the formation of dry bands. They are regions on the insulation surface that reach the dry condition quickly. In this region, the electric resistivity and consequentially the voltage drop are higher. As a result, during the dry process, the voltage increase cumulatively until the dry band's formation. Then, the concentration of surface voltage is at the dry bands. If this voltage overcomes the dielectric supportability surrounding, partial discharges will be present on the insulation surface.

This electrical activity on the insulation surface can lead to different effects: The first would be if the discharge becomes extinct quickly, causing carbonization on the region where the current pass through (characterization of electrical tracking). In case the discharge extends in length until the complete dielectric rupture, that is, a phase-to-ground failure.

At the beginning of the electrical activity causing by the formation of dry bands, the spark or discharges can increase slowly, and the process can be stopped. Alternatively, the spark can rapidly propagate, becoming an irreversible process due to stress concentration at their extremities.

Figure 6 illustrates the process of dry and wet bands formation on the insulation surface. It also shows the drop voltages and the surface currents. Initially, the surface is damp, and there is a leakage current circulation, which is responsible for the uneven heating and the formation of dry bands. Then, the surface current decreases due to a higher impedance in the circuit. Drop voltage on the dry bands increases the heating generation and dry band's extension, until the occurrence of partial discharges. These partial discharges are transverse to the insulation surface.

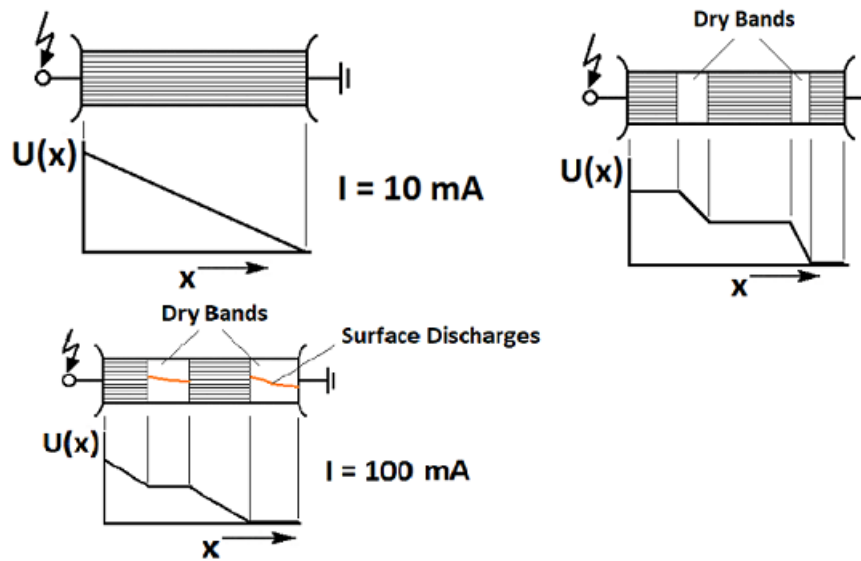


Figure 6 – Region Formation Phenomenon - Dry and wet Band - Formation of External Partial Discharges

The partial discharges on dirty surfaces occur under operating conditions between 0,02 and 0,04 kV/mm. On the other hand, at normal circumstances, the dielectric rupture occurs at 3 kV/mm for uniform electrical fields.

2.1.2.3 Transient Voltages

Transient voltages in rotating machines can result from many causes, such as atmospheric discharges, switching operations, and faults in the electrical systems. Typically, the insulation is designed and qualified by test during the manufacturing process to hold strong solicitations, as atmospheric impulses and switching. Therefore, fast transients are the cause of failures due to their extreme non-uniformity of voltage distribution. Switching operations at gas-insulated substations can generate fast transient. Moreover, even small-amplitude transients can cause failures in aging equipment due to many years under thermal, electrical, mechanical, and ambient stress. Therefore, part of the project procedures and qualification test need prior knowledge of the electrical environment and possible electromagnetic transients that may occur when the equipment is in operation. That is an essential strategy to make more efficient projects.

2.1.2.4 Mechanical Solicitations and Aging

The mechanical solicitations can cause different levels of damage to the insulation of a stator bar. In general, mechanical stress is due to relative motion between the insulation components and result in mechanical and electrical forces, resonances, defective components and parts fixation, abrasion, and other solicitation that can affect the mechanical insulation properties. Often, the cause of these processes is due to manufacturing,

transport, or installation, affecting specific machines. When the mechanical process occurs in sequence, affecting many units of the same project, the cause is problems in the machine project and design.

2.1.2.5 Environmental Solicitations and Aging

The dielectric system contamination by water, oil, or chemical products can lead to insulation aging and degradation. The thermal aging process is accelerated when occurring in the air rather than neutral atmospheres, such as in hydrogen.

In general, the effects of moisture and water absorption by the insulation are well known. Under these conditions, the most common aspects of the aging process are reducing dielectric properties of insulation and a propensity for deficient mechanical performance. However, the damage level by the presence of moisture depends on the insulation' type. Old insulation system made by organic material and varnishes is more susceptible to mechanical degradation when moisture and water absorption is present than moderns insulation made by inorganic material and synthetic resins such as epoxy. Polyester Based Materials also can lose their electrical and mechanical properties under the presence of moisture.

Hydrolysis is a mechanism in which moisture causes the rupture of chemical bonds in the insulation. In this way, it is possible to observe insulation delamination and puffiness. As a result, these conditions can lead to electrical, mechanical, or thermal failures. Oils, acids, and solvents can also affect the insulation systems and turns the organic material prone to develop degradation and aging. The dust contamination of the insulation surface also can result in dielectric failure by electrical tracking.

2.2 Useful life of electrical equipment

The term aging is applied to the internal process in all equipment and systems that gradually approximates the failure [3]. This process contrast to another, external to the equipment, in which the machine load increase as the demand for electrical energy increase until a level in which the machine can not fulfill the load. Moreover, the equipment becomes obsolete over time due to the emergence of new technologies. The solution to the problem due to load demand rise can be by increasing the system's redundancy. On the other hand, the deterioration problem in the equipment can be slowed by the application of preventive maintenance actions.

The *IEEE PES (IEEE Power Engineering Society)* defines preventive maintenance as a periodic activity where equipment has, from time to time, its deterioration contained, reduced, or eliminated [22]. It is an integral part of the so-called asset management. In the presence of deterioration, the equipment has a reduced economic value.

Figure 7 shows the connection between value, time, maintenance, and reliability.

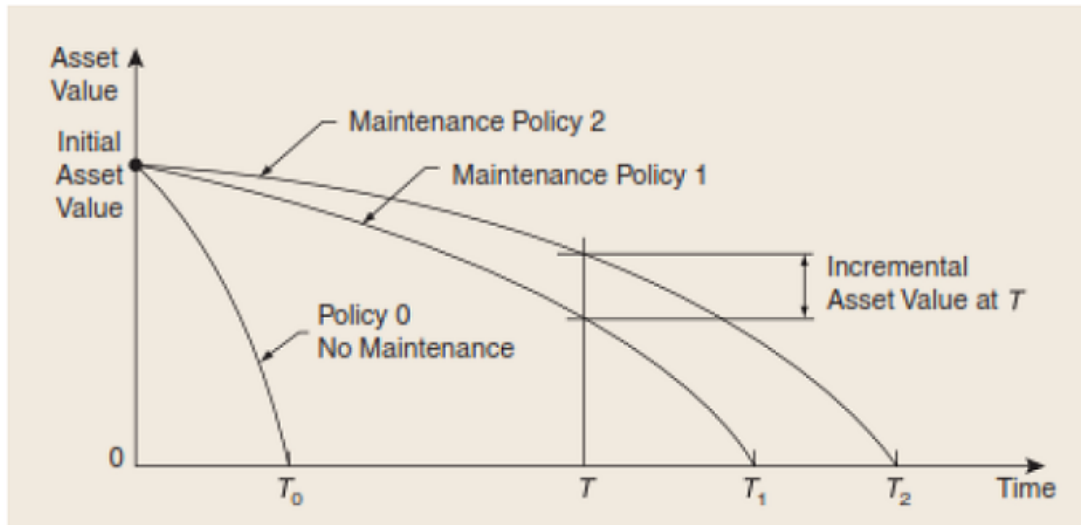


Figure 7 – Life curves [3]

The graphics illustrated in figure 7 represent life curves of equipment with different maintenance conditions: Policy 0, that is, there is no maintenance done in the machine; Policy 1 and 2, where the base of maintenance has two distinct rules. Assume that the fault is a condition in which the equipment economic value became equal to zero, and the life is the time necessary to reach this condition. Also, assume that reliability is a measure of equipment performance related to time.

The Life extensions T_0 and T_1 (when is applied the policy 1 instead of the policy 0), and between T_1 and T_2 (when Policy 2 replaces Policy 1) are shown in figure 7, as changes in the equipment conditions(charge in its economic value) in any time.

Note that the equipment condition becomes better with the maintenance. In terms of reliability, policy 2 is better than policy 1, demonstrating that the maintenance is capable of modifying component life.

Nevertheless, maintenance has a cost and must be taken into account when comparing different policies. Rising costs caused by more frequent maintenance actions must offset the gains arising from a more reliable operation of the system. So, if policy 2 has a costly implementation, it will not be superior to Policy 1, as previously thought.

In many cases, the power system operators are more concerned with equipment reliability rather than the economic aspect. However, the current competitive scenario of the electric sector, safety, and operation costs become equally important, requiring mathematical models (usually complicated) for cost optimization.

2.3 Aging, life time and reliability

2.3.0.1 Aging in equipment

Aging occurs in all the electrical system components, although there are distinct causes for each type of equipment [23]. For transformers and reactors, aging is due to the deterioration of winding insulation material. For generators and motors also occur damage caused by fatigue of mechanical parts.

The equipment experience stages of infancy, regular operation, and aging. Equipment passes to failure more often and requests more time every repair until reaching the end of its life. Aging causes a rise in the risk of failure and aggravation of damage to a system.

Frequently, the companies perform regular inspections and preventive maintenance to extend the equipment's life. However, the maintenance action can become too expensive, or unlivable, for equipment in the aging phase. So, proper consideration of one solution between maintenance or replacement of the equipment.

2.3.0.2 Life Time Concepts

There are three main lifetime concepts for electrical systems' equipment.

- **Physical Life:** One equipment starts its operation and stays in this condition until it can no longer operate, being necessary to take it off from service. The maintenance can increase the physical life.
- **Technical life:** There are situations where the equipment withdrawn from an operation for technical questions. However, they still have conditions to keep in use. For example, equipment in action is replaced by another because there are no more spare parts on the market, or it has a prohibitive cost for repairing.
- **Economic life:** Equipment can have null economic value, although they have conditions to keep in service. There is two way for calculation of the equipment economic value: First, Equipment economic value depreciated annually, and when the value becomes zero, it means that the equipment life is over. Another way, operation and maintenance costs are added to equipment depreciation. Regularly, these costs increase over time and, at a given moment, can overcome the actual equipment value. In this case, it is necessary to analyze the advantages and disadvantages of withdrawing the equipment from the operation, even before reach the null economic value.

2.3.0.3 Estimation of the Average Lifetime

In general, manufacture provides the estimation of the average life of its equipment based on some assumptions and theoretical calculation. However, this estimation is not appropriate because it does not consider the equipment's real operation condition.

It can be estimated the average life, using the simple mean lifetime values already observed of a group of individuals from a large population. Unfortunately, this estimation is not ideal for electrical equipment. Most electrical system equipment such as transformers, reactors, cables, and generators have a relatively long lifetime. As a result, the records of the mean lifetime available in the company's' database are limited [24]. The number of the sample still can be considered small for a reliable estimation, even using data from different companies because there are probably differences in the operation strategies and environmental conditions between the companies.

The disadvantage of this method, which uses a simple mean lifetime value, it is the use of information only from failure equipment. Methods based on Weibull and normal distribution allows the estimation of the average and standard deviation lifetime considering both, equipment in operation and failed [25], [26]. Then, even with a small number of samples, the models can provide accurate estimations.

The reference [24] shows a group of data of in-service year and retired year of 500 *kV* reactors from British Columbia Transmission Corporation.

The method using a simple mean indicate a mean lifetime equal to 25 years, obtained by the four failed reactors in a total of 100 reactors in the system. The values of mean life estimated by the methods using Weibull and Normal distributions are 38,4 and 37,6 years, respectively. That is, the values for a lifetime using these distributions are close to each other but distant from the estimated value using a simple mean (25 years). Note that, among the 100 reactors, 35 reactors have more than 30 years old, indicating the values estimated by the Weibull and Normal distributions are more reliable than the estimation by simple mean.

2.3.0.4 End-of-life Failure Calculation

The use of aging equipment implies a higher risk for the system, and than, this justifies the determination of the failure probabilities for the equipment that is in old stages. Figure 8, extracted from [24], presents the behavior of the failure rate for electrical equipment with relating its age.

The bath tube shape shows a sharp failure rate increase in the wear-out stage region compared to the typical operating stage region, where the life has a constant failure rate.

At the infant mortality stage region, the equipment also presents a higher failure

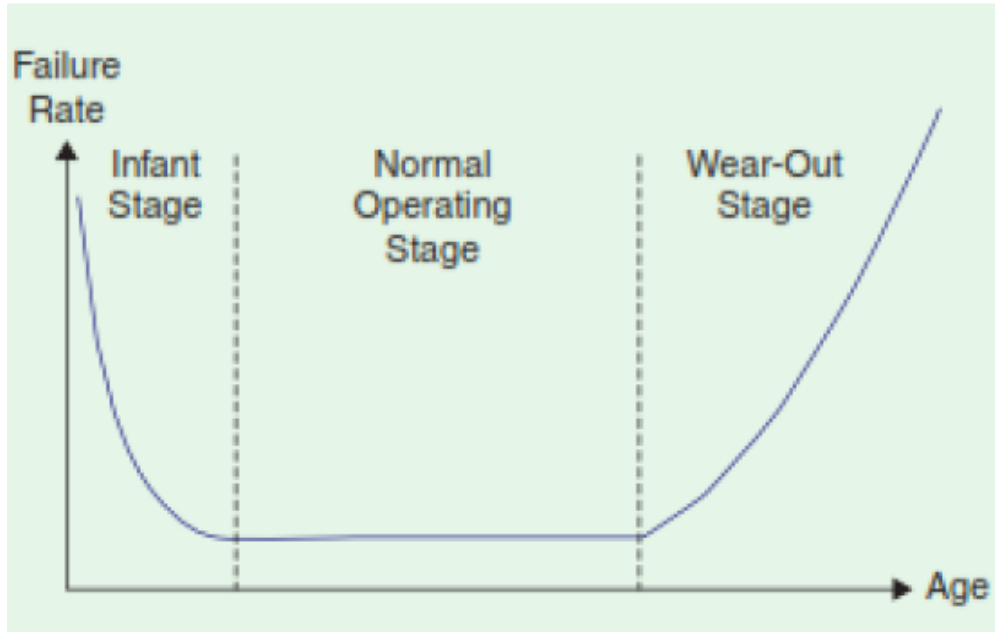


Figure 8 – Bath Tube For Failure rate [4]

rate due to possible problems in the manufacture, assembly, installation, and adaptation of operators to the use of equipment.

Normal and Weibull distributions can model the failure rate. Figure 9 shows the behavior of the failure rate relating to the age, using the normal distribution, where μ and σ are average and standard deviation for the lifetime, respectively.



Figure 9 – Failure Rate For Normal Probability Density Function [4]

Figure 10 depicts the same relation for Weibull distribution. In this case, the distribution parameters are α (scale factor) and β (form Factor).

The Weibull distribution can model lifetimes for three characteristics regions only

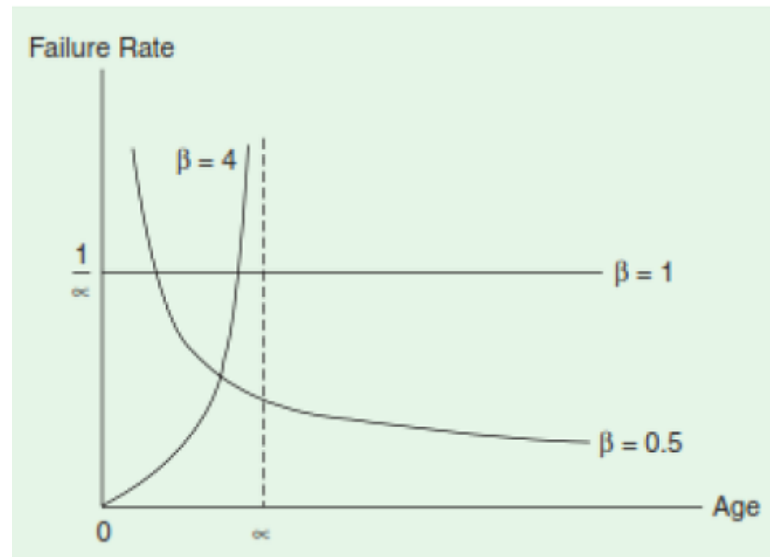


Figure 10 – Failure Rate For Weibull Function [4]

by adjusting the form factor β . Then:

- At Infant stage: $\beta < 1$;
- At Normal operation stage: $\beta = 1$
- At Wear-Out stage: $\beta > 1$

2.3.0.5 Evaluation of the Remaining Life of insulation of Rotating Machines

According to [27], the estimation of the remaining life of insulation of big generators and motors has interested many companies for the following reasons:

- Ensure that the insulation has failure probability lower than an acceptable value in the period between the equipment's inspections (usually every five years for big generators);
- Evaluating the winding condition to determine the type of maintenance is necessary to recover the situation "good as new," which is possible to detect the deterioration problem at the beginning stages;
- Estimation of the remaining useful life as part of a generator's life extension program. If the remaining useful life is too short, it can be plan more instance repair actions or even the equipment replacement;

However, the determination of the remaining useful life has been the most challenging part of this analysis for reasons like lack of data and well-defined models for deterioration. Moreover, the existence of many failure mechanisms that are not well known quantitatively also contributes.

The failure mechanisms interact with each other, being highly dependent on the operation and environmental conditions. To estimate the remaining useful life of some electrical equipment is necessary to understand the deterioration process and know the symptoms that appear with the deterioration.

The factors that can affect the occurrence and the state of deterioration of generators and motors insulation are:

- Temperature and voltage levels;
- Mechanical stress;
- Usage cycle;
- Type of insulation and quality of used materials;
- Manufacture and Assembly quality;
- Frequency and quality of maintenance;
- Random events, such as inadequate operation, surge voltages, among others.

The wide diversity of important factors result in a high number of the deterioration process. The different failures process presents in turbo-generators are:

- Thermal Aging, resulting in loss of dielectric and mechanical proprieties;
- Insulation wear caused by mechanical forces correlated with the electrical system frequency;
- Insulation crack by thermal expansion;
- Partial Discharges;
- Electrical Degradation.

The reference [27] discuss two methods to determinate the remaining life of insulation systems of generators and motors:

- Monitoring the factor that causes the insulation wear;
- Observation of symptoms through inspections and tests.

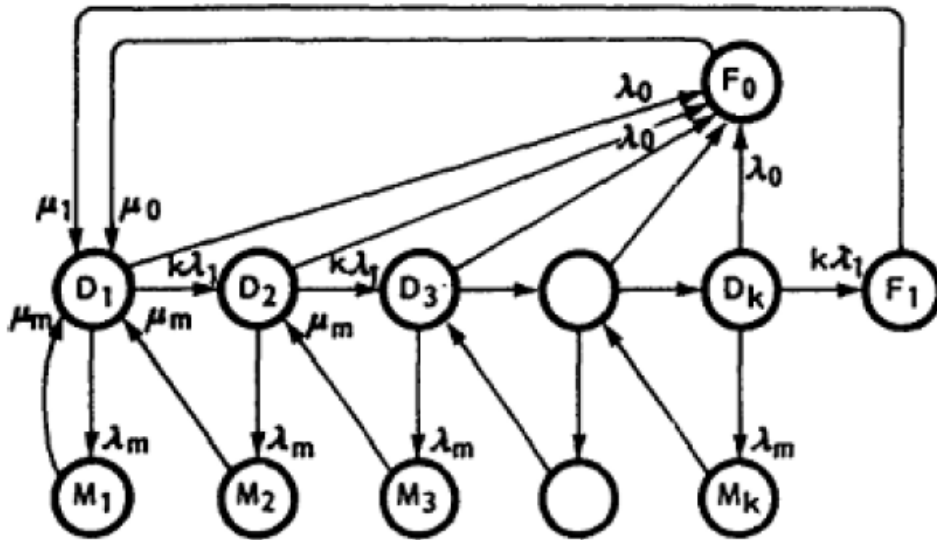


Figure 11 – Markov model(discrete-time) with deterioration stages

Further, the authors proposed a model based in Markov to estimate $MTTF$, as illustrated in figure 11.

A similar model is applied [5], where the differentiation of maintenance actions is made between the types M and MM to model minor and significant maintenance, respectively, as shown in 12.

Another attractive characteristic of this method is the capability to provide the probability distribution for the remaining life, obtained through Monte Carlo simulation [28] [29].

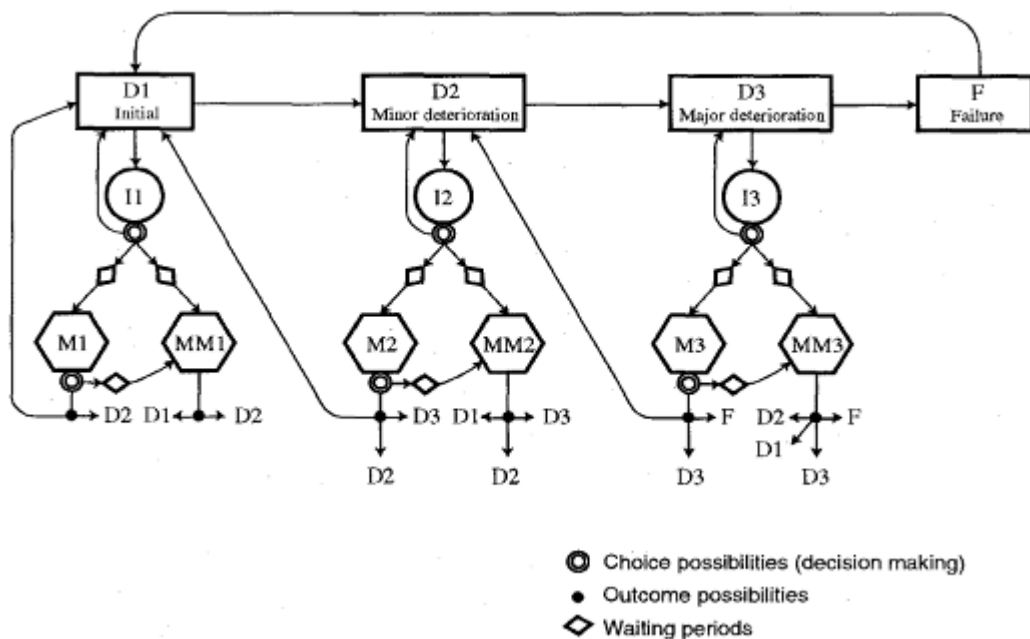


Figure 12 – Markov model with two maintenance categories. [5]

2.3.0.6 Evaluation the remaining useful life of the insulation system for transformers

The reference [4] presents a model-based in chronological Monte Carlo Simulation to determine the probabilities distribution for the remaining lifetime of substation transformers. The method combines the aging model of the insulation material from the Arrhenius theory 2.14 with reductions on life caused by short circuits, surges, and atmospheric discharges.

Figures 13 and 14 show histograms of lifetimes for a new and used transformer, respectively. The new transformer has an average expected life of 74 years. On the other hand, the current transformer (used transformer) has an average remaining useful life of approximately 40 years.

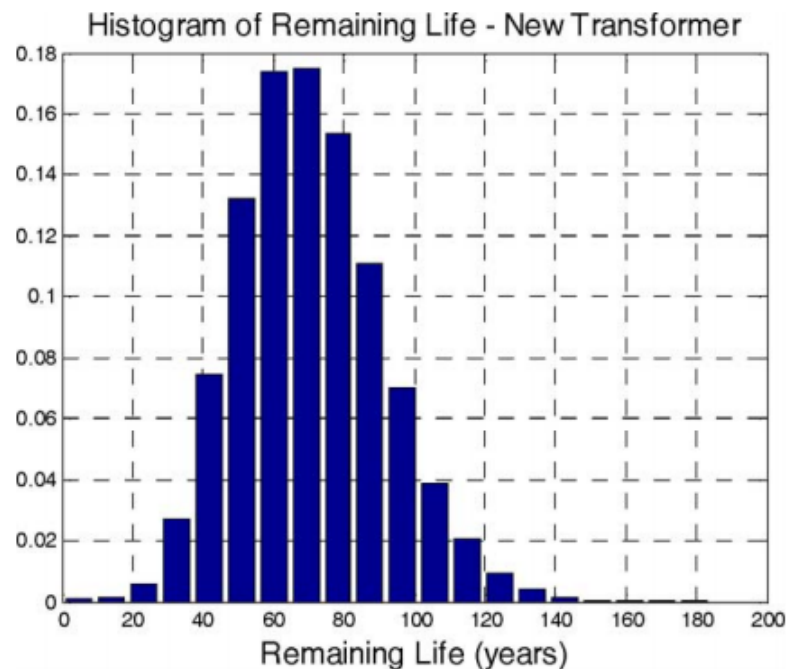


Figure 13 – Average life time - New Transformer [4]

2.3.0.7 Aging and Maintenance

As verified, the failure probability increase with aging. However, aging can be controlled or slow down with maintenance actions. There are two types of maintenance that are conceptually different: corrective and preventive.

The corrective maintenance consists of equipment restoration, which suffered a repairable failure. On the other hand, preventive maintenance is an inspection activity performed without failure equipment. Preventive maintenance has its primary objective the deterioration reduction and equipment life extension, which applies to both repairable failures and end-of-life failures.

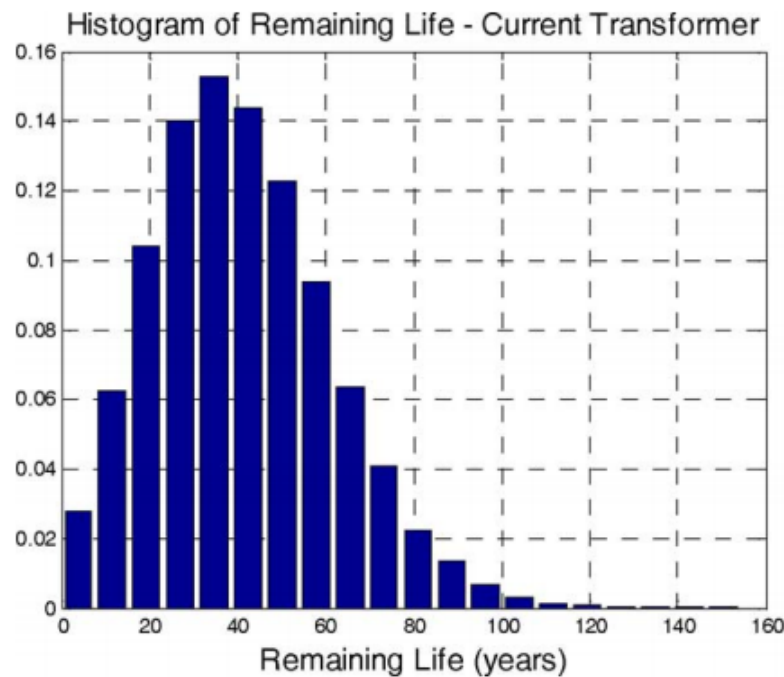


Figure 14 – Remaining life time - Used Transformer [4]

2.4 Predictive Maintenance

As shown in figure 15, the maintenance integrates the global group of activities performed in asset management, which might be considered technical criteria and shall comply with the financial restrictions.

The maintenance programs can vary from the most simple (inspections from time to time with predetermined activities) until the most sophisticated, based in *RCM (Reliability Centered Maintenance)*.

The optimization of the most simple model can be though the identification of the maintenance frequency, which minimizes the costs. The most complex maintenance schemes, incorporate ideas of equipment condition monitoring where the decision about the maintenance moment and level is according to the deterioration components stage.

2.4.0.1 Reliability Centered maintenance

Definition

RCM is a strategy of maintenance applied to optimize the company maintenance program. The procedure used in each company's assets is the final result of the *RCM* program. The maintenance strategy is optimized to maintain plant functionality through low-cost maintenance techniques.

There are four fundamental types for *RCM* program:

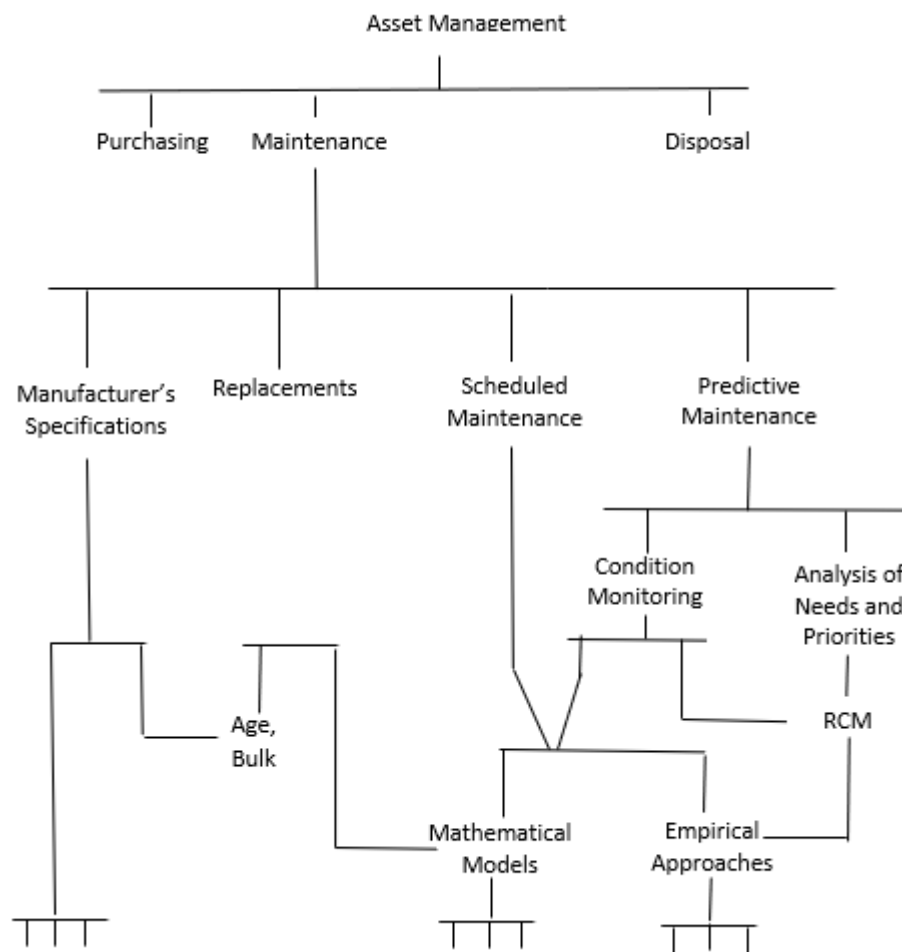


Figure 15 – Overview of maintenance Policy [6]

1. The main objective is to preserve the system function
2. Identification of failure modes that can affect the system operation
3. Prioritize the failures modes
4. Selection of applicable and efficient tasks to control the failures modes

Objective

The equipment reliability, achieved by the minimization of system failures probabilities, is the focus of RCM. Though this maintenance strategy, it is taken into account the equipment function and the possible failures modes and their consequences are identified. Maintenance techniques that are cost-efficient to minimize the failure probability are determinate. Then, the use of more efficient methods is applied to improve the reliability of installations as a whole.

Questions

An RCM effective implementation evaluates the installation as a series of function systems. Each system has inputs and outputs that contribute to the installation success. It is the reliability, instead of its functionality, of these systems that are considering.

The seven questions that need to be done for each asset are:

1. Which are the functions and performance wishes for each asset?
2. How can each asset not fulfill its functions?
3. Which are the failure modes for each operational failure?
4. What causes each failure mode?
5. What are the consequences of each failure?
6. What can be done to predict or prevent each failure?
7. What should be done if an appropriate proactive task cannot be determined?

RCM identify the most critical functions of the company and then try to optimize its strategy by using applicable and profitable techniques. The most vital company assets are those that tend to fail often or those that cause significant problems in case of failure.

Steps to RCM implementation

There are many different methods for RCM applications that are recommended by various organizations. However, in general, they can be summarized by the seven following steps:

- Step 1: Equipment selection for RCM analysis. The selected equipment for RCM must be critical in terms of effect in operation, repair, and maintenance costs.
- Step 2: Definition of limits and functions of the system that contain the selected equipment: The equipment belongs to a system that executes a critical role in the process. The system can be big or small as necessary, but the system function must be known as well as its inputs and outputs. For example, the purpose of a conveyor belt is to transport goods. Its inputs are the goods and mechanical energy that supply the belt while its outputs are the goods on the other side.
- Step 3: Define the ways the system can fail (Failure modes). In this step, the main objective is to list all the ways that the operation can be interrupted.

- Step 4: Diagnostic of failure modes. It is possible to identify the causes of each failure mode with the collaboration of operators, sophisticated techniques, RCM, and equipment specialists.
- Step 5 Assess the effects of failure. In this step, there is an assessment considering the consequences of each failure. It includes the security, operation, among other effects. It is also possible to evaluate the criticism of each failure mode.

After the systematic analysis of each failure mode, it is determinate the most critical failure mode, by doing questions such as: - Does this failure mode have security implications? - Does this failure mode lead to a total or partial stop of operations? For further analysis, the most critical failure modes have priority. It is important to note that these failure modes only include those that have a real probability of occurring in operation conditions.

- Step 6: Select a maintenance strategy for each failure mode. In this step, the most suitable plan for each failure mode is determinate. It is important to emphasize that the selected method should be technically and economically viable.
 - Condition-based maintenance is selected when it is technically and economically viable to detect the start of a failure mode.
 - The time or Usage-Based Preventative Maintenance is selected when it is technically and economically viable to reduce the failure risk by using this method.

For failure modes that there are not options of maintenance based in satisfactory condition, it should give consideration a system redesign to eliminate or modify the failure mode. The failure modes do not identify as critical in step 6 can be identified in this phase as good candidates for a maintenance program type run-to-failure.

- Step 7: Regularly Implement and evaluate the maintenance strategy selected. It is important to emphasize that the methodology RCM only will be useful with constant review and the renovation of its recommendation when it finds additional information.

2.4.0.2 Mathematical Models

The maintenance is capable of increasing the time until the failure of equipment under aging. Thus, any mathematical model that represents the benefices of a determinate maintenance policy should list the maintenance results due to the deterioration process.

Failure modes

Component failures can be divided into two categories:

- Random Failures
- Failures due to deterioration process (Aging)

Figure 16 presents two models for components. The first (indicated by letter a) applied to Random failures, where W and F represent the states of work and failure, respectively. The second (indicated by letter b) used to describe stages of deterioration designated by D1, D2, etc. In both cases, the effect of preventive maintenance in the equipment was disregarded, although in the model b is necessary periodic inspection to classify the deterioration stage.

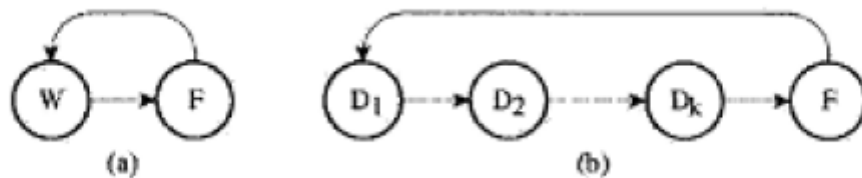


Figure 16 – State Space [6] a) Random Failure b) Deterioration

Probabilistic mathematical models can represent the process present in figure 16. The models are Markovianos if the transition rate between the stages are constants. For this type of model, there are techniques well know to solve them [30].

The **MTTF** for case (a) corresponds to the meantime of stay in the state W (working). In the case (b), **MTTF** corresponds to some of the meantime of remaining in the deterioration states. In the case of constants rates, the time until failure for case (a) has an exponential distribution. However, for case (b), some of the exponential times haven't exponential distribution.

Maintenance Effects

The models present in figure 17 include maintenance actions in the process illustrates previous in figure 16.

In the case in figure 17, assuming constants rates implies admitting that repair after a random failure gives the component a new equipment status. As the failure rate is constant, the preventive maintenance does not modify the equipment condition, according to the model. Then, the probability of occurring a random failure in a given future time interval is the same doing, or not, the preventive maintenance [6].

This situation is different from the illustrated in figure 17-b, where the performance of preventive maintenance makes the equipment come back to the previous deterioration stage. In this process, it doesn't matter the distribution of transition time, between the

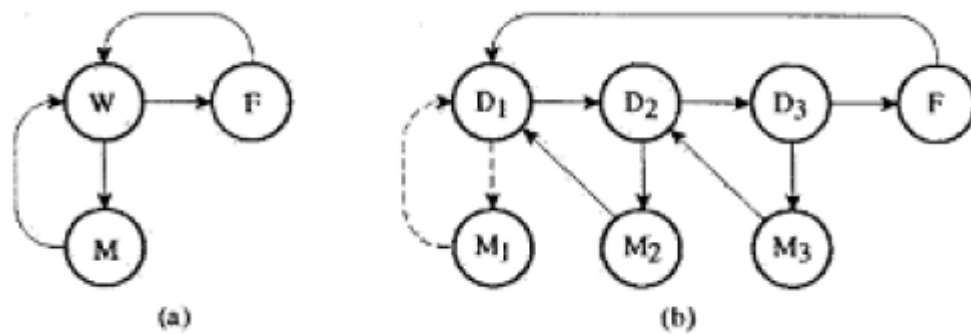


Figure 17 – State Space Considering Maintenance [6] a) Random Failure b) Three stages for Deterioration

deterioration stages, the maintenance will improve the equipment condition. Thereby, the rule [6]: Equipment conditions do not modify with random failures repair, but preventive maintenance has a vital function to perform when the failures are due to aging.

2.5 Aging factors

Aging is an irreversible degradation in the insulation system. The nature of this degradation can manifest in many ways. The properties of an insulation system that are most influenced by aging depend on the material insulation type and the type of the imposed influence. The factors that cause aging are called aging mechanisms. There is a division of such mechanisms: Electrical, mechanical, thermal, and environmental [31].

One of these mechanisms can cause aging, or some of them acting simultaneously or sequentially can cause aging. The action of one mechanism or many mechanisms along the time results in equipment failure.

In general, equipment failure means the insulation breakdown. The time until insulation breakdown determines the insulation lifetime. Instead of wait for the insulation breakdown under regular operation, which can last several years or decades, accelerated processes in laboratories are performed to determinate this time. Increasing the action of aging mechanisms minimize the insulation lifetime. On the other hand, if there are enough data, it is possible to use the statistical technique for these analyses.

Though the results of the accelerated aging tests, It can perform the estimation of a useful lifetime in specific operation conditions by appropriated models. However, it is necessary attention in any extrapolation. Other aging mechanisms may become dominant, or the aging process is not linear regarding the influence factor applied.

Additionally, it is unlikely that the aging rate remains constant during the life of an insulation system. The dominant processes at the beginning of aging can not be the same over the insulation lifetime. It is important to note that extrapolation of accelerated

aging results can be very risky. The best way to increase the estimation reliability of the remaining useful life is by better understand the chemistry and physics of fundamental aging processes.

The paper presents the failure mechanisms of stator windings [32]. They are thermal deterioration, thermal cycle, inadequate resin impregnation, voltages surges, losing winding in the slot, end-winding vibration, contamination, among others. Many statistics studies have approached the causes of failures in rotating machines and generators. However, these statistics focus on machine failure without worrying about the mechanism that cause failure [1]. The survey considering 1199 hydro generators by the committee SC and EG11.02 from CIGRÉ is a clear example of this type of investigation. The results present 69 incidents, among which 56% of the failure machines give insulation problems.

Seven groups can represent the root cause that leads to these failures, as shown in figure 18.

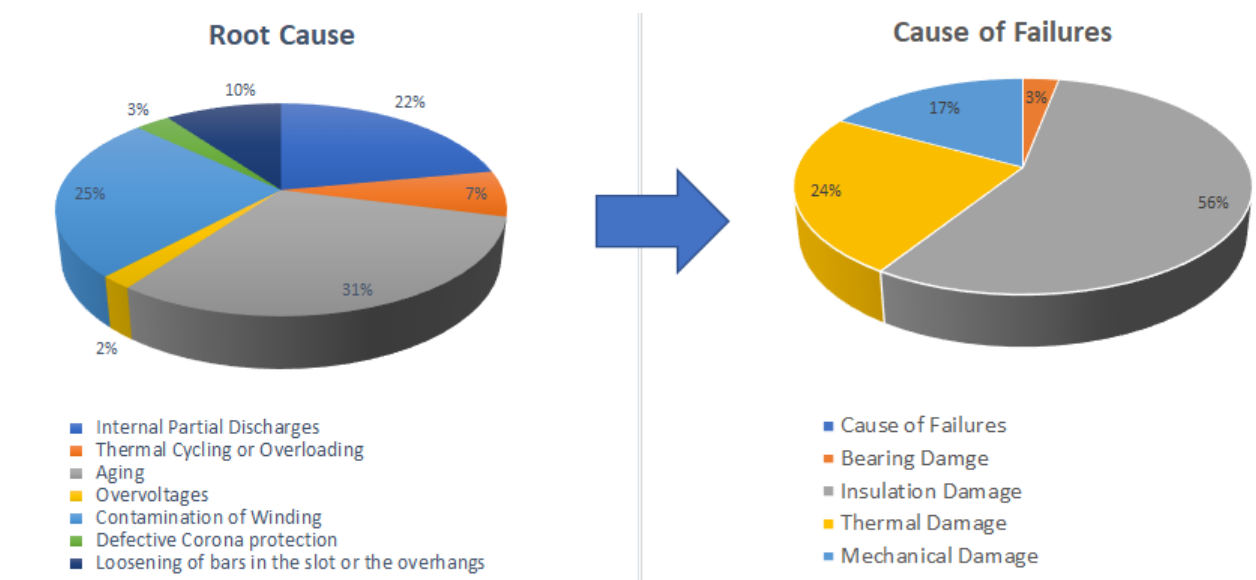


Figure 18 – Root Cause of Failure in Rotating Machines [7]

The applied voltage is not the determining factor in aging, although the dielectric rupture is the final cause of an insulation breakdown [1]. The thermal degradation of the resin, mechanical vibration, impulses from switching, and efforts provoked by different coefficients of thermal expansion are the dominant aging mechanism.

The aging under thermal, mechanical, and electrical stress show an increase of lifetime under moderate temperatures up to 130 °C, and a fast reduction of a lifetime when the temperature is above 180 °C.

These facts can be partially explained by the increase of thermal degradation of the organic material and the reduction of internal action and breakage of the resin layer at high temperatures. The insulation system's stress can also be accidental(short term)

and permanent(long-term) and, the operating regime determines them.

Thermal stress lead to the mass reduction of insulation, as well as thickness and moisture insulation resistance reduction. These effects on insulation produce a decrease in its electrical and mechanical properties.

Usual or accidental electrical stress begins the development of partial discharges. This effect causes worsens the electrical characteristics of the insulation and its degradation until failure. Mechanical stress between conductors and core cause abrasion of the insulation and delamination, becoming them susceptible to insulation failures. This mechanical stress also occur between conductors (coils/bars)

The ambient stress with the incidence of oxygen, moisture, radiation, among others, increases the chemical reactions and start new degradation reactions of the insulation [33].

The analyses of degradation action of insulation systems over time show the beginning of the development of three distinct phenomenons: Aging, degradation, and breakdown. The appearance of Microscopic channels with high electrical conductivity is how an insulation breakdown starts manifest [34].

These channels cross insulation between conductors causing insulation loss. The insulation degradation and aging are phenomenons that facilitate insulation loss, but they are different. The paper [35] presents an analysis of these phenomenons, depending on the electric field intensity and duration, as well as electrical trees dimensions and other effects. Figure 19 illustrates the above [1].

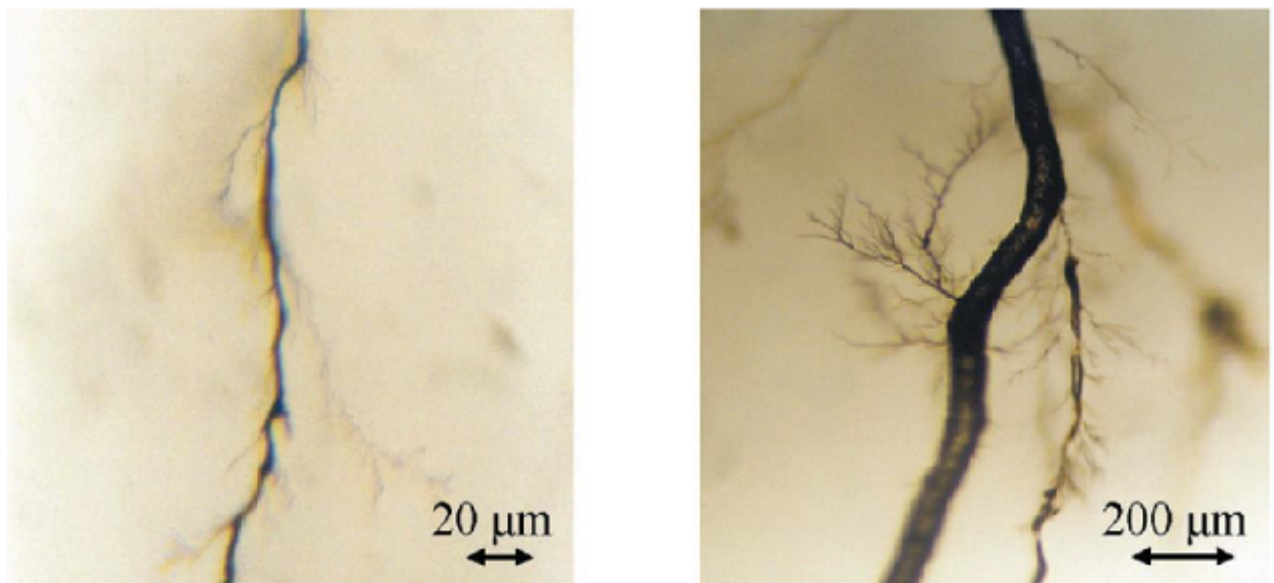


Figure 19 – Electrical trees [1]

Figure 20 shows an approximate time scale for the action of these phenomenons [8]

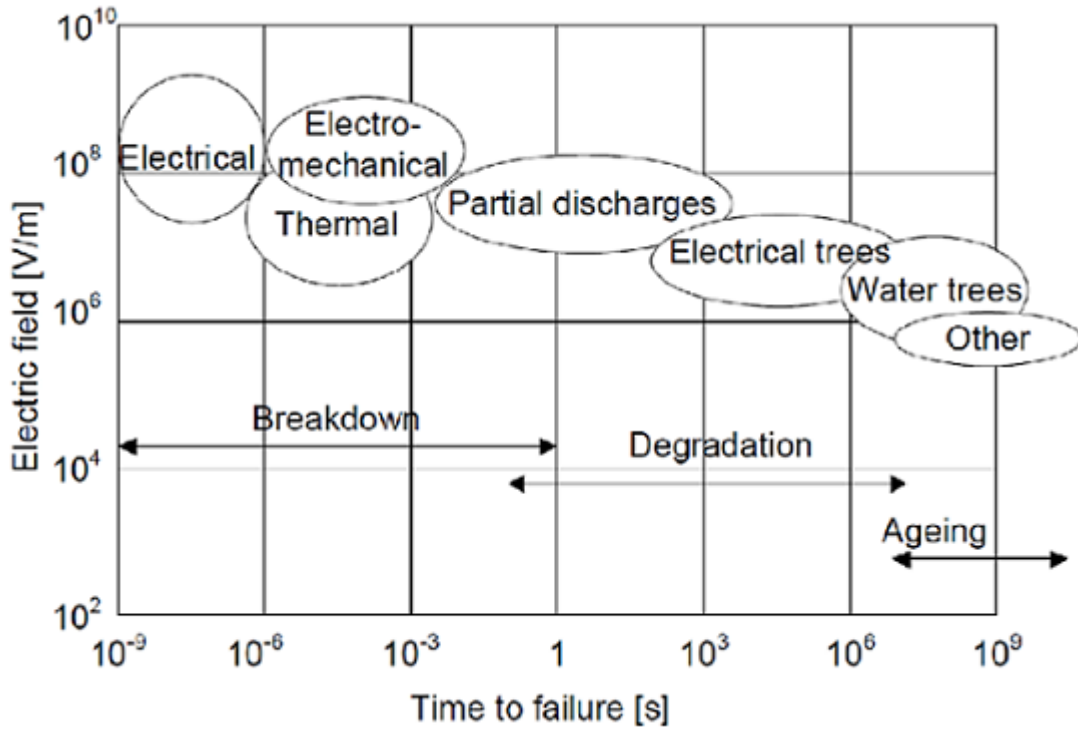


Figure 20 – Breakdown, Degradation and Aging [8]

Table 3 shows the breakdown, degradation, and aging characteristics [8].

The degradation occurs over a long period. On the other hand, failure is a process that occurs suddenly, and it is catastrophic. The insulation became utterly unusable after a breakdown. That is the fundamental difference between degradation and breakdown. For example, degradation can lead to electrical trees, and it can take hours, days, or even years until an insulation breakdown occurs. [36].

Even though the influence of the aging process under the insulation, the deterioration is less clear. It is widely accepted that the time until a breakdown decreases with the increase of intensity and time of electrical field application. On the other hand, aging is a process that develops on a molecular scale [37] [38]. Many types of stress can deteriorate the insulation of equipment over time [39]. As previously observed, the aging mechanism includes temperature rise due to equipment load, applied voltage, mechanical stress, operation mode, internal failures, vibration, contamination, among others. These factors may be continuous, cyclic, or intermittent. The contamination is due to the presence of radiation, water, corrosive material (solid, liquid, or gaseous), which may lead to insulation breakdown or accelerate the aging process. Figure 21 shows the aging factors.

The combination of these factors results in many failure processes. Since aging is an inevitable process, one practical question arises. This question is about the remaining useful life that we want to model. Moreover, we want to understand the influence of these factors on the insulation life.

Table 3 – The breakdown, degradation and aging characteristics [8]

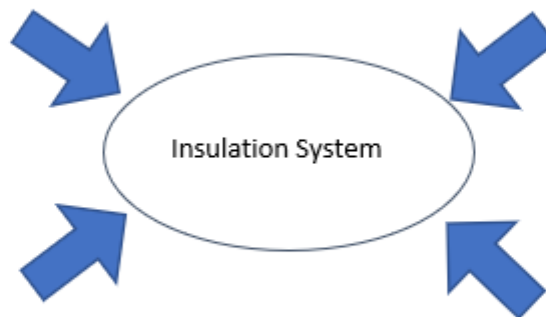
Process/ Characteristic	Breakdown	Degradation	Aging
Evidence	Direct observation (normally by eye - hole through insulation)	Observable directly (may require microscope or chemical techniques).	Difficult to observe (may even be difficult to prove existence)
Place	Continues filament	Occurs in weak pars	Assumed to occur throughout insulation
Size	>mm (dependent on energy of event)	μm (may form large structures)	> nm (molecular scale)
Speed	Fast (occur in < 1s)	Less than required service life (hours - years)	Continuous process (whole service life)
Effects	Catastrophic (insulation cannot be used afterwards)	Leads to breakdown (reduces breakdown voltage)	May lead to degradation (may not reduce breakdown voltage) Reduces the breakdown voltage
Examples	Thermal, Electrical, mechanical, and multiple	Partial discharges, electrical fractures, electrochemical fractures	Oxidation, delamination, electrochemical changes

Thermal

- Oxidation
- Hydrolysis

Electrical

- Partial Discharges
- Overvoltage
- Electrical Tracking

**Mechanical**

- Cracking
- Tension
- Vibrations

Environmental

- Gas, Acids
- Pressure
- Radiation
- Moisture

Figure 21 – Aging Factors [1]

Voids in the material or the interface of materials are one of the primary sources of problems in solid electrical insulation. These voids are under an electrical field due to the voltage applied. In the case of the electrical field inside the voids overcome a critical value, partial discharges will manifest. The partial discharges cause material degradation, as a result, may lead to insulation breakdown [40]. The discharge can occur through insulation surfaces, typically between the solid insulation and the surrounding atmosphere. It can increase surface discharge activity. The difference of electric permittiveness causes an increase of the electrical field in the gas, generating partial discharges and erosion, as well as tracking on the insulation surface. The electrolysis is another phenomenon which electrically demanding the insulation (ions in movement due to moisture and dust).

The electric current in the windings generates losses by the joule effect in the conductors. The conductors dissipate most of the heat generated. Since the dielectrics are not good heat conductors, permanent, periodic, or transient temperature gradients may appear during operation. It leads to the degradation of the insulation material. The dielectrics' losses also can cause temperature elevation. Each material has a specific form of degradation. The papers [41] [42] [43] widely explore the thermal aging process.

The concept of assessing the behavior of thermal aging for the windings of a machine goes back to the works of Arrhenius, Montsinger [44], Bussing [45], and Dakin [46]. The chemical reaction is the basic principle. Decades of accumulated experience allows the insulation system in rotating machines to be economical and reliable [13]. Today, there are several standards IEC and IEEE that define the procedures to the qualification of the insulation system of windings. These standards use comparative evaluation, where the new behavior of a candidate system is compared to a reference system, which has already been tested and proven.

The work presents [47] a first revision of the insulation systems functions and historical evolution. It also shows the main mistakes of models, from that time, with the main emphasis on aging due to multiples factors and multiples ambient conditions.

Important Chemical degradation mechanisms are oxidation and hydrolysis reactions. Ambient Mechanisms that reduce the useful life, such as solar radiation, radiation in nuclear power plants, moisture, pressure, are also very important.

Factors such as vibration, thermal expansion, flexion of cables may generate fractions on the insulation material, giving rise to partial discharges.

The work of Giaerd did an introduction of aging factors and a review of aging models for singular stress. It also treated about multi stress, where many aging mechanisms act simultaneously. An example is an insulation material that is under temperature elevation and an intense electrical field. The failure occurs before when compares to a situation that these mechanisms are acting separately [48].

The work [9] brings a first revision about the results of thermal cycles in hydro generators. It also presents an interaction model between different stress during the insulation aging, as depicted in figure 22.

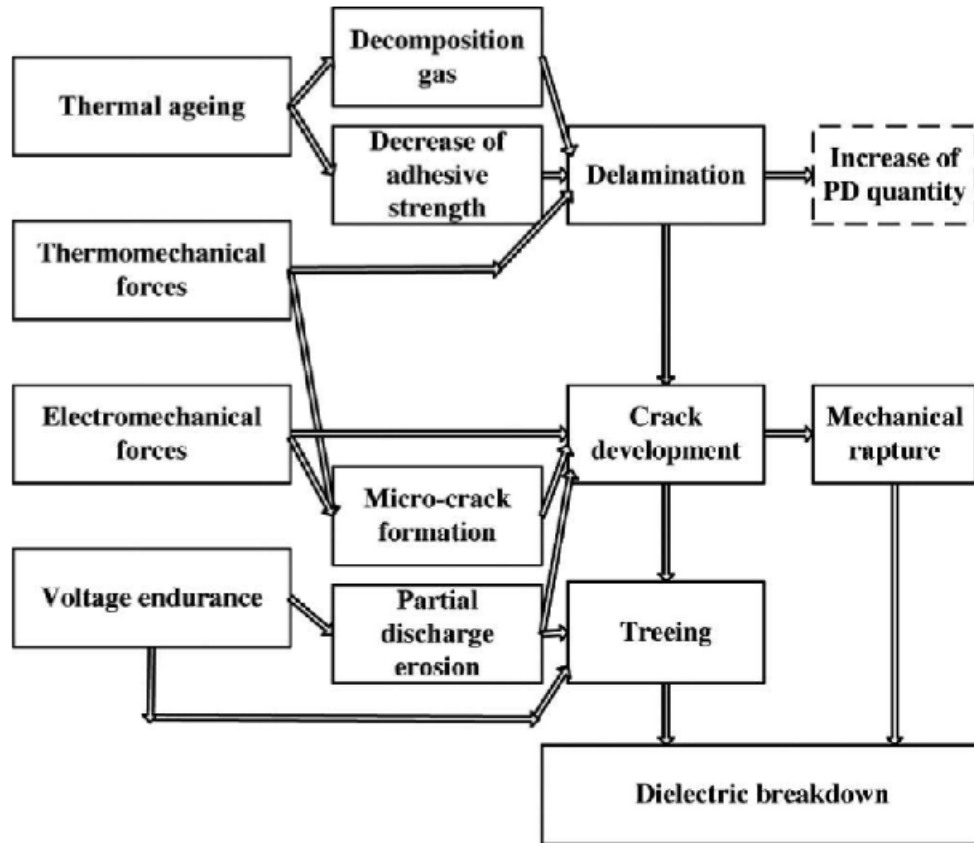


Figure 22 – Model for interaction between different stresses during aging [9]

Batnikas and Morin [10] used a three-phase stator model to perform electrical, thermal, and mechanical tests simultaneously, in a stator bar. This work evaluates partial discharges activity after every thermal cycle. The temperature has a strong correlation with discharges. Tests with twice the rated voltage did not provide any failure in the specimens under up to 1500 thermal cycles. On the other hand, tests with twice the rated electrical current cause failures in less than 1000 cycles. Figure 23 shows the stator model and bar used in the test.

The work [11] uses the results of accelerated aging tests. The test in stator bars presents three thermal overloads with many cycles. After each thermal cycle, mechanical and electrical stress is applied, as well as moisture. During the cycles, electrical measures such as insulation resistance, dissipation factor, and partial discharges are taken. In the end, VET (*Voltage Endurance Test*) verify the remaining useful life. Figure 24 shows the sequence of the test procedure.

Botts evaluated the corona effects in rotating machines [49]. It manifest when the electric field around the solid insulation ionizes and breaks gas molecules, causing

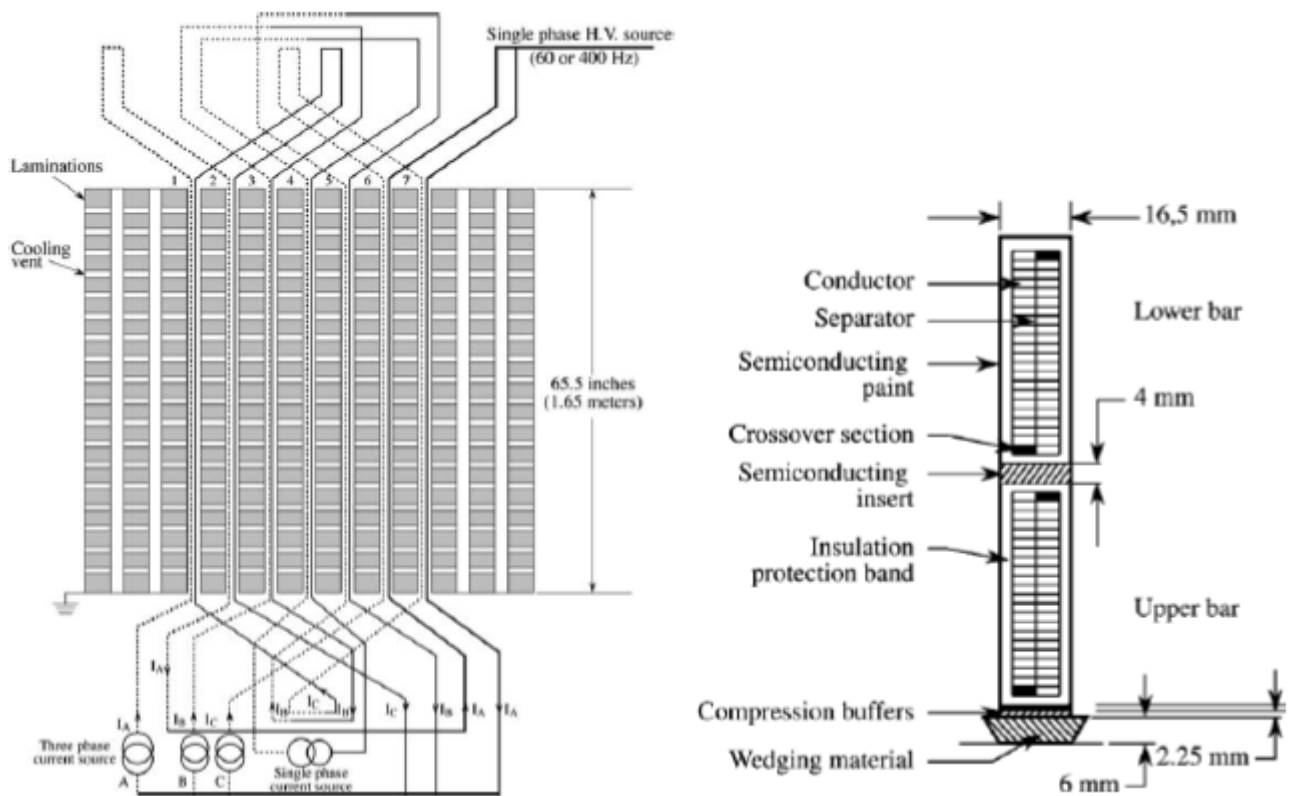


Figure 23 – Model for interaction between different stresses during aging [10]

discharges that deteriorate the insulation over time.

The work treats the influence of vibration and presents results of aging experiments with the combination of electrical, thermal, and mechanical (vibration) stress. The evaluation of the results shows the consistent increase of dissipation factor and partial discharges magnitude, as a consequence of the reduction of the dielectric insulation capacity.

The work [50] evaluates the thermal aging influence on the insulation using dielectric Spectroscopy, or frequency response. The experiment consisted of the application of 186 °C in a coil for 7000 hours. The basic premise was warming in high temperatures could cause a different chemical process of aging, unlike what happens during normal operation. The time and frequency domain allow the observation of these chemical processes.

Measurement of the charging and discharging current of the stator winding insulation under high voltage DC is one of the tests used in assessing the condition of rotating machines [51]. This reference performs VET in 12 and 13.8 kV Roebel bars. Half of these bars was subjected to 35 kV AC voltage and 110 °C. Failures between 25 and 150 hours were observed. VET with 59,5 kV AC voltage was performed in other bars. There was not any failure over 2000 hours of the test. Then, the test bars were again tested with DC voltage to compare the effects. Moreover, corona and partial discharges tests were

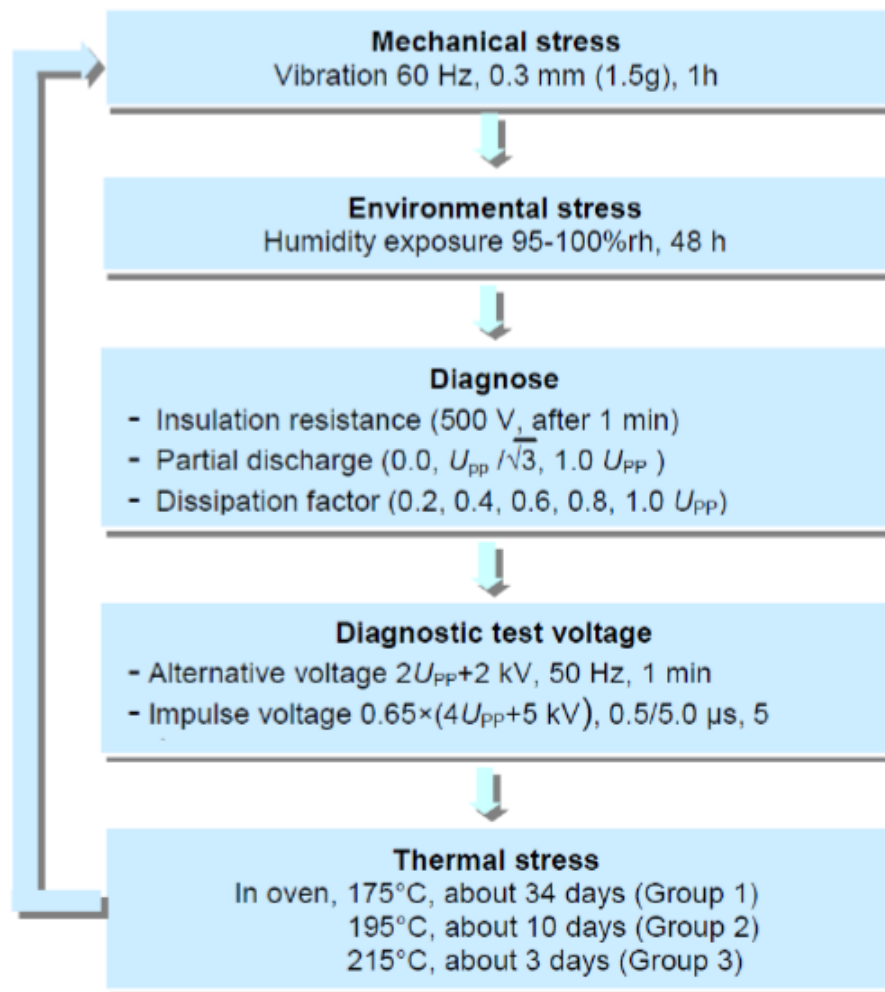


Figure 24 – Sequence of the test procedure. [11]

performed in the bars. The paper concludes that VET with DC voltage using 1,7 times of the applied voltage in VET with AC has the same effect.

Kokko presents a work that estimates the effects of the applied voltage over the useful life of generators windings [12]. Since the application of accelerated aging test to evaluate the useful life requires the extraction of bars/coils from generators, the author gives effaces to mathematical models based on experimental studies for that evaluation. In this work, Kokko proposes a schematic flowchart of the influence of aging mechanisms and necessary information to estimate the remaining useful life of generators. It includes information about project, manufacture, history of faults, operating conditions, maintenance activity, among others. Figure 25 shows the flow chat.

The inverse power electrical aging model was found to estimate the insulation lifetime. Figure 26 depict the results comparing the expected life and the electrical field.

The work [52] presents an analysis of multiples stress degradation. The authors execute multi stress accelerated aging tests in 300 MW, 18kV stator bars of generators

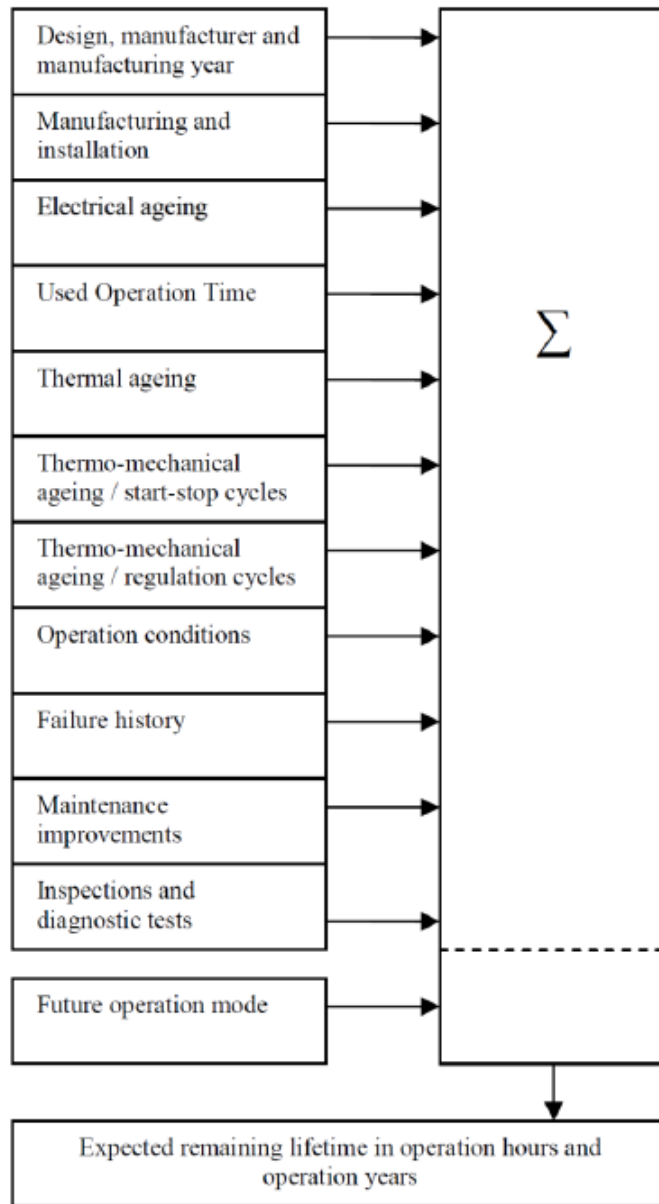


Figure 25 – Schematic Flowchart for Life Time Estimation of Stator Windings [12]

combine thermal and electrical stress, as well as mechanical vibration and thermal cycle (thermal-mechanical stress). The authors also measure partial discharges and dissipation factors to quantify the insulation degradation. In the sequence, VET in the tested bars were performed to identify the breakdown voltage. The partial discharges asymmetry presented the best correlation with the breakdown voltage.

The work investigates specimens of stator bars, and observe the formation of electrical tracking with 50 to 200 length, which can lead to phase to ground failure [1]. Figure 27 shows the presence of treeing caused the burning of the binder and delamination. Moreover, tests with vibration and temperature elevation caused delamination, abrasion, and degradation of the corona protection layer.

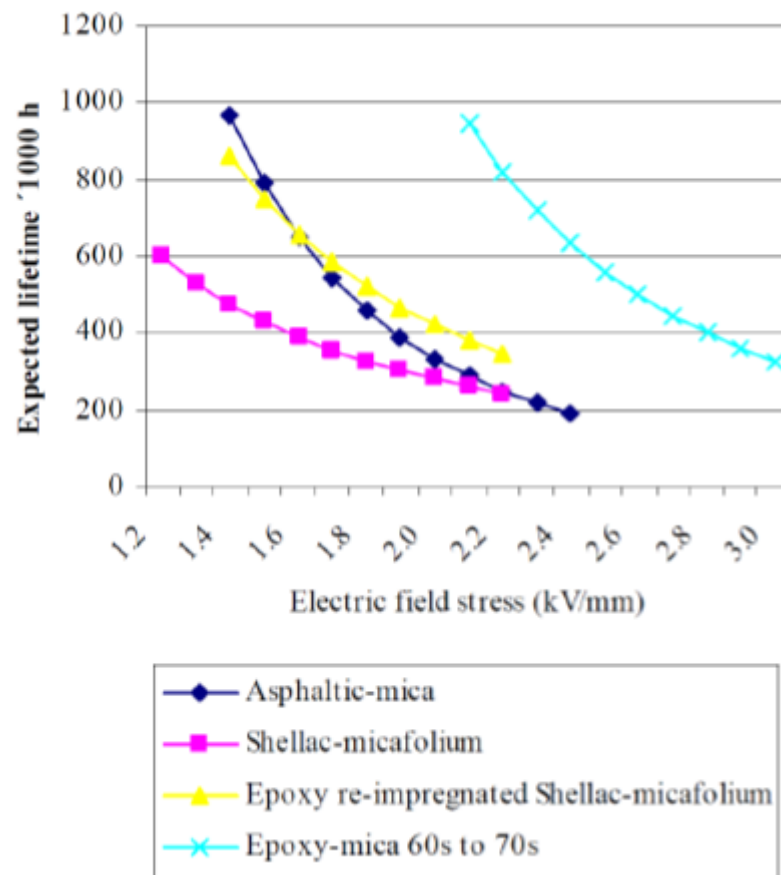


Figure 26 – Formed electrical ageing curves vs. electric field stress for various stator winding insulation systems [12]

The work [53] treats the consequences of local defects on stator winding insulation. Generator bars with mica-bitumen insulation and mica-epoxy insulation were investigated with the application of Visual inspection and VET. The mica-epoxy bars were from 10,5 kV generators with 35 and 36 years of operation, and the mica-bitumen were from 12 kV generator with 42 years of operation. Replacement bars from the same generators were tested as well. The replacement bars did not present failures.

On the other hand, both types of in-service aged insulation failed due to the high electrical stress and delamination between the copper and the ground wall insulation. The authors estimate the time to breakdown, in the bars that did not fail, using VET and adjusting a Weibull with two parameters for the results.

As well know, electrical, thermal, mechanical, ambient process are factors that cause aging in insulation systems of rotating machines. Partial discharges can be a symptom and a cause of insulation aging [54]. In insulation based on mica-epoxy, the coating material (epoxy) is decomposed by partial discharge activity, causing irreversible changes in their proprieties[55].

Thermal-mechanical stress cause delamination and formation of voids between the

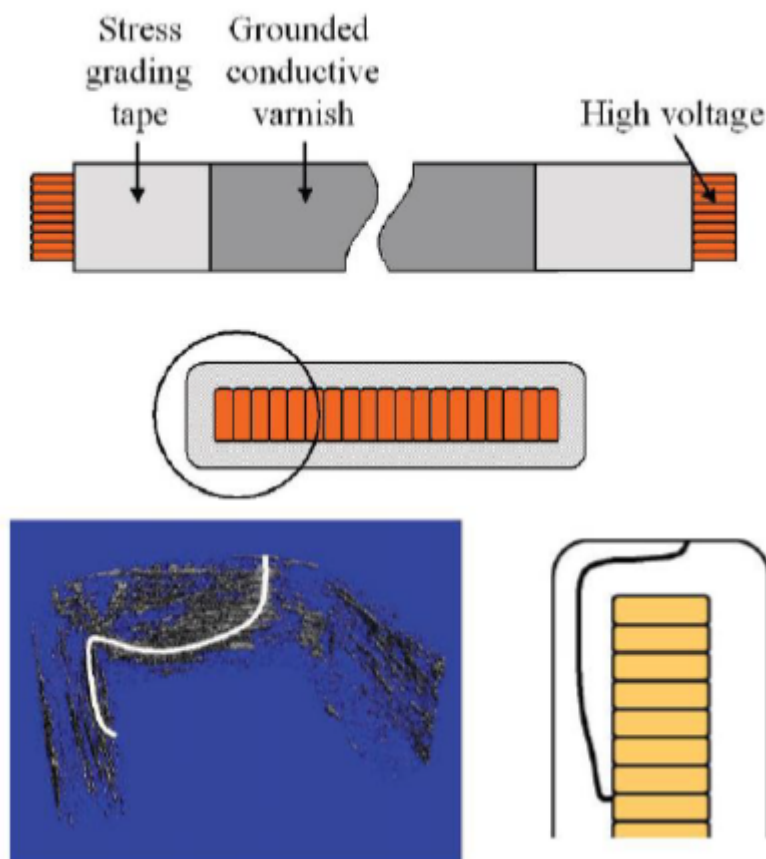


Figure 27 – Formation of Electric Micro fractures from 50 to 20 μm [13]

ground wall insulation and the copper conductors. The origin of this stress is the operation regime and the different coefficients of expansion of the insulation parts. Considering the copper ($170\text{E-}7$ 1/K) and epoxy resin ($1,1\text{E-}7$ 1/K) coefficient of expansion, and having a temperature variation from 20°C to 140°C , the linear displacement is approximately 2 mm. That is sufficient to break the insulation in case the effect manifests repeatedly [53].

Weiers carried out tests to examined bars of generators with 37 years of operation that had failed an overpotential test [56]. After examination, the diagnostic of water absorption is positive. Bars were dismantled from these generators, and VET carried out. The in-service bars failed in a period 27 times shorter than a spare bar in the right conditions. The conclusion is water absorption significantly reduces equipment remaining life.

The evaluation of bars/coils condition is critical since this forms the basis for evaluating maintenance strategies, risk assessment, and decision to replace or invest in new equipment. A diagram of the activities and measurements in condition assessment is shown in figure 28.

The dielectric measurements are an important tool for the diagnostic of insulation systems. Partial discharges, dissipation factor, polarization, depolarization index represents some of these test. The work [9] presents the evaluation criteria of mica resin

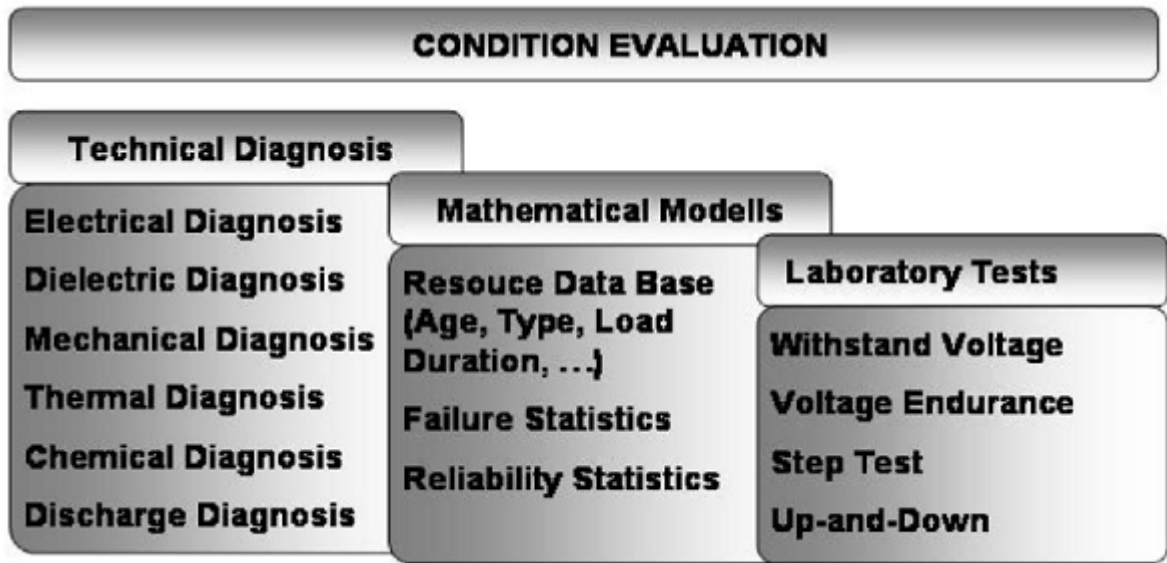


Figure 28 – Condition Evaluation [14]

insulated windings by results of partial discharges and tan delta(δ) test, as shown in figure 29.

2.6 Accelerated Aging and Diagnostic tests

2.6.1 Accelerated Aging test

Aging is a prolonged process that takes decades in generators. The evaluation of stator winding condition by natural aging through operation condition stress would take decades. The alternative to accelerate aging is by the intensification of the aging stress above normal condition, becoming this evaluation feasible in a short period. That is how the accelerated aging test is performed in laboratories by manufacturers to improve the stator isolation system to hold the operation stress for a longer time.

As can be seen in figure 30, the insulation systems have significantly been change over time, and the accelerated aging tests have a contribution to this.

The insulation material, for example, in the beginning, was made by asphalt mica. Latter, asphalt mica was replaced by natural resins, and nowadays, the state of art insulation systems has an epoxy resin as the base component material [15].

The insulation system's dimensions have reduced as the insulation systems became able to hold more and more electric field strength. As can be seen in figure 30, the ground wall insulation thickness had significantly decreased over time. On the other hand, the rated electric field strength made a permanent increase from 0.75 kV/mm for asphalt systems 100 years ago to up to 3.5 kV/mm for newer isolation systems [15]. Indeed, the older isolation systems were overrated. It leads to a longer useful life, as some statistical

Test item	Criteria	Judgement	Figure of characterisation
Partial discharge	I $q_m < 1 \times 10^4$ pC	Good (a)	
	II $q_m \geq 1 \times 10^4$ pC	Careful (b)	
	III $q_m \geq 3 \times 10^4$ pC $N_q < 2.0$	Critical (c)	
	IV $q_m \geq 3 \times 10^4$ pC $N_q \geq 2.0$	End discharge (d)	
tanδ	I $\Delta \tan \delta < 2.0$	Good	
	II $\Delta \tan \delta \geq 2.0$	Careful	
	III $\Delta \tan \delta \geq 6.5$	Critical	

N_q : Ratio of the slope of $q_m * V$ characteristics [$= 10 \log(q_{m1.25E/\sqrt{3}}/q_{mE/\sqrt{3}})$] (E : rated voltage).

Figure 29 – Evaluation Criteria for mica Resin Insulated stator windings [9]

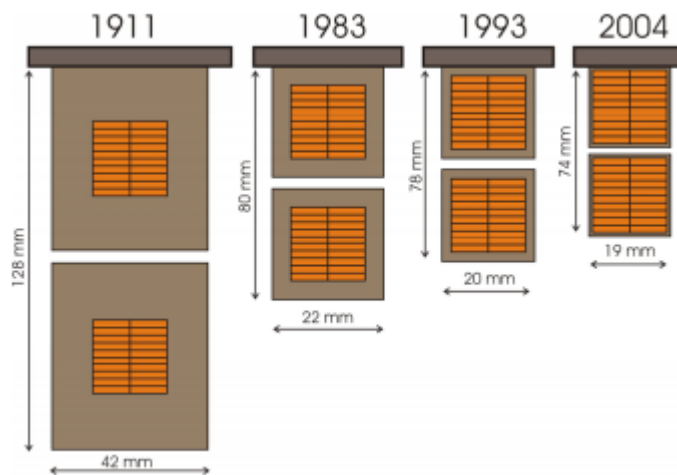


Figure 30 – Isolation System Evolution Over Time [15]

analysis pointed out that the old generator lasts longer.

The accelerated aging tests have helped the generators manufacturers on this evolution, comparing similar constructions to determine the best. That is why the accelerated

aging test is crucial to the generator's winding manufacture evolution.

Another important application of the accelerated aging test is to improve the maintenance schedule of generators. The use of accelerated aging tests along with the diagnostic test is possible to set up dangerous conditions that require maintenance on windings or even the replacement of them. That is part of the preventive maintenance, based on the equipment's conditions, and represents a vital tool for companies to manage their assets better.

The Accelerated Aging test is generally executed by increasing one or more aging stress above the normal condition operation level. For example, Voltage Endurance Test is performed in stator bars/coils at 30 or 35 kV for generators rated at 13.8 kV. It means that the electrical stress is upper to 4 times more intense.

The most widely applied accelerated aging test for stator winding, are shown below:

- Voltage endurance test
- Thermal cycle test
- Thermal test

Standards represent not all *TEAM (Thermal, Electrical, Ambient, and Mechanical)* aging stress. For example, mechanical stress has not any well-accepted test. However, it is correlated to the root cause of some stator failure mechanisms.

In the sequence, these accelerated aging tests are present in details.

Voltage Endurance Test

The armature insulation must be able to isolate the generator's parts in different potentials. Then, the main objective of machine insulation is to prevent discharges between parts in different voltages levels.

The insulation system must be properly designed to withstand voltage, avoiding insulation puncture. The main characteristic of one insulation material is the breakdown strength. Each insulation material has its breakdown strength. It means a voltage level that the material loses its insulation properties and starts to works as a conductor. The air is an example of gas insulation material and has a breakdown strength of about 3 kV/mm at atmospheric pressure (1 atm, 20°C and 60%) . However, its insulation properties cannot be compared to the solid insulation material. Typically used in the insulation system of rotating machines, the solid insulation materials present breakdown strength ranging about 200 kV/mm [57].

The breakdown strength of an insulation system can be calculated using the breakdown voltage divided by the insulation thickness.

The breakdown voltage is a short-term voltage that causes insulation breakdown. Moreover, the breakdown voltage can be understood as the voltage that causes insulation puncture in some minutes, without any electrical aging of the insulation system.

In practice, the operating electrical stress level of a rotation machine is very low comparing to the breakdown voltage. However, in air voids present in the insulation system, that are inevitable in rotating machines, the breakdown strength is much lower. Then, Partial discharges manifest in these voids in all rotating machines rated above 8 kV. This phenomenon is responsible for a good part of the electrical aging in the insulation.

The electrical aging, along with other aging stress through the time, can degrade the insulation system, leading to the loss of the isolation properties. The final result would be an insulation puncture.

In conclusion, to design an electrical insulation system, taking care only by the breakdown strength is not suitable to yield a long life for the insulation system. It is necessary to take into account electrical aging over time that is inevitable during operation. In this scenario, the VET was introduced, fitting as a tool for the determination of the best insulation system design. The procedures using by the machine manufacturer to perform VET vary widely. The primary standards reporting about the VET for hydro generators are:

-IEEE Std 1043 - IEEE Recommended Practice for Voltage-Endurance Testing of Form-Wound Bars and Coils [58]

-IEEE Std 1553 - IEEE Trial-Use Standard for Voltage-Endurance Testing of Form-Wound Coils and Bars for Hydro generators[59]

-IEEE Std 930TM-1987 , IEEE Guide for the Statistical Analysis of Electrical Insulation Voltage Endurance Data [60]

The IEEE Std 1043 gives the details of the test procedures to develop voltage endurance tests. This standard is for form-wound stator winding bars and coils of hydro generators rating from 4 kV until 22 kV and frequency of 50 Hz or 60 Hz [58]. The recommended voltage for the test in the specimens of stator bars or coils depends on the machine rated voltage, as predicted in Table 4.

Despite voltage, the test temperature is also an essential factor for a Voltage endurance test. The recommendation is to perform the test with a heating source to simulate the aging stress under operating conditions. The application of heating plates is described in detail at [58]. The temperature during the test must be constant and around the operating temperature. For example, a specimen stator bar or coil class F, the

operating temperature is about to 110 °C.- 120 °C. However, many manufacturers perform the test without any heating source. The test can also be at room temperature. The execution of a pretest to evaluate the initial condition of the specimen is recommended. A diagnostic test such as Power factor, and PD are some options of a pretest to perform. Other parameters such as humidity, ambient temperature, frequency voltage, time to failure, and failure location are essential to record as well.

The IEEE std 1553 [59] defines the number of specimens necessary, the acceptance criteria, and the procedures for retesting in the event of a premature failure during the VET. The number of specimens shall be at least four bars or two coils but not more than 1% of the number of bars/coils in the winding. If all the specimens hold the test time (400 hours or 250 hours) without insulation puncture, the winding met the test requirements. If a failure occurs before 50% of the test time, the insulation under test does not pass in the test requirements, and further analysis to determine the appropriate corrective action is necessary.

Instructions for statistical analysis of the test results are given at the IEEE Std 930TM-1987 [60]. Failures Probability plotting using Weibull distribution are present. Moreover, there are statistical methods to compare the failure data of two types of bars/coils. This comparison is essential to the determination of the type of insulation and design that yields a long life.

Table 4 – Test Voltages for voltage-endurance test

Rated line-to-line voltage of the winding	Rated line-to-ground voltage	Voltage Scheaduale A (400 h)	Voltage Schedule B (250 h)
4.0	2.31	8.7	10.1
6.6	3.81	14.3	16.7
11.0	6.35	23.9	27.9
11.5	6.64	25.0	29.1
12.0	6.93	26.1	10.1
12.5	7.22	27.1	16.7
13.8	7.97	30.0	35.0
15.0	8.66	32.6	38.0
15.5	8.95	33.6	39.3
16.0	9.24	34.7	40.6
17.0	9.82	36.9	43.1
18.0	10.39	39.1	a
19.0	10.97	41.2	a
22.0	12.7	a	a

A variation of the voltage endurance test consists of performing the test in higher frequency, as proposed by the reference [61]. Since the bars/coils aging are related to the PD in the voids present in the insulation system, and this phenomena are related

and tend to repeat each voltage cycle, the increase in the frequency voltage leads to the intensification of discharges, accelerating aging by electrical stress. Then, the insulation might fail faster, as represented in equation 2.13 [57]. Many manufacturers perform VET with 400-500 Hz for the AC voltage frequency.

$$L_2 = L_1(f_1/f_2), \quad (2.13)$$

Where: L_1 and L_2 are the voltage endurance lifetimes at AC frequencies f_1 and f_2 , respectively.

VET is destructive test that it is possible to use as a diagnostic test to estimate the damage caused in a bar/coil after aging. Thus, the estimation is possible with bars/coils of a machine under operation or specimens used in previous agings tests in laboratories. The quantification of damage is measured by the time to isolation breakdown with the bars/coils under test conditions.

Thermal cycle test

The Thermal cycle test is an important accelerated aging test that simulates the thermal-mechanical stress incident on generators. The standard [62] reports the thermal cycle test for stator bars/coils, where it is present all the procedures in detail.

The test consists of applied temperature variation to set up thermal-mechanical forces in the stator bars/coils. The temperature range for thermal cycles depends on the thermal insulation class of the insulation system under test, as shown in table 5.

Table 5 – Temperatures limits to Thermal Cycle Test

Thermal Class	Temperatures limits (°C)
H	40 - 180 (°)
F	40 - 155 (°)
B	40 - 130 (°)
A	40 - 120 (°)

Table 5 shows the thermal insulation class and the temperature limits for the cycles. The lower limit is 40 °C for all thermal class. On the other hand, the upper limit depends on the thermal insulation class. For example, considering an insulation class F, the upper limit temperature for the cycle is 155 °C. It means the upper limit temperature is the rated temperature of the insulation system under test.

The rate of temperature variation must be 2,5°C/min (+/- 1.0 °C), and this is applied for both heating and cooling half cycles of the thermal cycle test. It is important to emphasize that this rate influences the rate of degradation applied to the bar/coil

under test. It is recommended for the heating half cycle the application of a current through the windings to provide the desired rate of temperature variation. Appropriate instrumentation is necessary to measure, due to all reference temperatures being in copper, the internal part of the windings.

A cooling system can be used during the cooling half cycle but is not essential to test development. The winding can cool naturally by the environmental surrounding. However, the rate of temperature variation must be within the recommended limits. The winding has to be cooled evenly because the temperature difference between areas of the same bar/coil cannot exceed 5°C.

The test requirement is to complete a total of 500 thermal cycles. After that, the recommendation is to perform a diagnostic test. There are many options, such as partial discharges, tangent delta, VET (destructive test), among others, to the quantification of the damage caused by the intense thermal-mechanical stress. A previous diagnosis test must compare the results before and after bar/coil aging.

2.7 Thermal aging tests

The thermal stress represents a critical agent of aging in all electrical equipment. As will be discussed in subsection 3.1.1, the causes of aging by thermal stress are basically by oxidation reactions, which are speed up with temperature rise. Thermal aging test of an electrical insulation system is well documented in various standards, and the following references are essential for performing thermal aging tests:

- IEC 60505:2004, Evaluation and Qualification of Electrical Insulation Systems;
- IEEE Std 1-2000, IEEE Recommended Practice—General Principles for Temperature Limits in the Rating of Electrical Equipment and the Evaluation of Electrical Insulation;
- IEEE Std 98-2002, IEEE Standard for the Preparation of Test Procedures for the Thermal Evaluation of Solid Electrical Insulating Materials.
- IEEE Std 101-1987, IEEE Guide for the Statistical Analysis of Thermal Life Test Data.

Before performing a thermal aging test, it is essential to consider that thermal evaluation of an insulation system involves the following thermal factors of influence [63]:

- a) Exposure temperature
- b) Ambient temperature
- c) Temperature gradient
- d) Rate of temperature change

An aging test aims to establish a thermal endurance relationship, which is an expression of a thermal lifetime as a function of the test temperature. Equation 2.14 represents this expression, the Arrhenius rate law:

$$L = Ae^{(B/T_k)} \quad (2.14)$$

- Where A and B are constants;
- L is machine life in years;
- T_k is temperature in kelvin.

The correlation is typically a linear function of a lifetime at a logarithmic scale in hours by test temperature [64]. In order to have reliable information and ensure that the test data is providing a liner pattern, the IEEE Standards suggest at least three different test temperatures. The temperatures chosen for the test must be high enough to provide useful results in an appropriate time.

The test must have a heating source to reach the test temperature. Oven heating is a method that provides the most control in temperatures. In this method, all the insulation system may have a single temperature. However, oven heating does not simulate service conditions. For rotating machines under operating conditions, the insulation of the stator windings may operate at variable temperatures, and the heat is by a temperature gradient from the copper to the insulation surface.

The use of heating plates in the insulation surface is another alternative method. To better emulate the service condition in a rotating machine, it can execute the application of current in the bars/coils under test to provide heating by Joule effect.

The thermal aging test is fully employed for classification purposes to determine the thermal class of an insulation system. Table 5 report the insulation system class designations.

Table 6 – Thermal class

Thermal Class (°C)
Class 90
Class 105
Class 130
Class 155
Class 180
Class 200
Class 220
Class 250

The thermal endurance relationship is applied to the determination of the rated temperature. Usually, the measured temperature is the temperature that corresponds

to 20 000 hours of life in the expression of thermal endurance life. This point can be determined graphically by the Arrhenius Plot of life or mathematically by the Arrhenius rate law 2.14.

Table 6 is a numerical designation for the insulation system class. The number used for insulation classification represents the rated temperature of the insulation. There is also an older classification by letters. Table 7 represents both the letter and numerical classification. For example, in rotating machines, an insulation system with letter classification as B corresponds to the insulation system with numerical classification 130, and the rated temperature for this class is 130 °C.

Table 7 – Thermal Classification of the insulation system for rotating machines

Numerical Classification	Letter Classification	Rated temperature (°C)
105	A	105
130	B	130
155	F	155
180	H	180

2.7.1 Diagnostic test

Two reasons motivate the application of the diagnostics tests: Diagnostic the deterioration problem; Quantified the isolation health stage. Many electrical and mechanical tests can be applied in large rotating machines. The choice depends on the main objective defined by the machine inspectors. Some diagnostic tests are suitable to carry out in laboratories or factories, others for field application. In a factory or lab, the test in the stator windings is to attest to the quality of the manufactured process, to estimate the useful life, and to compare insulation's systems designs. For field application, the diagnostic test is used for the detection of a deterioration problem as well as to evaluate the current health status.

The following topics discuss the main tests usually applied for the evaluation of the rotating machine. The diagnostic of the main insulation problem is an essential step to predict the time to failure. Since each kind of insulation problem has a different rate of deterioration, only the actual condition of the machine is not enough to estimate the isolation life. Consequently, a suitable prognostic of remaining useful life has a previous step, the diagnostic.

Insulation Resistance

The test evaluates the insulation between conductors and phases, and between phase and ground. The measures are taken using DC current under a reduce voltage ap-

plied, a fraction of the rated voltage, over one minute period time. The insulation condition evaluation also depends on the machine size, test equipment, and engineer experience. It is important to note that all tests under significant value of voltage applied in the winding have to take into account the current insulation condition. Therefore, the choice of which voltage will be applied must be based on the machine rated voltage and its health status in order to avoid unexpected failures.

It is also important to note how the results of this test lightly depending on the voltage range applied. However, for machines with dry insulation and in the right conditions, this dependency is almost irrelevant and can be neglected.

In general, the insulation resistance test is performed with the equipment generically known as MEGGER. It is also possible to perform the test using bridge circuits for measuring, a stable current source DC, voltmeter, and a special amperemeter able to measure small currents. The results using AC sources do not have to match with those using DC sources because the dielectrics' reactions are distinct.

The reading of the insulation resistance test is sensitive to external factors such as humidity and winding surface contamination. Thus, the recommendation is to standardize, correcting the readings to a base of 40 °C, according to the equation. 2.16.

$$R_{40} = K \cdot R_{measure} \quad (2.15)$$

Where R_{40} is the resistance at 40°C, K is a coefficient that depends on the test temperature, and $R_{measure}$ is resistance measure in the test. The coefficient K depends on the temperature, and it is defined according to standard IEEE std. 43-173, by the equation 2.16

$$K = 0,00635e^{0,06895\theta} \quad (2.16)$$

Where θ is the temperature in degrees Celsius.

The minimum value for insulation resistance is subjective. Therefore, most users of big synchronous machines adopt the IEEE std.43-1974 recommendation, defined by the equation 2.17

$$R_{MN}[M\Omega] = kV + 1 \quad (2.17)$$

Where kV is the machine rated voltage in kV.

After one minute of applied voltage, for better comparison, the measured value must be corrected to the reference temperature of 40°C. The test needs to be performed for both stator and rotor windings.

Polarization Index

The insulation resistance measures depend on the time of voltage applied, because of the polarization phenomena of the dielectrics. The polarization varies from machine to machine, and with the amount of insulation humidity. In general, the insulation resistance measures are negligible for measures time above to 15 minutes. On the other hand, the rate of variation for insulation resistance measures in the first minutes of the voltage applied depends on the insulating condition and the presence of contaminants (water). This behavior allows defining a correlation called the Polarization Index, which represents the ratio of the 10 min resistance value to the 1 min resistance value [16]. The polarization index does not need correction to 40°C.

Figure 31 shows the variation of measures of insulation resistance for a rotating machine as a function of its drying and measure time. That is, the readings were taken after 1 and 10 minutes, which allows the determination of the polarization index value and the minimum drying time of the unit.

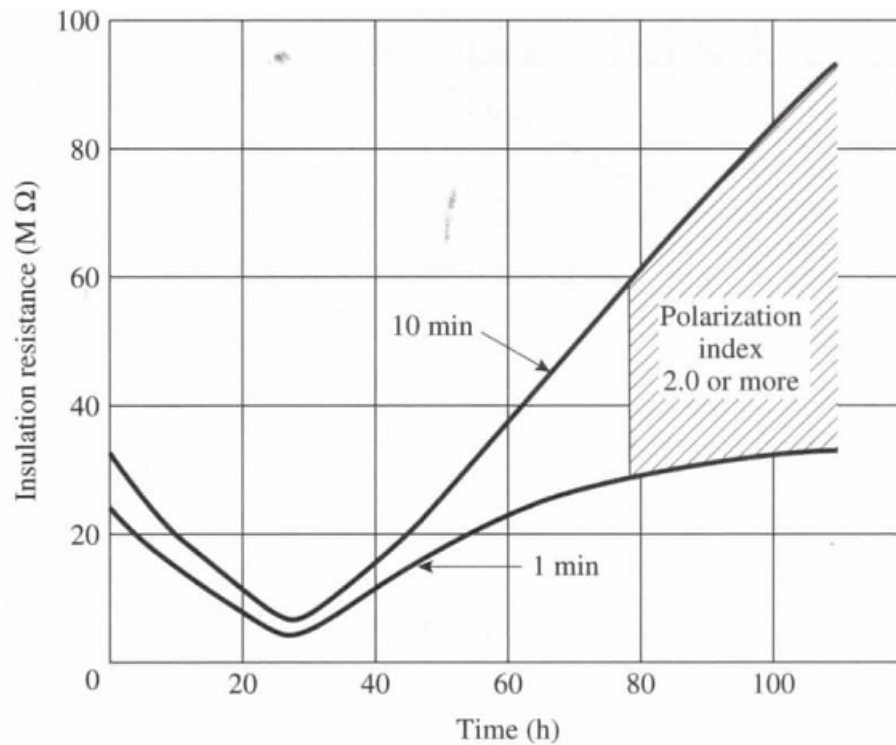


Figure 31 – Insulation resistance as a function of Measurement and Drying Time [16]

The indexes for the polarization index are used to evaluate the degree of cleanliness and humidity of the windings. As depicted in figure 32, the polarization Index also depends on the way the insulation is made and its components. Therefore, the windings build with insulation materials Class B usually have higher values for the polarization index than insulation Class A. This fact is also correlated with the presence of semiconductor layers.

The minimum values for polarization index recommend for IEEE Std.43-1974 [16]

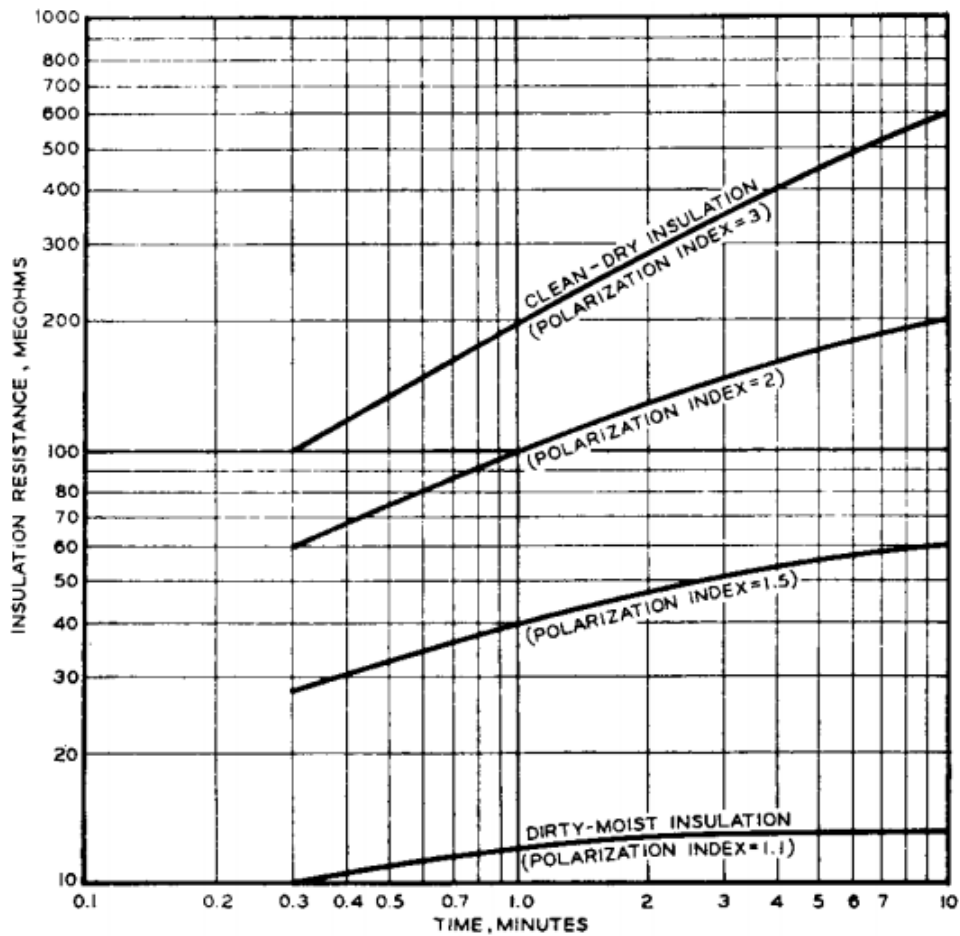


Figure 32 – Insulation resistance over time for insulation Class B [16]

are shown in the table 8

Table 8 – polarization Index

Insulation Class	Polarization Index
A	1,5
B	2,0
F	2,0

The values for the polarization index are taken under low levels of applied voltage. It is a requirement before the Hi-POT test since the application of high voltages in humidity insulation can generate unnecessary insulation failures.

HI-POT

The applied voltage test, HI-POT, is performed in order to demonstrate the windings capacity to hold its rated voltage without insulation breakdown. The test consists of applied voltage in all three phases or in one phase per time, with the other phases grounded. The voltage is applied over one minute. It can be used both DC or AC voltage.

For AC voltage, it is possible to use the rated frequency or lower. The choice depends on the machine power, winding dimensions, the relation between machine and test equipment, stray capacitance, among others. Therefore, several divergent points also make this choice depends on personal work experience.

The recommended voltage applied to performed the test, according to IEEE 62-1958, range from two times the rated voltage plus 1 kV, when the test is executed in the manufacturing process, to values lightly above the rated voltage, when the test is executed in an operating machine. In this case, it is also recommended to take into account the machine age and its actual condition.

Power Factor

The power factor test is performed in stator windings and measures the dielectrics lost per volume unit. Thus, it is capable of providing results that can be correlated to the actual insulation condition. This test is highly dependent on the dielectric under test. The results are better in polar dielectrics. The power factor test results are expressed in percentage, that is, dimensionless. The increase in the insulation power factor along the machine operating time can represent more air voids in the insulation. However, it also can be due to the increase of contact resistance between the coils and the slot. Both phenomenons can be explain by the dielectric lost models, in series or parallel forms, according figure 33.

Thus, Building a histogram with the evolution of measures values for tangent loss along the time can be a handy tool to evaluate the actual insulation condition.

The procedures to care out the insulation power factor test are further discussed in standards, as IEEE Std 286 -2000 [17]. The test is applied in machines rated voltage above 7 kV. The temperature strongly influences the power factor measures because of the phenomenons that control the dielectric losses. The power factor depends on the voltage applied as well, that is, of electric field gradient and the phenomenons which activate by voltage. Therefore, in order to compare different tests, it is necessary to take into account these phenomenons, having at least applied voltage near.

It can be assumed that the values records for power factor are also associate with the presence of voids in the insulation. This phenomenon is the base for the power factor tip-up test.

Power Factor Tip-Up

The Power factor Tip-up test is used to evaluate the number of voids in the insulation, as well as the influence of losses for ionization by slot discharge and corona. The test

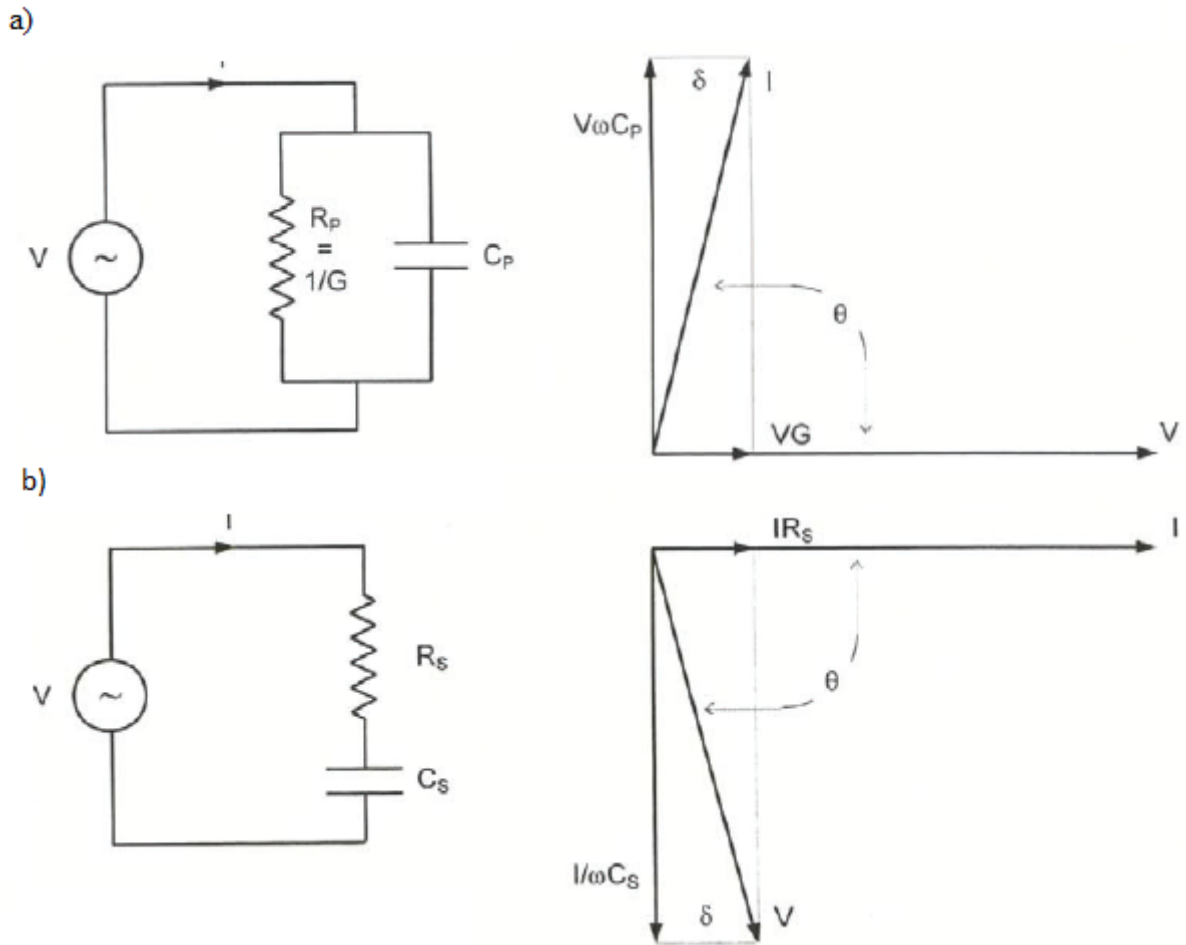


Figure 33 – Models for dielectric losses : a) Parallel model b) Series model [17]

is based on physical considerations that state the internal (voids) and external (corona) ionization phenomena are voltage-dependent. Equation 2.18 expressed this idea.

$$P_I = A_1 f(U - U_o) \quad (2.18)$$

where: $A_1 = \text{Constant}$

$U_0 = \text{Ionization Onset voltage}$

$f = \text{frequency}$

$U = \text{Applied Voltage}$

In this way, it is possible to obtain a rising curve by the measures values for the insulation power factor under different voltage conditions. Fast variation in the insulation power factor, as shown in figure 34, indicates a large number of voids in the insulation or elevate electrical activity that can lead to a failure involving the stator winding and the grounded core.

In practice, the power factor tip-up test is a performed under a voltage of 25% and

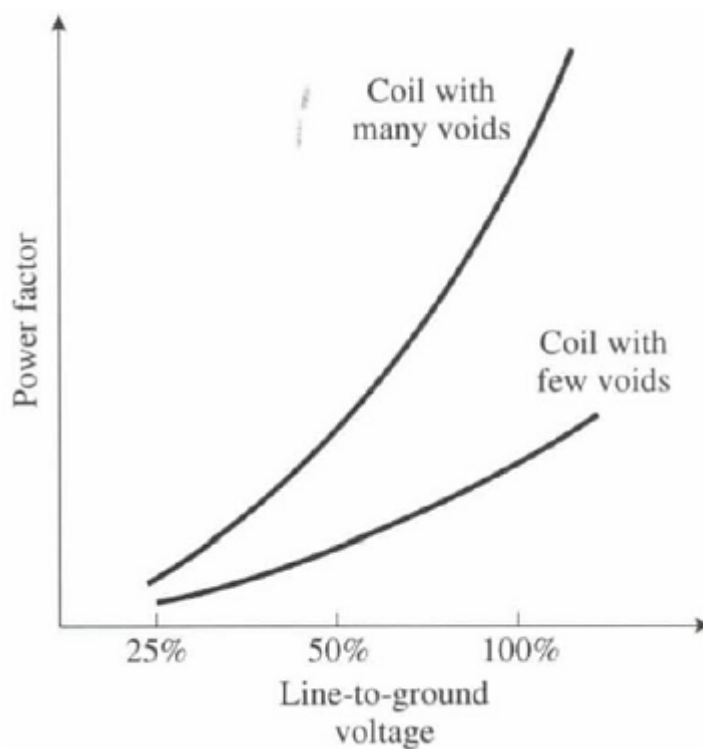


Figure 34 – Typical correlation between insulation Power Factor and applied Voltage

100% the phase to ground rated voltage. Thus, the tip-up value is the difference between the measures for high and low energy.

The tip-up test is widely applied for the rotating machine manufacturers. They performed the test in the individual coils to check the presence of a problem in the manufacturing process that results in a significant volume of voids in the insulation. The test is executed in individual coils, since the application of the test in an entire phase may overlap the effects.

Partial discharges

The PD test evaluates the electrical activity internal to the insulation. Thus, it might be a good indicator of the number and size of voids in the insulation system. In addition to the tip-up, power fact, and other test methods, the partial discharges can be measure by the acquisition of high-frequency pulses, generated by the PD phenomena. There are many methods to measure PD. However, the technique using coupling capacitors has the most use. This method allows measure discharges in the entire winding or in one phase per time. Then, to evaluate the discharges manifest in a winding section, it is necessary to disconnect this part form the machine.

In general, the methods that allow the PD detection or evaluation in a winding section are based on electromagnetic or sonic probes. The partial discharges test is further discussed at IEEE Std 1434-2014 [65]. The test is performed from voltages lower than

partial discharges inception voltage until the machine rated voltage. This test provides results that can be used as an indicator of the winding health stage. It is also useful for compare the deterioration level between the coils under higher electrical stress and others, such as the coils close to the grounded core, submitted to a lower electrical stress level. This comparison is beneficial to determine to switch the direction of the coils, a low-cost strategy that can provide a more extended machine useful life.

The partial discharges signals in the insulation voids tend to be masked by strong signals from slot discharges. However, theses phenomenons present different frequencies. The partial discharges signals are in the MHz frequency band. On the other hand, slot discharges are in the kHz frequency band. Then, by adjusting the suitable frequency band is possible to differentiate and qualify the phenomena.

3 Theoretical Basis of the Methodology

After a further literature review, it was observed that the stator insulation is submitted to four principal stress during operation: Electrical; Mechanical; Thermal; Ambiental. These are the primary stresses that cause insulation aging.

Aging is an irreversible and slow process that degrades the insulation over the years. However, aging is not an aggressive process that leads to failures at an unexpected time. Aging cannot be slowed or avoided with proper maintenance activities.

The combined action of these stress along the time can trigger failure mechanisms. Installation and manufacture problems can also facilitate the emergence of failure mechanisms.

It is essential to understand each type of stress. Section 3.1 discusses each of the TEAM aging stress [66].

It is also important to enumerate all fault mechanisms incident on hydro generators, their causes, forms to diagnostic, and quantify their deterioration over time. Section 3.2 deals with the stator failure mechanisms.

Section 3.3 presents the diagnostic test widely in this thesis to evaluate the insulation condition, the partial discharges test. Finally, section 3.4 introduces the tool used in the proposed methodology for data storage and management.

Nevertheless, the base of the methodology of this thesis is present here. Better understand this chapter helps to understand the method used for estimating the remaining useful life of hydro generators.

3.1 Aging Stress

The operating condition of a generator is related to the rate of insulation deterioration. Measures condition variables, such as voltage, current, power energy, winding's temperature, a vibration of the stator bars/winding, provide information about the operation condition of a given generator. Every condition variable is associated with one aging mechanism, for example, voltage with electrical stress, and the temperature of windings with thermal stress.

It is important to note that aging stress can be continuous over time, or transient where is present just for a brief moment. Operation voltage, the temperature of windings, environmental conditions, among others, represents continuous stress [57]. For this type of stress, the operation life is proportional to the time of exposure to stress. Temperature

variation during a load rejection, machine start/stop, transient voltages, represents transient stress. In the case transient stress is predominant in a machine, its life is proportional to the numbers of transients.

The TEAM aging stress [66], or aging mechanism as known as well, represents the most damage stress that regular operation imposes on the generators. Thermal, Electrical, Ambient, and Mechanical stress represents TEAM stress. They are the principal aging stress that affects the isolation system and causes aging by a natural, irreversible, and slow process of degradation. The next sections give special attention to TEAM stress.

3.1.1 Thermal Stress

Thermal stress is one of the most recognized causes of insulation degradation. The windings temperatures are responsible for thermal stress. The heat is generated by the joule effect through the circulation of current in the copper conductors. As a result, the stator winding temperature strongly depends on the machine load. Chemical oxidation reactions govern the thermal aging process of the insulation system in air-cooled machines. Like many chemical reactions, enough level of energy is necessary for activation. Then, there is thermal aging just above a threshold, which is determinate by the insulation material.

The thermal aging is related to useful life by a simple's law, the Arrhenius rate law, depicted in by equation 2.14.

The equation works above a threshold where there is thermal aging. Equation 2.14 is described as:

- For every increase of 10 Celsius in the winding temperature, the useful life by thermal stress decreases by half.

The equation 2.14 is valid only if a single chemical reaction controls the insulation failure [64].

Thermal stress is responsible for setting up many deterioration processes. For example, high temperatures in the windings can cause the delamination of the insulation system. Thus, intense partial discharge in isolation may manifest, causes severe degradation, and leads to an insulation breakdown.

A variation of thermal stress is well known like as Thermomechanical stress. Due to load cycles, the windings temperatures vary. Since the stator winding is mainly composed of a conductor made by copper and insulation made in most of the cases by epoxy mica or asphalt, in the presence of thermal variation affecting the windings, expansion, and contraction forces will be present. This phenomenon is cause due to the difference between the coefficient of thermal expansion of the winding materials. Because of this phenomenon,

the thermal cycle represents another deterioration process present in generators that have constant starts/stops and load cycles in their operation.

Intermittent operation is more present in the generation nowadays because of the liberalization of the power market [67]. The transition from mostly continuous operation of generators to more frequent starts and stops, known as intermittent operation, intensified the deterioration by thermomechanical Stress. It represents a column deterioration mechanism and one of the most damaging to the isolation system. To better understand, after many load cycles, possibly exist loss of bond between the ground wall insulation and the copper, leading to the presence of air voids between these layers, and, consequently, intense local partial discharges active.

3.1.2 Electrical Stress

The electrical aging is present only in generator rated above 6,9 kV. This fact is due to electrical aging manifest manly by the phenomenon of PD. As happens with thermal aging, electrical aging is present just above a threshold when PD is manifested. PD is small electrical sparks in air voids present in the insulation when the local electrical field is above $3 \times 10^6 \text{ V/m}$, *sufficient level to air dielectric rupture*.

Using accelerated aging tests is possible to quantify the insulation deterioration over time by exposure to the electric field. Thus, when partial discharges are present, the equation 3.1 is used to describe the relationship between lifetime and electrical stress:

$$L = a.e^{(bE)} \quad (3.1)$$

Where:

- a and b are constants.
- E is the electric field in V/m

Modern's isolation systems such as mica and polyester are very resistant to partial discharges. In most cases, electrical aging is not associated with insulation degradation. Although, the transients overvoltages are the final cause of isolation breakdown.

Usually, other aging stress causes loss of the isolation properties in such a way that even small overvoltages can lead to a generator failure.

3.1.3 Ambient Stress

The ambient stress refers to the environmental conditions that surround the generator, and the following factors may contribute to insulation degradation [68]:

- Moisture condensed on the windings

- Oil from the bearings or seal oil system in hydrogen-cooled machines
- High humidity
- Aggressive chemicals
- Abrasive particles in the cooling air or hydrogen
- Particles from brake shoe wear (if fitted) or carbon brush wear (if fitted) within the machine
- Dirt and debris brought into the machine from the environment, such as insects, fly ash, coal dust, and powders that are by-products of associated industrial processes (cement, pulp, chemical residues, etc.)

Many environmental factors can affect insulation useful life. However, none environmental factor by itself causes insulation deterioration. It is necessary a combination with another aging stress. For example, the rated voltage causes electrical stress that should not be harmful to the insulation system. However, in the presence of a high level of humidity, surface tracking can manifest.

Surface tracking is a failure mode that causes acute deterioration of insulation and leads to isolation breakdown quickly. In summary, a high level of humidity affects insulation conductivity, and the combination with the electrical field generates a failure mode. In general, environmental stress change some critical properties of the insulation materials became them weak to other stress.

3.1.4 Mechanics Stress

Mechanics stress affects the electrical machine in three different ways. One of these mechanics stresses touches the rotor windings, caused by the high centrifugal force. As reported in chapter 1, the objective is to focus on stator insulation problems. There are two types left for mechanical stress affecting the stator winding. The circulation of AC currents in the stator induces electromagnetic force causing oscillation with twice the AC frequency in the winding. To avoid problems, it is necessary suitable installation the bars/coils in the slots. Otherwise, the vibration may cause surface isolation damage by abrasion in the stator core. The abrasion of bars/coils represents one of the leading causes of premature failure of high voltage rotating machines [69]. The vibration of bars/coils are the cause of many failure modes, such as corona discharges, loose bars in the slot, and others.

As exhibit in the equation 3.2, the magnetic induced forces are proportional to the squared of the electrical currents:

$$F_{mag} = k_1 I^2 / d, \quad (3.2)$$

Where;

F_{mag} : Magnetic induced forces, expressed in kN of force acting per meter length (kN/m) of the coil/bar in the slot

k_1 : *Constant*

I : Current through the bar/coil

d : Width of the stator slot

The other mechanical stress is due to the magnetic forces as well, but it is associated with transients in the electrical current. Out-of phase synchronization, generators' start/stoop, and other transients that can give rise to AC currents five times or higher than the normal operating current. As can be observed at 3.2, the magnetic force varies with the square of the current. It can reach 25 times the regular operating forces during transients in the electric current.

The other mechanical stress is due to the magnetic forces as well, but it is associated with transients in electrical current in the stator windings. Out-of phase synchronization, generators' start/stoop, and other transients that can give rise to AC currents up to five times greater than the normal. As can be observed in equation 3.2, the magnetic force varies with the square of the current, then, magnetic forces value 25 times more potent than usual can be present during transients in the electric current.

Magnetic force is responsible for both types of mechanical stress. Continuous mechanical stress, present during regular operation and transient mechanical stress present just to a brief time and under a specified condition.

There is no model well applied and accepted considering mechanical stress to predict the lifetime of the machine, such as the models for thermal and electrical stress. Researches are using a mechanical aging test, in a try to come up with a good model for a mechanical lifetime, as well as evaluate the machine and the isolation damage through the time. Nevertheless, there is no standard about accelerated aging tests using mechanical stress. The coil/bars oscillation has a little damage at stator insulation, and consequently, low impact in their lifetime.

The coils/bars vibration plus abrasion in a surface (stator core), results in acute deterioration of stator bars/coils. It is a failure mode and only occurs under certain circumstances. There are many root causes for this problem, such as contamination, weak bars/coils installation, corona discharges, and others. That makes mechanical stress important to insulation lifetime estimation.

3.1.5 Multiple Stress

Multiple stress simulates the aging process affecting the machine during operation. It is easy to understand why Multiple stress is essential. Since generators are under multiple stress during regular operation, an accelerated aging test with the simultaneous action of multiple stress more accurately represents machine aging.

Applying single stress does not reproduce the rate of deterioration of a real machine in operation. Many authors support the theory that simultaneous multiple stress aging has a different deterioration rate than sequential multiple stress aging.

When the intensity of particular stress under a test is above the regular condition operation, this stress is acting as accelerated aging stress. Multiple stress tests can have many accelerated aging stress or just singular accelerated aging stress with the presence of other stress at a reasonable level.

It is difficult to analyze data from aging tests with multiple accelerated aging stress. The approach adopted is to perform multiple stress tests with only one accelerated aging stress.

3.2 Stator Failure Mechanism

This section list the main mechanisms that cause deterioration of stator windings over time. The list contains aging and failure mechanisms, their symptoms and possible reasons. It only discusses the failure mechanism in form-wound stators, because the hydro generators are the focus of this thesis.

Since the goal is the mechanisms that cause a gradual deterioration of stator bars, it excludes the failure mechanisms that rapidly cause failures events, such as out of phase synchronization, incorrect winding connection, among others.

Thermal Deterioration

An oxidation chemical reaction governs thermal deterioration. Thus, the higher is the temperature, the faster is the deterioration. For hydro generators, the oxidation process leads to loss of the adhesive characteristics of the insulation, causing delamination, and insulation color change. There is no thermal deterioration below a threshold. For the modern insulation system, such as mica and polyester, this threshold is around 110 °C. For old machines insulation class B with asphalt as a component, the limit is about 70 °C, and the operation above this level has an aggravating factor. The asphalt is a component that becomes soft at this temperature level. The cause of thermal deterioration has many reasons: inadequate operation, overload, weak cooling system, unbalance of voltages, harmonics, and others.

Thermal Cycle Deterioration

Insulation system delamination is mainly caused by the thermal cycle. That happens because of the different coefficients of copper and insulation expansion, causing thermomechanical forces inside the stator winding. The consequence is delamination and voids formation, mainly in the interface between the copper conductors and the ground wall insulation. Starts and stop of generators and load cycles are operations procedures that can lead to thermal cycle deterioration. Visual inspection signals for the thermal cycle include puffy insulation, and a hollow sound when tapped (Hammer test). The partial discharge analysis also can identify discharges between copper and ground wall insulation due to delamination. Another diagnostic test helpful for the identification of thermal cycle deterioration is the power factor tip-up.

Inadequate Resin Impregnation

Insufficient resin impregnation affects the insulation system's thermal conductivity. Thermal deterioration and vibration can be observed in the stator coils at different levels depending on the quality of the impregnation. Both thermal degradation and vibration lead to abrasion of the stator coils surface, and this scenario is very critical to the insulation lifetime. Improper impregnation also results in voids in the ground wall insulation and partial discharges, which degrades the insulation and consequently can cause failures events. The degradation process by PD activity is prolonged and takes a long time to lead to machine failure.

In general, improper manufacturing procedures leads to inadequate resin impregnation. It is possible to make a list of the leading cause of this failure mechanism in rotating machines, such as improper resin viscosity, chemical contamination during the manufacturing, improper preheat, and other problems in the manufacturing procedures. The PD test can diagnose this deterioration process, as well as a tip-up test. It is difficult to find any clue of inadequate resin impregnation by visual inspection.

Semi-Conductive Coating Problems

The semi-conductive coating, also called stress relief coating, provides to the surface of the coils a conductive layer important to prevent PD. Since space between the bar surface and core are tiny, machines rated above 6 kV would inevitably have PD in these spaces if there is no semiconductor layer.

The cases of problems on semi-conductive coating is related to poor manufacturing processes. It is necessary to make the coating layer and testing it to ensure that it has the appropriate resistance. Since the manufacturing process is weak, the semi-conductive coating will present a high resistance. As a consequence, slot discharges manifest during

machine operation. The intense PD activity deteriorates the semi-conductive layer and the ground wall insulation that can lead to a phase-ground fault in the machine.

In the air-cooled machine, slot discharges will yield ozone, a very reactive component, that can lead to faster deterioration, and machine failure. Visual inspections that indicate the presence of a white powder is indicative of ozone. The PD test can detect slot discharges. Since the slot discharges and white powder is also symptoms of the loose bar in the slot, an additional factor is a need for diagnostic problems in the semi-conductive coating. The failure mechanism loose bar in the slot is dependent on the machine load, and semi-conductive coating problems is not.

Loose Coils in the Slot

Circulation of electrical currents through the windings induces magnetic forces that cause their oscillation. If the coils are not tight enough, they become loose in the slot. This may result in abrasion of insulation surface on the metallic parts of the stator core. The abrasion will generate friction of the semi-conductive coating and, consequently, in the ground wall insulation. The deterioration of this coating leads to intense slot discharge, which accelerates the degradation process. This failure mechanism leads to insulation breakdown in a short time since it is very harmful to the insulation.

The identification of loose coils in the slot can be by PD test, with the identification of slot discharges and noticing the strong relationship between discharges intensity and the machine load. As the coils are loose in the slot, the higher is the machine load, the higher will be the magnetic forces that cause the vibration of the coils. Visual inspection signals such as the presence of ozone in air-cooled machines, the powder produced by abrasion, and greasing (in case of oil contamination) are indications of this failure mechanism. A resistive test of the semi-conductive coating will indicate a high resistance.

Semi Conductive/ Grading Coating Overlap Failure

The hydro-generator present a silicon carbide coating above the semiconductive coating in the stator windings, only in some centimeters outside the slot, as shown in Figure 35. As the electrical field is intense in this region, the silicon carbide has an attractive electrical property that perfect fit for this region: the higher is the electric field, the lower is its resistance. That factor avoids problems around this region with PD and deterioration.

An overlap between the silicon carbide coating and the semiconductive coating is responsible for ground the silicon carbide coating. The root cause of this failure mechanism is problems in the overlap, mainly by poor connections. As a result, a high-level voltage is present on silicon carbide coating and discharges between this part and the semiconductive

coating (at 0 V) manifest. It is unlikely these discharges lead to machine failure. But they present a high magnitude. By visual inspection, it is easy to detect a white band in the overlap position at high voltage coils/bars. PD tests also can identify this failure mechanism.

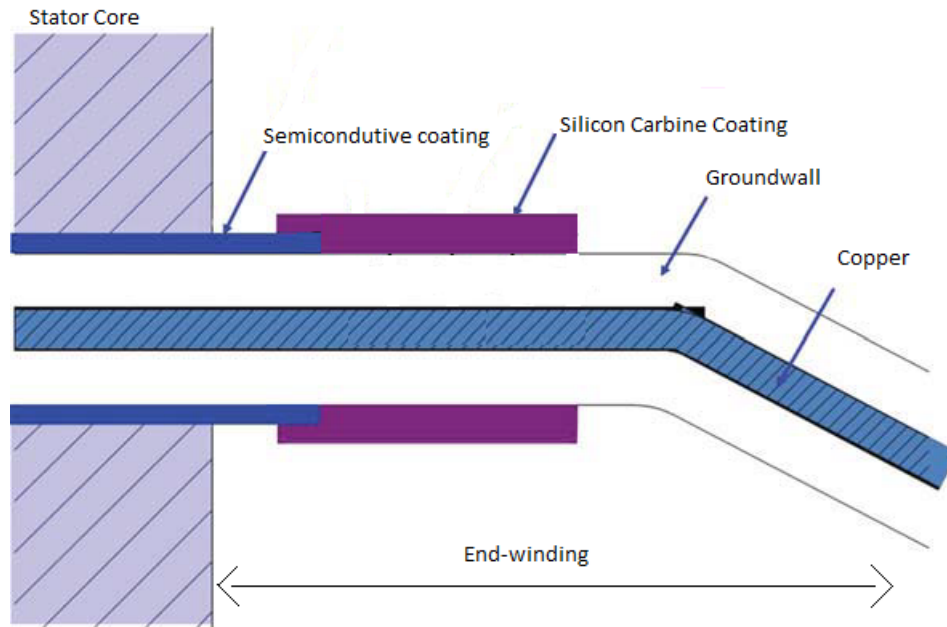


Figure 35 – End-winding Region [18]

High Intensity Slot Discharges

High-intensity slot discharges is a failure mechanism similar to loose bar in the slot. Although slot discharges are symptoms of other problems such as the loose bar in the slot and semiconductive coating failure, the root cause is different. Hydro generators develop intense slot discharge activity when there is inappropriate manufacture for the supports system of the slots. Slot discharges are also present in machines with a weak grounding system for the semiconductive coating.

This failure mechanism leads to machine failure in a short time. Since it is very harmful to the insulation system, it is quickly necessary the diagnostic of the problem. The symptoms include high levels of slot discharges, usually higher than 98% of similar machines. Visual inspections present signs of burning and pitting, present at coils/bars at high-level voltage, and white powder, due to discharges. The partial discharges test can also detect slot discharges activity. Unlike to loose bar in the slot, which also presents slot discharges, this failure mechanism does not depend on machine load.

Transient Voltage Surges

Voltage surges is an atypical failure mechanism. It either causes the insulation breakdown immediately or has no lasting effect. It is well known that voltage surges are the final cause of insulation failure, and this failure mechanism does not gradually deteriorate the insulation. The insulation deterioration is governed by any other aging or failure mechanism, which degrades the insulation system and reduces its electric strength.

The voltage surge in the stator windings briefly increases the electrical stress above the rated condition. The cause of such voltage transients is mainly due to transients in the power systems. Lightning, faults in the power system, motor circuit breaker closing/opening, out-of-phase generators, are examples of events that cause voltage surges.

Since it is not possible to avoid voltage surges, it is necessary to design the insulation system of stator windings that withstand these voltage transients. Because of that, all the stator windings have to be submitted to the AC hi-pot test, where the stator bars are under twice the rated voltage plus 1 kV during the test. It is also widely used equipment to generator protection from high transient voltages, such as surge arresters and capacitors.

Electrical Tracking

Electrical tracking is a failure mechanism that combines electrical and environmental stress present in the stator windings due to the electrical field and the contamination. The contaminated insulation surface of the stator becomes conductive, allowing the circulation of electrical current. The presence of electrical current in the insulation surface causes degradation and can lead to failures. In cases where the failure mechanism is intense, it is possible to observe tracking, that is, the formation of ways where the electric current circulates.

The cause of electrical tracking in form-wound stators is due to the presence of partly conductive contamination in the end-winding region. Dirt, insects, plant by-products, among other elements, contaminate the generator. The partly conductive formation, in the insulation surface, occurs when these elements mix with moisture or oil, forming a conductive coating on the insulation surface. It is a failure mechanism often present in high voltage generators, and the process until fail leads many years or decades.

Abrasive Particles

Abrasive particles are a failure mechanism that combines particles, such as sand, glass fibers, and fly, with high velocity. As a result, the collision of these particles with the stator winding causes deterioration and damage to the insulation. These particles are capable of grinding the insulation, especially in the end winding region. The root cause

of this deterioration process is the presence of abrasive particles in the cooling system. For example, in air-cooling generators, the ventilation to cooling the stator windings, also lead these particles to high velocity. As a result, the abrasive particles will abrade the insulation because of the energy of their motion. This failure mechanism is most likely to occur on open-ventilates machines [18]. The inadequate maintenance of the filters of the cooling system, which are supposed to block these particles, speed up the degradation. In severe cases, the deterioration can disintegrate the groundwall insulation, getting the copper exposed. Visual inspection can easily detect this failure mechanisms, observing signs of abrasion of the stator end-winding. In the early stages, no diagnostic test can detect this failure mechanism.

Chemical Attack

Chemical Attack is another failure mechanism that involves environmental contamination, as electrical tracking and abrasive particles. That is, environmental stress is the cause of all these failures mechanism. Chemical Attack occurs when the insulation is contaminated by chemical substances present in the local environment, such as acids, paints, solvents, oil, and moisture. The process of clear the stator winding use material that also causes the chemical attack. For example, high-pressure water, commonly used to clear winding, can be absorbed by old insulation made of asphalt mica.

The consequence of a chemical attack depends on the insulation material and the chemical element. In general, the old insulation system is prone to softening, swelling, and loos of mechanical and electrical strength under chemical attack. All the effects mean insulation deterioration. For example, the loss of mechanical and electrical strength, lead the insulation to no longer hold some high voltages surge or transient mechanical forces that eventually occur during operation.

The modern insulation system is more resistant to chemical attack. However, epoxy insulation might degrade under a long time of contact with water or oil.

Visual inspection is the best way to diagnose this failure mechanism. Loss of color and puffy insulation are sings of a chemical attack. Chemical analysis of insulation samples also can detect the problem. It is complicated to find signals of this problem by diagnostic tests. Insulation resistance and polarization index test are the more efficient test to detect chemical attacks.

Inadequate End Winding Spacing

If there is inadequate space between adjacent coils in the end-winding, the generators rated above 6 kV can develop PD. The discharges usually occur between the coils, causing insulation degradation and ozone formation. Since ozone generates nitric acid,

the deterioration is not only caused by partial discharge, but also by the ozone. Both may lead the generator to phase-to-phase or phase-to-ground failures. However, this is a slow process that can take ten years or even more. PD in different locations, such as circuit ring buses, and coil connection insulation can also occur if that space is too small.

Visual inspection easily identifies the presence of ozone in the end-winding region, by signals of a white powder. PD test can also provide the diagnostic of this failure mechanism, as well as the blackout tests. Poor machine design and manufacture are the root cause of this failure mechanism.

End Winding Vibration

The magnetically induced forces, early present at 3.2, cause winding vibration. In case of inadequate support in the end winding region, the insulation may abrade over time. This failure mechanism is more likely to occur in machines that present long end windings, such as the turbo generator. Then, end winding vibration is not common in the hydro generators. Since the focus is hydro generators, no further details about this failure mechanics will be present.

Poor Electrical connection

A given generator has many electrical connections in the stator, especially the hydro generators. If the resistance of the connections is very high, thought circulation of the current the joints will reach elevated temperatures, causing acute thermal deterioration, and in severe cases, failures. As the thermal deterioration of the connections increases, the tendency is their resistance increase as well, further aggravating the problem. For example, the copper can melt, resulting in machine failures due to elevated temperatures around the joints. Moreover, the high temperature in the connection causes intense insulation degradation. Eventually, the deteriorated insulation over the connections can crack due to possible current surges. In this scenario, the risk of failure with copper exposed is very high.

Due to the number of connections in the stator, the form-wound machines are more likely to present this failure mechanism. Signals of discolored insulation are symptoms of a poor connection. This signal is usually apparent in the connections under the risk of failures. The insulation also cracks easily. An excellent alternative to detect this failure mechanism is using infrared imaging cameras and monitoring hot points over time. The root cause of overheat is due to poor brazing, poor soldering, or inadequately tightened or designed bolted connections [18].

3.3 Diagnostic Test

After the presentation of all aging stress and failure mechanisms that are incidents in the stator windings, the basis of physical and chemical phenomena to the estimation of the remaining useful life is exposed.

It is possible to observe in many failures mechanism changes in the electrical and physical proprieties of the insulation as deterioration reaches a critical condition. The monitoring of these proprieties over machine aging can provide valuable information about machine current health state, possibles pre-failure conditions, and trends to failure. These are the information we are looking for, and they are the key to the success of this work.

By the acquisition of variables such as the temperature of the windings, voltage, currents, resistance, and environmental conditions, it is possible to access the insulation operation conditions. By diagnostics tests, such as partial discharges, power factor tip-up, insulation resistance, among others, it is possible to monitor the electrical properties of the insulation system. Among the diagnostic test, the partial discharges test it is cleary the best. The test are able to detect many failure mechanisms and provides information about the health status of the insulation. It is widely used for monitoring the stator condition. It is also possible to measure the partial discharges under machine operation, being able to track the partial discharges trend over a machine lifetime. This feature makes the test perfect fit in our proposal: monitorization of variables to have information about the insulation health state, detection of pre-failure conditions, possibles trends, and change of pattern.

3.3.1 PD Measurements Systems

The application of PD measurements to monitoring the condition of the stator insulation has more than forty years. The diagnostic test is the most qualified to verify the hydro generators' windings condition. Assuming the isolation system of the stator is the weakest part of the machine, the PD test is an essential tool for developing maintenance strategy, avoiding unexpected failures, and increasing the reliability of the system.

Any failure process that creates PD as a symptom of insulation aging can be detected with PD measurements [18]. There are many methods of PD detection. They have as a base the physical characteristics in the occurrence of PD. For example, the partial discharges generate electric impulse currents, dielectric loss, light, sound, chemical reaction, gas pressure rise, and phenomenons. The methods for partial discharges detection works through the identification of these phenomena.

For on-line and off-line PD test in the synchronous machines, the most applied method for measuring partial discharge has as base the electric impulse generated during

the PD phenomenon. This method detects the high-frequency pulse of current generated by the PD. The current typically will capacitively couple from the voids to the copper, travel along the coils conductors [18]. Because of the surge impedance of the coils, the voltage pulse will also manifest. The electrical current generated by the PD pulse has a full frequency band, and it may reach up to hundreds of megahertz depending on the discharge location.

The pulse duration is concise. Since the electrons travel through the small voids in the speed of the light during a PD occurrence, the pulse has nanoseconds. The movements of these electrons that generate the electrical current. The positive ions also move during a PD phenomenon. However, these particles are massive, and their movements are prolonged compared to the electrons. Theoretically, the positive ions contribute a portion of the current generated by the PD, but because of its speed, they are neglected.

Then, to provide accurate PD measurement, suitable sensors have to detect high-frequency pulses of current, as the coupling capacitors widely applied in on-line and off-line PD tests.

On- line partial discharges test

On-line partial discharge tests are performed with machines under regular operation. The great advantage of this test is PD acquisition with all the operation stress present. Hence, it is possible to perform diagnostic of many failure mechanisms by partial discharges analysis.

On-line partial discharges test is performed in the entire stator with at least two coupling capacitors per phase. It is required a *PDA (Partial Discharge Analysis)* instrument or oscilloscope with a wide frequency band detection connected to the coupling capacitor through suitable cables for data acquisition. There are many possible configurations. The most used configuration is depicted in figure 36, with two coupling capacitors per phase and noise elimination by time delay.

The connection between machine and electrical systems during the test allows different types of noises, such as lighting, harmonics, machine vibration, to affect the measurements. Indeed, these characteristics are the main disadvantage of this test. Thus, it is important to provide noise reduction to avoid false positives.

Off-Line partial discharges test

Off-line partial discharges test is normalized and recently reviewed at IEEE std 1434 – 2014, where further details can be accessed. It is performed with the machine turned off, and an external source applied voltage in the stator bars/coils under test. The application

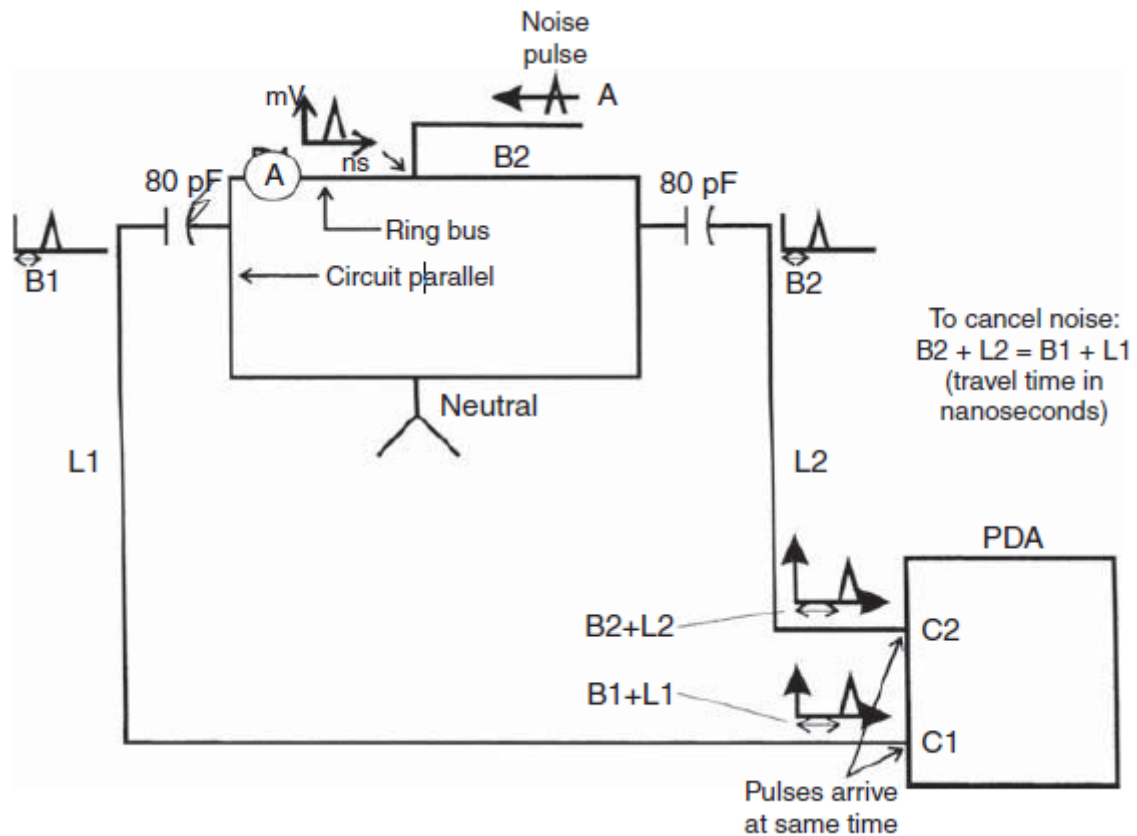


Figure 36 – Detection method using differential time of two-way signals [18]

of voltage is by an external source. The test execution is usually by one phase per time. The test can also be performed in individual coils/bars before the machine installation.

The measures of partial discharges are through coupling capacitors connected in the higher potential of the stator bar/coils. The purpose of the test is for quality control at the manufacturing stage. It is also applied as a maintenance tool with the machine already in operating. Figure 37 shows a configuration usually apply to off-line partial discharges detection.

Figure 38 show the electrical circuit that models the detection method for off-line PD measure.

The main advantages of this test are the possibility of control the applied voltage and the reduced amount of noise involved in this test. The possibility to control the voltage during the test enables the identification of the partial discharge inception and extinction voltages. The variables can be useful to the determination of the insulation condition, as well as prognostics of a lifetime. Since this test is performed with machine short-down and disconnected from the electrical systems, the reduced amount of noise is a significant advantage comparing to the on-line partial discharge test.

The off-line partial discharges test cannot simulate all the stress existing in the

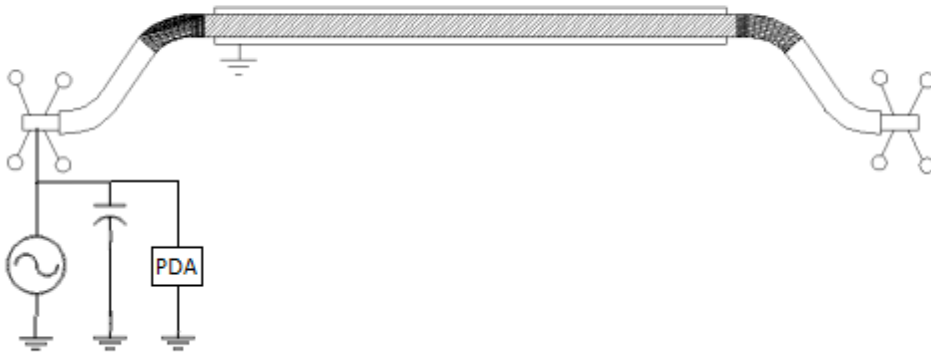


Figure 37 – Detection method for off-line partial discharges measures

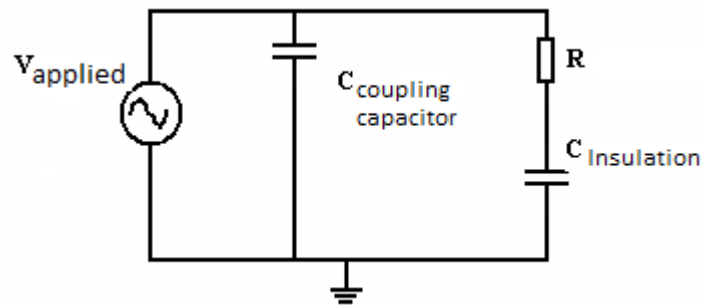


Figure 38 – Equivalent circuit to Detection for off-line partial discharges measures

machine under regular operation. Moreover, slot discharges and phase-to-phase discharges do not occur in this test. Consequently, it is impossible to perform diagnostics of failure mechanisms using only off-line partial discharges test results.

Coupling capacitor

The coupling capacitor is connected to the high voltage side to detect high-frequency current. The impedance of the coupling capacitor is very low for the high-frequency PD pulses, attracting them. On the other hand, the coupling capacitor works like an open circuit for signals with low frequency, blocking them. It is the most common sensor for PD data collection. Usually, the capacitance are from 80 pF to 10000 pF, according to standards [70].

Detection

Since most PD instruments are sensitive to voltage, it is necessary to convert the PD current signal into a voltage signal. Then a simple resistor can be used to convert

current signals into measurements in mV accurately. There are also more sophisticated mechanisms for the conversion, using an RLC converter. Though this equipment, it is possible to control the input signal and manipulate the output voltage to represent proportionally and adequately the PD pulse.

The charge involved in a PD can be easily calculated. For example, considering the configuration of figure 37, the obtention of the charge involved in the PD phenomena is possible by the application of equation 3.3.

$$Q = C_{ins} \cdot V \quad (3.3)$$

where:

Q : Charge

C_{ins} : Insulation Capacitance

V : Voltage applied

Thought the equation 3.3 in the form of variation, we have the Equation 3.4

$$\Delta Q = C_{insulation} \cdot \Delta V \quad (3.4)$$

where:

ΔQ : Discharge (pC) or (nC)

ΔV : Voltage pulse (mV)

Then, it is possible to observe the PD phenomenal as the charge involved in the ionization of the gas, or as the electrical voltage pulse measured by the partial discharge instruments. That is why there is the representation of partial discharges magnitude in Coulomb (C) and Voltage (V).

Because PD pulse rise times may be in the nanosecond range at the injection site, the initial voltage wave has frequencies from the kilohertz to the gigahertz range [70]. The PD frequency varies with the size, volume, pressure, temperature of the voids, and many other factors. The discharges location, that is, internal voids, slot discharges, or winding discharges, also influence the PD frequency. However, the impedance of measurement circuits and components, such as the coupling capacitor, cables, stator winding, among others affects the bandwidth of the measurement. Equation 3.4 is the equation to obtain the charge involved in PD.

Instrumentation

It was common the use of an analog oscilloscope to measure and display the PD pulses and the phase-ground voltage in a visor. Most applications today use digital means, allowing a digital oscilloscope to provide the measurements and the graphics. That is a significant advance as the results now can be assessed for further analysis at any time. It is important to emphasize, the measurements of PD are in Coulomb. For this proposer, it is necessary the integration of the PD current signal. Moreover, the base of most of the PDA instrument is on pulse-peak detection, proving the magnitude, number of pulses, polarity, and the angle position. Other features such as frequency, shape, length typically are not explored. A vital tool developed with digital means and widely applied today is the *PMA (Pulse Magnitude Analysis)*. The PMA consists of two-dimension graphics with the magnitude versus the counting of pulses. Usually, the graphics display the positive and the negative pulses that make the analysis and identification of failure mechanism easier. Figure 39 shows an example of PMA graphic.

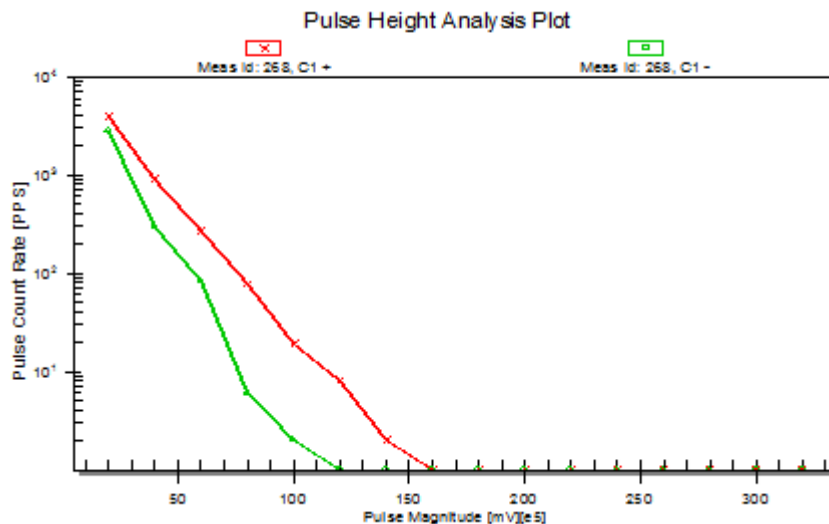


Figure 39 – PMA graphic extracted from an off-line partial discharge test at LAT-UNIFEI

Another essential tool is the *PPA (Phase Pulse Analysis)*. The PPA displays the pulse magnitude, the counting of pulses, and the phase angle in two or three dimension graphics. The recommendation is to use this tool or detecting the main isolation problems though recognizing the pattern of the PD. The two-dimension graphics are more applied for analysis, and, in this case, a color code represents the pulse count rate. Figure 40 shows an example of the PPA graphic.

Noise Separation

The contamination of partial discharge results can occur due to different types of noises such as corona, lightning, harmonics, next phase induction, and others. Nevertheless, the analysis of PD pulses can lead to false positives due to the presence of noise. In

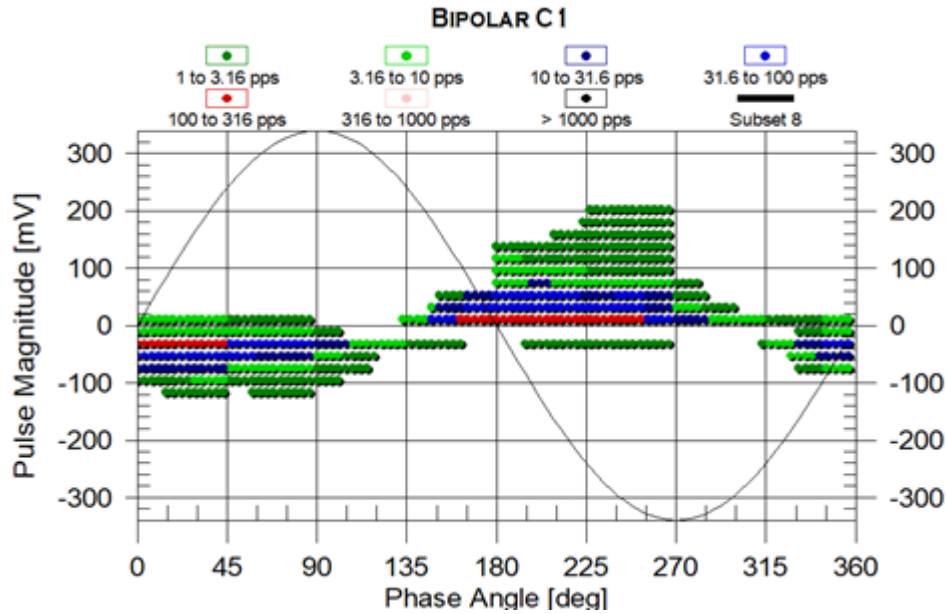


Figure 40 – PPA graphic extracted from an off-line partial discharge test at LAT-UNIFEI

that way, noise separation or de-noising is a necessary process that leads to more positive results, avoiding mistakes in the analysis. Unfortunately, the on-line PD test is subject to more noise than an off-line PD test. This is because the machine is under normal conditions and connected to the electrical system in the on-line PD test. For noise reduction proposes, there are some hardware methods applied. For example, the detection method using differential time of two-way signals: The application of this method and the elimination of noise occur by the time of flight. Figure 36 represents a scheme of this configuration method for noise separation.

The detection of PD signals by the coupling capacitors C1 and C2 have the same time delay ($T_{L1}=T_{L2}$). The detection of Noise by C1 and C2 have a different time delay. Then, the separation of PD and noise is possible by the arrangement by the elimination of signals with a different time delay ($T_{L1} \neq T_{L2}$)

The use of filters is a method for the reduction of noises in an off-line PD test. The filters installation between the sensors (coupling capacitor), and the PDA equipment provides elimination of noise by allowing the passage of only pulses in the typical frequency range of PD pulses.

Features for PD Analysis

The instrumentation process provides data to PD analysis. Thought this data, the evaluation of the insulation condition is possible to analyze. The identification of the main deterioration problem and a prognostic of the reaming useful life for the insulation can also by evaluate. It is present here the description of basics PD features. It is fundamental to understand these features for a better performance of diagnostic and prognostic thought

PD analysis. The measures using the coupling capacitor detect high-frequency current pulses generated by the PD phenomena. The factors' extraction from the high-frequency currents pulse results in the following variables widely find in PD analysis:

- **Apparent charge**

The apparent charge (Q) definition according to IEEE std 1434 is: Q of a PD pulse is that charge which, if injected within a very short time between the terminals of the test object in a specified circuit, would give the same reading on the measuring instrument as the PD current pulse itself. Q is not equal to the charge locally involve of a PD pulse, which it is not possible to measure for many reasons. Q is normally express in Picocolumbs (pC).

- **Partial discharge quantity**

Partial discharge quantity represents the charge of one pulse of PD express in terms of Q . The calculation of the electrical charge involve in one partial discharge by the PD instruments is made by the time integration of this current pulse. It is usually represented in Coulomb. The PD quantity is dependent on the size and volume of the voids that occur the phenomena. It is an excellent feature to evaluate the insulation condition.

- **Normalized Quantity Number**

Normalized Quantity Number (NQN) represents a quantity that is proportional to the total PD activity registered in a time interval. Figure 41 represents the calculation of NQN thought the normalized area under the straight-line curve. As shown in figure 41, the graphics represent the pulses per second detect by the instruments in a two-dimensional graphics: The magnitudes of the pulses in the horizontal axis and their respective rate of repetition on the vertical scale. The acquisition date of PD forms a correlation depicted by in a straight line fitted to the pulse counts in each magnitude window of a pulse height analysis. The area under this straight line represents the value of NQN . Positives values for NQN means the calculation for PD with positive polarity. Negative NQN values mean the calculation for PD pulses with negative polarity.

Equation 3.5 [71] is use to the calculation of NQN . The use of logarithms of pulses counts in the equation 3.5 reduces the contribution of pulses with high repetition rates, comparing to low repetition rate pulses.

$$NQN = \frac{FS}{G \cdot N} \cdot \left(\frac{\log_{10} P_1}{2} + \sum_{i=2}^{N-1} \log_{10} P_i + \frac{\log_{10} P_N}{2} \right) \quad (3.5)$$

Where

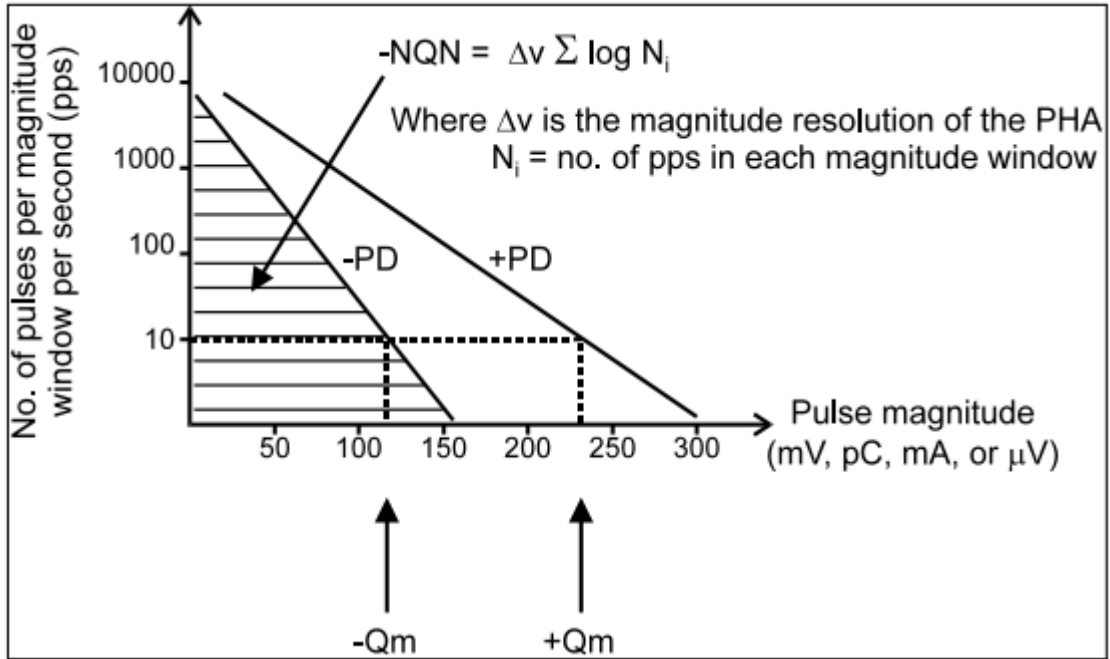


Figure 41 – Partial Discharges Quantity Calculation

P_i is number of pulses per second in magnitude window i ,

N is number of magnitude windows,

G is gain of the partial discharge detector,

FS is maximum magnitude window in millivolts at unity gain.

- **Largest repeatedly occurring PD magnitude (Q_m)**

There are several partial discharges with different values for Q per second. Q_m represents the higher valor of Q with a repetition rate of 10 pulses/second at least. Q_m obtention is also shown in figure 41. It is important to observe that pulses with higher magnitude are detected, but they do not reach the condition of at least ten pulses per second. In general Q_m is given in pC, mV, mA. The value of Q_m is associated with the condition of the insulation. The higher is Q_m , the higher is the insulation degradation. Typically, the insulation must have faults at a specific portion of the insulation system that has the most deterioration. As the magnitude of discharge is associated with the size and volume of the voids, Q_m gives the value of the most critical void/portion of the insulation. That is why this feature is critical to monitorization of the actual insulation condition.

- **Average Discharge current (It)**

It is the current generated by the PD pulses during a certain time interval. Equation

3.6 [65] show the calculation by the some of the absolute magnitudes of PD pulses:

$$I_t = \frac{\sum_{t_0}^{t_1} (Q_1 + Q_2) + \dots + Q_n}{t_1 - t_0} \quad (3.6)$$

Where:

I_t is the average discharge current, A

t_0 is the starting time, s

t_1 is the completion time, s

Q_1, Q_2, Q_n are apparent charges transferred in a partial discharge pulse 1 thorough n, C

- **Pulse repetition rate**

The number of pulses is also an important feature normally access by the PDA instruments. This variable represents the number of PD pulses that originated in a time interval. Generally, the number of pulses is represented per second.

The number of pulses strongly correlates with the number of insulation voids involved in partial discharges. If the number of pulses increases over time, probably the number of voids involved in partial discharges increases as well. This is a signal of insulation deterioration. The connections between the features the number of pulses and Q provide valuable information thought the representation of the number of pulses within ranges of Q.

- **Polarity**

A PD pulse can be classified according to its polarity as positive or negative. The pulse polarity is an important feature to localize the voids inside the slot. That is, it is important to diagnostic of the insulation problems. The factors can be represented according to their polarities: Q_+, Q_{m+} , and $NQN+$ represent the values for positives PD pulses; Q_-, Q_{m-} and $NQN-$ represent the values for negatives PD.

- **Position of the PD relative to the voltage phase to ground**

This feature represents the angle of PD pulse occurrence in the phase to ground voltage applied in the stator bar. It is also called angle position of PD. Equation 3.7 represents the phase angle.

$$\phi = 360 \cdot \frac{t_i}{T} \quad (3.7)$$

Where:

ϕ is the phase angle, degrees

t is the moment of the partial discharge occurrence, s

T is period of the voltage signal on the insulation, s

As pulses polarity, this feature is very useful to detect the main deterioration problem in the machine. That is, it is a feature to perform the diagnostic of the machine problem.

These are the basic features extract for PD analyses. It is important to note that these basic features are not sufficient for yielding good results in pattern recognition algorithm. Therefore, it is possible to derive many other features by statistical analyses of the basic features described upon [72]. Statistic functions such as mean value, standard deviation, Skewness, and Kurtosis are used to improve the results of pattern recognition algorithms.

Signal analysis interpretation

The diagnostic of the primary failure mechanism by PD is of high interest, considering that the PD measurements can be performed on-line without shut-off the machine. Moreover, many failure mechanisms that affect the generators have a pattern in the partial discharges, thus the identification of the issue can be performed.

The most useful tool for diagnosing the failure mechanism based on the PD pattern is the PPA. However, the identification by only PPA graphics is not easy. Then, the execution of other diagnostic tests or visual inspection provides more reliable results.

Often more than one failure mechanism is present. Thus, combining two or more PD patterns can cover the failure mechanism, bringing more damage to the machine. This fact is often responsible for false negatives and, consequently, unexpected failures.

The presence of noises is another problem that interferes with the diagnostic. Even though suitable filters, some particular kinds of noises are difficult to be eliminated [73]. Consequently, the experts have to know how to sort out these problems for making a precise diagnostic.

Other factors, such as the couple capacitors and the means of propagation, also provide changes in the PD measurements. The couple capacitors cause little attenuation to PD signals in low frequency. In the same way, the different means of propagation will generate different attenuation in the PD signals.

There are two means of propagation for PD [19]. The first one is through the circuit of the stator, and the second one is through the air. The predominance of the mean of propagation is dependent on the type of Discharge. For example, the propagation of the partial discharges in the internal voids is primarily through the circuit of the stator. Otherwise, the propagation of Discharges in the end-winding is mainly through the air.

It is possible to separate the discharges into four different types: Internal Discharges, Slot Discharges, End-winding Discharges, and Delamination Discharges. The identification of the kind of discharge by PDA analyses is the first step of a diagnostic.

Generally, each type of Discharge is associated with two or three failure mechanisms, and its identification is the second step of the analysis. When more than one failure mechanism is present, it is vital to identify the most damage to the machine, avoiding unexpected failures.

Internal discharges

Internal discharges occur in small voids present in the ground wall isolation of the stator bars. Applying Off-line partial discharges test, which is possible to control the applied voltage, the incipient voltage (CVI) for internal PD is about 6.0 kV. Consequently, this activity is always present in operating machines rated at 13.8 kV.

At normal levels, these discharges are not a problem, since mica, the primary material in modern's isolation systems, is very resistant to discharges. However, if these discharges occur at high levels, they would generate deterioration of the isolation system.

The characteristic of Internal partial discharges activity is the symmetry in the pulse polarity. Since both sides of the voids have the same material, the electrodes in both haft cycles are the same. As a result, the magnitude and the number of pulses have the same value for both polarities.

Figure 42 shows internal PD. Observation: The positives of PD pulses between 50 and 75 mV are probably are noises captured during the measurement.

Slot discharges

Slot discharges occur in the air gap between the side of the stator bar and the slot (or magnetic core). Unlike internal discharges, slot discharges usually are not presented in regular operation and are very damaging to the machine. The discharges initiate due to a resistive problem of the bars/coils, or erosion in the semi-conductive coating paint. This resistive problem is typically caused by an inappropriate resin impregnation or other manufacture problem. The erosion is a result of excessive vibration of the bars in the slot, generating abrasion between the bar's surface and the slot. The asymmetry of Slot Discharges activity is due to the presence of different electrodes. The positives discharges will be predominant, having a larger magnitude and number of pulses in the negative haft cycle. The triangular shape is another feature that is possible to observe in PPA. Figure 43 is a graphic of a typical slot discharge pattern.

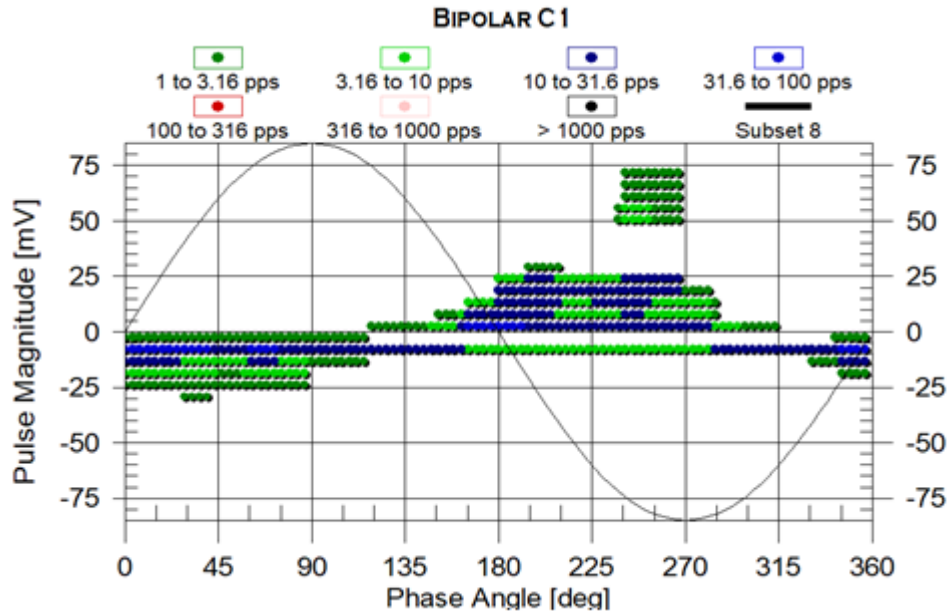


Figure 42 – PPA graphic extracted from an off-line partial discharge test at LAT-UNIFEI

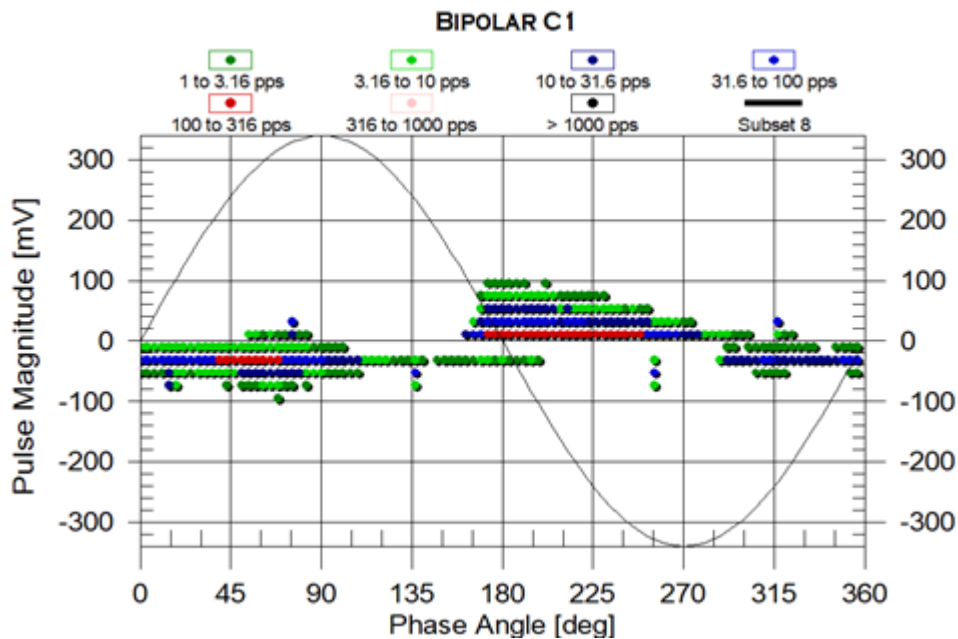


Figure 43 – PPA graphic extracted from the Hydro power plant Volta Grande CEMIG

End-winding Discharges

The end-winding is the portion of the stator localized out of the slot, being a region subject to different types of problems. The so-called end-winding discharges are the presence of electrical activity in this region, and many factors can initiate them. The contamination of the end-winding surface leads to end-winding discharges and, consequently, surface tracking. Another failure mechanism caused by end-winding discharges is the corona discharges, located at the junction of the semi-conductive coating and the grand paint area. The discharges between the surfaces of different generators' phases in

this region are also end-winding discharges. They usually occur due to inadequate air gap space between phases in the end-winding region.

The PD pattern for end-winding discharges is different for each type of failure mechanism. As a result, end-winding discharges assume three main types of PD partners. The first failure mechanism described, surface tracking has a PD pattern characterized by asymmetry in the pulse polarity—a few negative numbers of pulses with high magnitude in the positive half cycle. Typically, the phase angle of these high magnitude pulses is around 30° . Figure 44 depicts a typical pattern for surface tracking. The electrodes (semi-conductive counting and grand paint area) are responsible for the pulse polarity asymmetry with the predominance of positive pulses in number and magnitude for corona discharges. The patterns have the same features as slot discharges. Thus, the difference between them is only possible to detect by PPA graphics. The routed shape of corona discharges in PPA graphics is different from the slot discharges' triangular shape. Figure 45 shows a typical pattern corona for discharges.

The discharges between phases or bar to bar discharges are set up in the end-winding portion when the air gap is too small to support the phases' electric stress. Unlike other end-winding discharges, the PD pattern is symmetrical, and the magnitude of the pulses depends on both the level of voltage and the size of the air gap. That is, the electrical stress in the air gap between the bars. Figure 46 shows a typical pattern for discharge between phases.

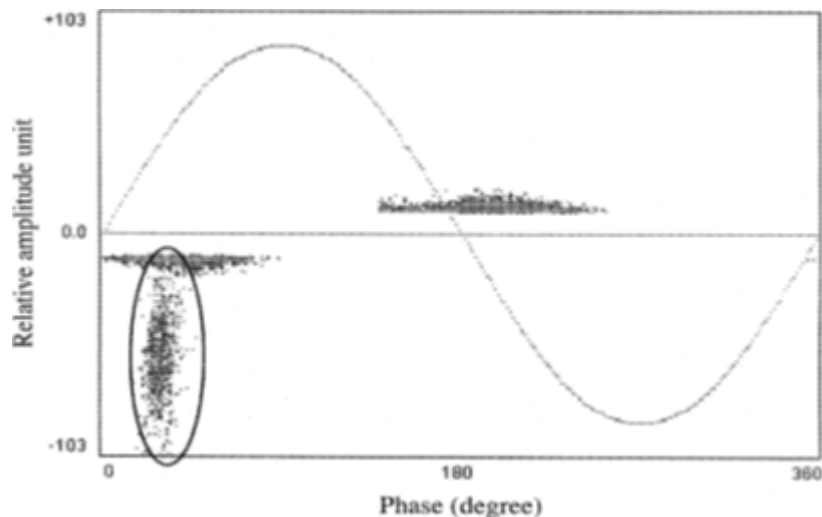


Figure 44 – PPA graphic-Typical pattern for surface tracking [19].

Delamination Discharges

The delamination occurs when the layers of the isolation system lose adhesion, generating voids in the isolation system. The delamination can create voids in the ground

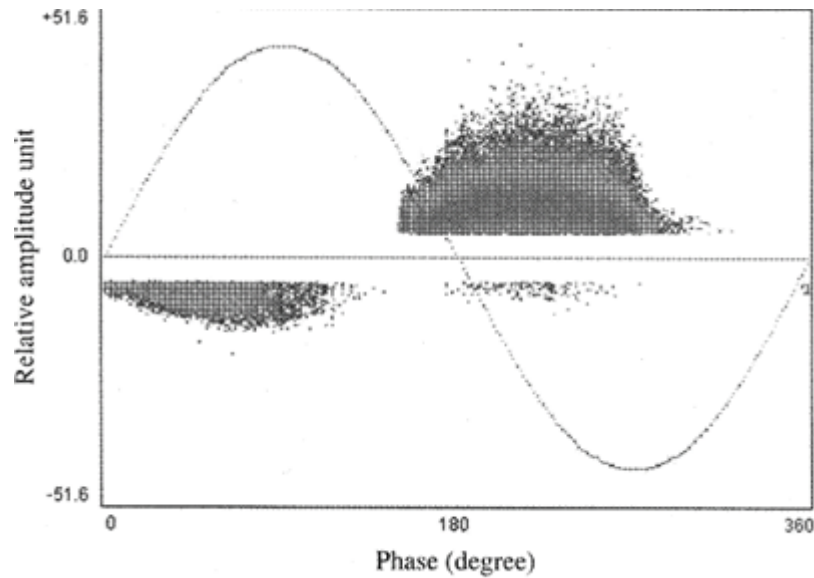


Figure 45 – PPA graphic-Typical pattern for corona discharge[19].

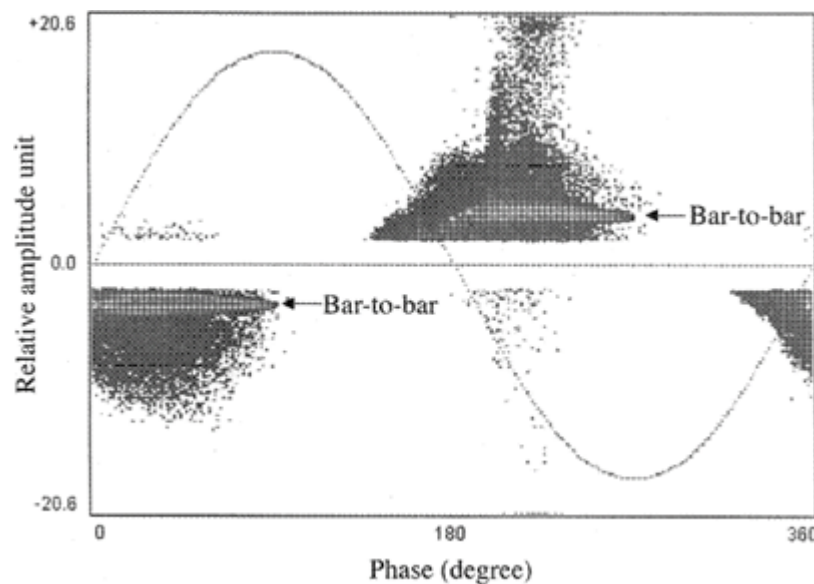


Figure 46 – PPA graphic-Typical pattern for discharge between phases [19].

wall isolation due to thermal stress or between the ground wall isolation and the copper conductors due thermal cycle. The PD pattern for delamination is dependent on the location of the void. If the voids are in the ground wall, then the PD pattern is the same as internal discharges. Otherwise, if the voids are between the ground wall and the copper conductors, then the PD patterns are asymmetrical, with the predominance of negative pulses in the positive half cycle.

Figure 47 depicts the typical pattern for PD between the ground wall and the copper conductors.

The diagnostic focus of this section is though PPA characteristics. However, a

spectrums analysis of PD pulses also can be used, but it is not widely applied.

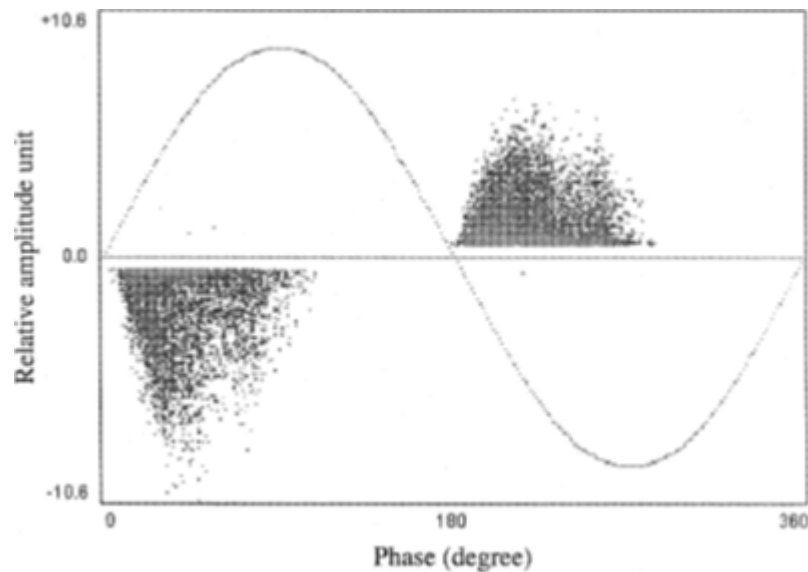


Figure 47 – PPA graphic - Typical pattern for PD between the ground wall and the copper conductors [19].

3.4 Data Storage and Management

The methodology present in chapter 4 of this thesis has as a base the monitorization of accelerated aging tests and the operation of a hydro-power plant (Emborcação-CEMIG). Both require the continuous acquisition of a bunch of variables such as temperatures, voltages, current, partial discharges; among others. Then, a significant number of data have to be stored and managed. The utilization of data infrastructure systems to easily store, manage, access, and visualize the data facilitates and contributes to achieving this objective and reach good results.

The PI system is applied in our monitorization to suppress this function. The PI system is an infrastructure system developed by OSIsoft. The great advantage of this system is the temporal database, which allows easy access and visualization of the variables.

In summary, the system works by acquisition data of different sources, generally from sensors, and sends to the server, which centers all the information. The server is responsible for the association of each monitored variable to elements that make more accessible the monitored plant's comprehension and the visualization of its data.

The three essential functions of the PI system is acquisition, store, and visualization of data. Not for coincidence, PI system infrastructure has three different levels: Interface, Server, and Visualizing tolls. Each level is responsible for executing one of these

essential functions. The figure 48 is a schematic of the PI System levels. A summary of each of these levels of the PI system is present in the sequence:

- Interfaces

The interface of the PI System is the stage where the Reading of data occurs. The information generally sends by sensors to the server is associated with a timestamp, being able to the formation of a temporal database. There are several interfaces in the PI System to allow the rending of data from different protocols or types of data sources. For example, PI interface for Mod-bus Ethernet Read-only, PI interface for mod-bus Ethernet Read-write, and the PI interface for UFL (interface to read text files).

- Server

The PI server has the PI Data Archive and the PI Asset Framework (PI AF). The Data Archive is the temporal database of the PI system. All the information sent by the interfaces is stored in this database as tags. The PI Asset Framework organizes the information store in the temporal database (PI Data Archive). The organization of the tags allows the users to quickly access and comprehension of the data stored.

- Visualization Tools

The Visualization Tolls is the level that represents the means of how the user visualizes the information/data. The are many platforms where the users can visualize the data, such as PI Datalink, PI ProcessBook, PI WebParts, among others.

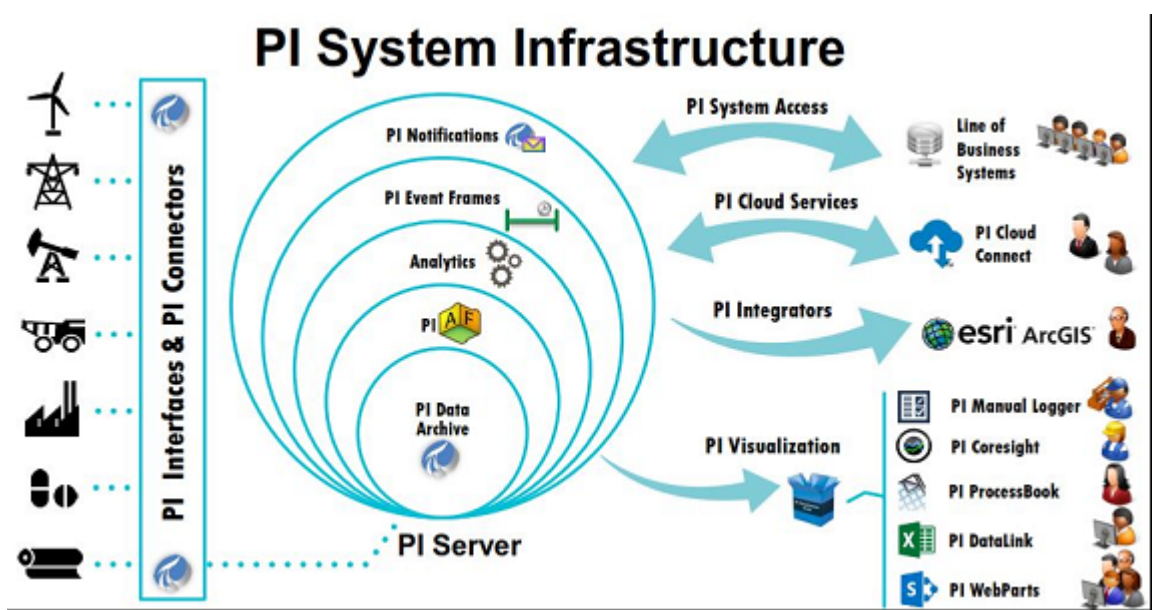


Figure 48 – Schematic of the PI System Levels [20]

4 Methodology

The applied methodology to estimate the remaining useful life of hydro generators is based present three big blocks:

- Statistical analysis of the operation database from CEMIG;
- Accelerated aging tests in stator bars/coils;
- Online monitoring of a hydropower plant.

Figure 49 depicts the scheme of the proposed methodology.

The statistical analyses have the importance of estimating the average useful life of hydro generators. The historical failure data of hydro generators from CEMIG is used to calculate the *MTTF*. Thus, the estimation of the remaining useful life of a given generator has an initial estimate.

The accelerated aging test will adjust the initial estimation value for a given generator based on its current insulation condition. For this proposal, the performance of accelerated aging tests under the observation of physical and electrical measures is the key to achieve the objective. The PI system is applied here to manage the measurement variables better and facilitate the analysis.

Like the previous observation in chapter 3, the insulation changes its electrical properties overtime during machine aging. Additionally, when the generators are under a failure mechanism, the deterioration and the changes in these properties might be faster.

PD measurements are continually taken for the stator bars under test to evaluate the electrical properties. The proposal is to track all the PD tendencies over insulation aging/degradation. Moreover, conditions variables of the insulation are assessed by measurements of voltage, currents, temperatures, and suitable sensors.

Thus, the execution of accelerated aging test in stator bars/coils, plus the continual observation of physical and electrical parameters, have the followings intentions:

- Simulate the failure mechanisms that are critical to the insulation health and may end with insulation breakdown;
- Track tendency of PD measures over the test;
- Identification of the start of critical conditions to establish acceptable and alarm values for Partial discharges;

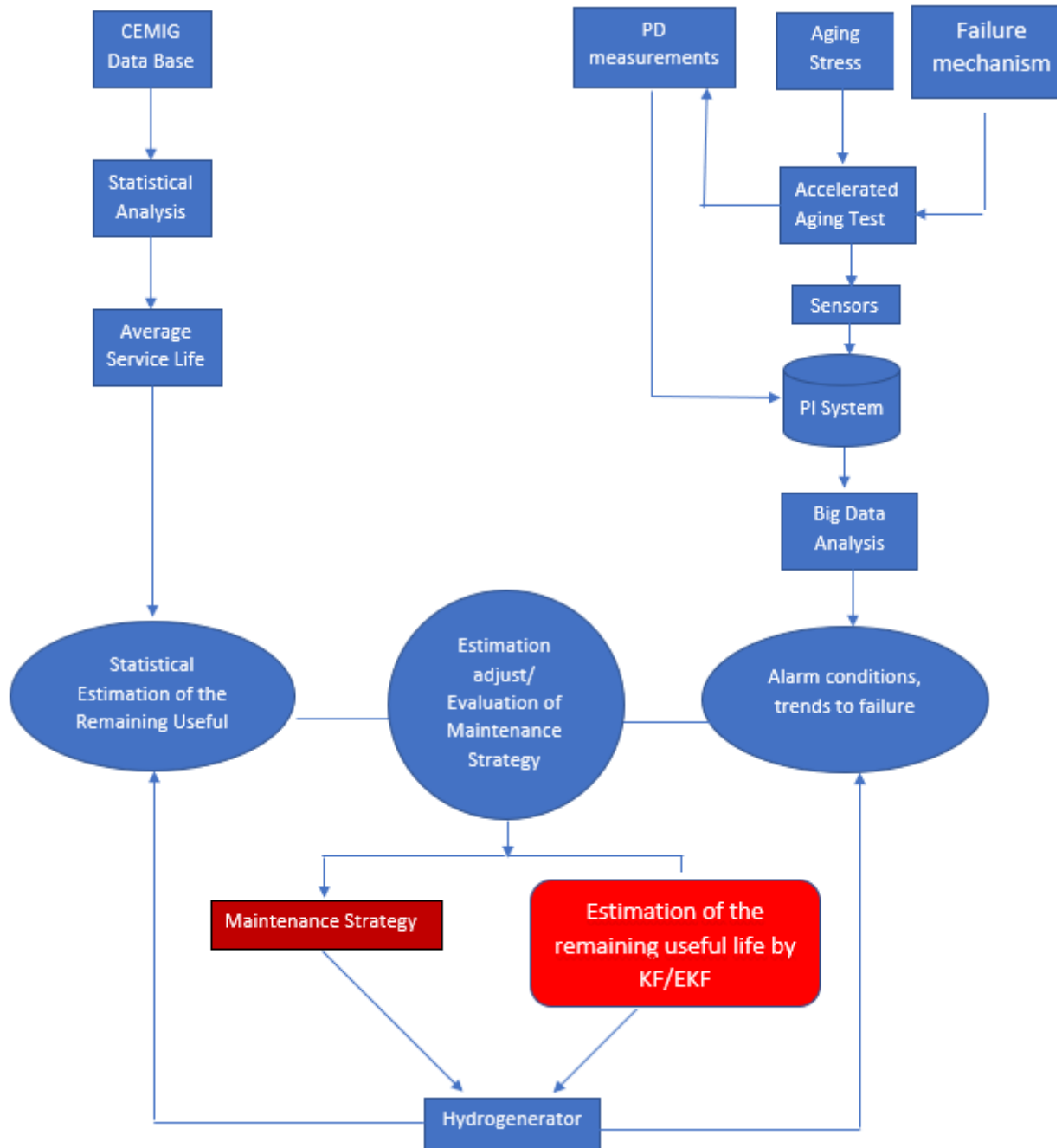


Figure 49 – schematic of the proposed methodology

- Correlation between the condition and electrical variables measures during the test;
- Observation of changes in the pattern of all variables that indicate pre-failure conditions;
- Observation of patterns and tendencies on the monitored variables that allow the prognosis of a failure and the remaining useful life (mainly in the PD)

In summary, the objective is entirely understand the aging/deterioration in the insulation system. The strategy of online and continuous monitoring of all measurement

variables over the accelerated aging test, give us the elements to achieve the objective.

If observed during the accelerated aging test clear tendency to fail in the partial discharges measurements, *EKF (Extended Kalman Filter)* and *KF (Kalman Filter)* will be applied to estimate the remaining useful life. Since each stator failure mechanism has a specific rate of degradation, the estimation will be valid only for the specific failure mechanism simulated in the accelerated aging test.

The third part is the monitoring of a hydropower plant EMBORCAÇÃO-CEMIG. It has the function to provide the reference insulation condition of a generator under regular operation. Thus, installing a PDA instrument in one generator to continually monitor the partial discharges is the principal part. All measurements already taken in this hydropower plant are continually monitored as well. PI system was implemented to store and better manage the measures.

Finally, the maintenance strategy is also a crucial goal of the proposed methodology. The maintenance strategy proposed is given in the figure 50. The following steps summarize the maintenance strategy:

- Step 1: Step 1: Continually evaluation of PD measurements. If the PD values are stable, the estimation of the statistical analysis for the remaining useful life is valid. In case of detecting an alarm condition, it goes to step 2. The alarm conditions are changes in PD pattern, critical values for PD, detection of the pre-failure condition.
- Step 2: Further investigation. PPA graphics can be used for failure mode identification. Visual inspection and other diagnostic tests must be performed, providing a definitive diagnosis of the problem. After the investigation, if it does not detect problems, the statistical estimation is valid, comes back to step 1. If a stator failure mechanism is detected, it goes to step 3.
- Step 3: Failure mechanism evaluation. Depending on the failure mechanism detect, there are two possibles alternatives: First, there is Suitable maintenance that can reduce or even eliminated the deterioration. Thus, this activity must be performed. After that, it returns to step 1. The second alternative, there is nothing to do to avoid deterioration. Thus, a prognostic of the remaining useful life based on the current insulation condition must be considered, which goes to step 4. It can propose some alteration in the generator operation regime to have time to plan its replacement. That avoids the emergence cost of manufacturing a new generator. The analysis is based on the deterioration problem affecting the machine.
- Step 4: Operation Regime. It is analyzed whether changes in the operation regime of the generator are necessary to extend the life. This strategy is necessary to avoid the emergence cost of manufacturing a new generator. The analysis is based on the

deterioration problem affecting the machine. Thus, for some deterioration problems, the change in the regime is effective. On the other hand, for others, it brings no benefit.

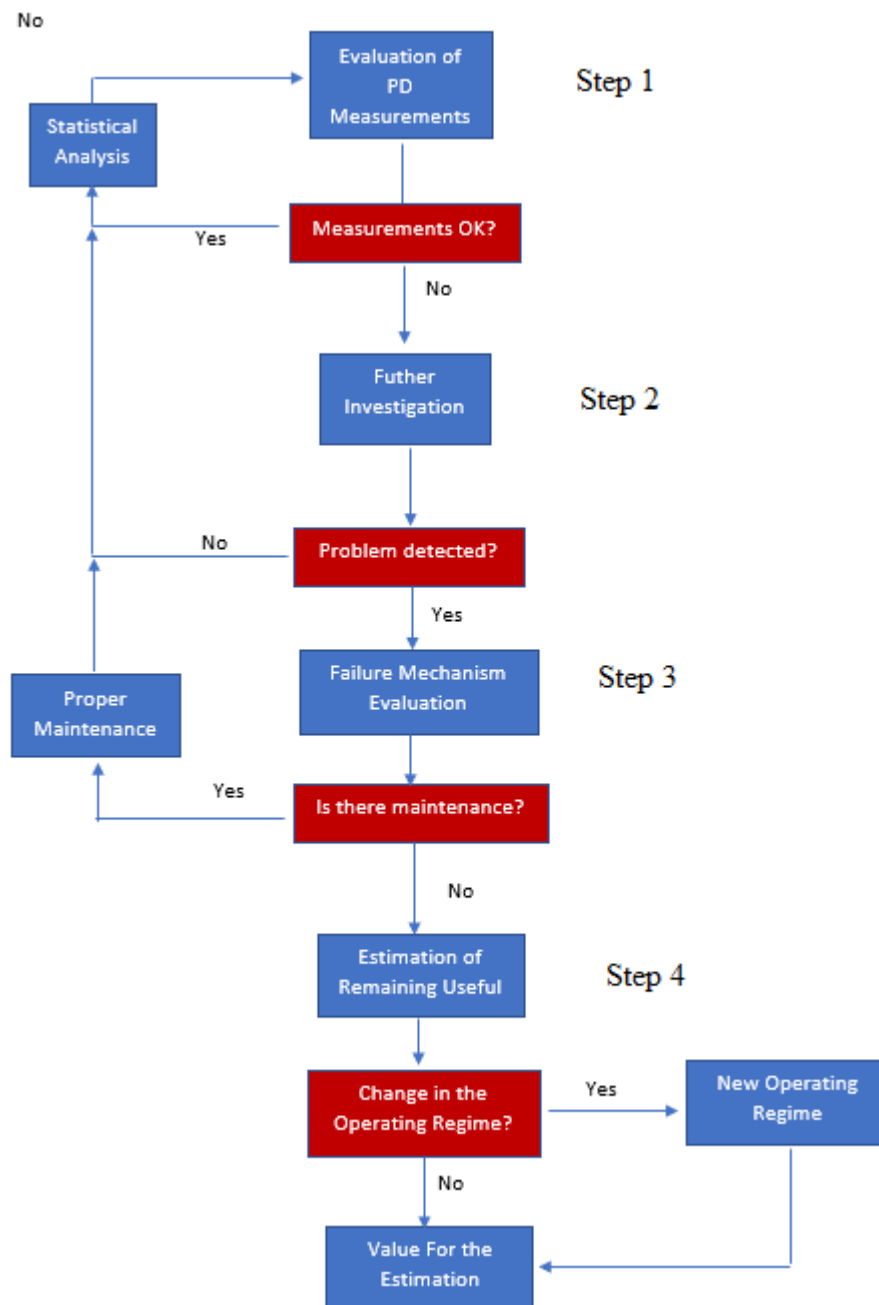


Figure 50 – Maintenance strategy scheme

4.1 Statistical Analysis of the Remaining Useful Life of Hydro Generators

The statistic evaluation of generators from Cemig is one of the bases of the methodology. The evaluation will provide the average lifetime of generators. The statistical estimation of the remaining useful life gives the initial value for estimating the useful life of a given generator. No considerations about the insulation condition are used here.

Tables 21 and 22, located in annex A, presents data of generators rated above 12,5 MW from CEMIG database.

The failure rate calculation takes into account the failure registers of these generators. The following events are assumed to be end of life:

- Replacement of a generator
- The complete stator rewinding

Using tables 21 and 22 is possible to construct functional tables 23 and 24 that present the actual age of each generator and the registered failure, replacement, or rewinding ages. Tables 23 and 24 are also located in annex A.

4.1.1 Overview of CEMIG Database

Here is presented a summary of the main information extracted from CEMIG database. Table 9 represents a overview of information from the tables 23 and 24. The information is used to calculate statistics variables for the generators, as their current average age, the average age at fault, the average age at end of operation, among others. These are essential variables for the next statistical calculations.

Table 9 – Statistical Overview of Cemig Database (History update date - 01/01/2018)

Current generator ages (year)		Statistics (year)	
Newest	0.0	Average age at fault	10.9
Older	67.0	Average age at operation output	52.9
Average ages	29.2	Total operating time (all generators)	2529.3

Failure Rate

The failure rate is essential to predictive the remaining useful life. It represents how often a generator will failure given its age and the whole number of operating units. Thus, the probability of a given generator to fail can be determined. As higher is this rate, the more likely an generator fails.

Equipment regularly experiments different failure rates over their lives. The bathtub curve is widely applied to model the failure rate of the equipment. There are different stages according to this curve. Infant stage; normal operation stage, and wear out (aging) stage:

- Infant stage: It is when the equipment starts the operation. The failure rate is high in the beginning and decreases along the time until it stabilizes at the rate observed in the normal operation stage. Many reasons explain the higher rate of failure. For example, the equipment can fail when it is not well modeled to its operating condition. Moreover, operators have to adapt to the new equipment in operation, and this leads to more failures than usual.
- Normal operation stage: It is also called useful life stage. Its main feature is the constant failure rate over time.
- Wear out or aging stage: It is the stage where the equipment is aging. It starts to present more and more defects over time due to degradation. Thus, the failure rate increase over time.

The exponential model represents accurately the generators under their useful life when the failure rate is constant. For this study, the failure rate for the normal operation stage is obtained through the simple division of the total number of failures observed by the total operation time, as depicted in equation 4.1.

$$\lambda(t) = \lambda = \frac{N_F}{T_{Ot}} \quad (4.1)$$

where:

$\lambda(t)$ is the failure rate;

N_F is the number of failures observed;

T_{Ot} is the total operation time.

Observation: The total operation time is the sum of the generators individual operating times.

After calculating the failure rate, it is easy to obtain the life expectancy:

$$E_l = \frac{1}{\lambda} \quad (4.2)$$

Where:

E_l is the life expectancy

Table 10 report the statistical results of Applying equations 4.1 and 4.2 in CEMIG database.

Table 10 – Failure rate and Life expectancy for exponential model

Total operation time (years)	2529.3
Total number of observed failures	12
Failure rate (failures/year)	0.004744
Life expectancy (years)	210.8

With the failure rate value, the calculation of the following statistics functions is possible to perform as a function of generators age, in years, represented as time (t):

- Probability density function $P(t)$;

$$P(t) = \lambda \cdot \exp(-\lambda \cdot t) \quad (4.3)$$

- Reliability function $R(t)$;

$$R(t) = \exp(-\lambda \cdot t) \quad (4.4)$$

- Cumulative distribution function

$$F(t) = 1 - \exp(-\lambda \cdot t) \quad (4.5)$$

A constant failure rate during generator life yields a life expectancy equal to 210,8 years for a generator.

Thus, we conclude modeling the generator lifetime using exponential distribution is overly optimistic. By the exponential model a given generator can overcome 200 years of operation with relatively high probability.

The adjusted model apply constant failure rate only in the normal operation stage (useful life stage), and an increasing failure rate over time to represent its aging.

4.1.2 Adjusted Model

Here is presented the adjusted model for a generator lifetime estimation. The exponential distribution represents the operation time at the normal operation condition, where the failure rate is constant. A model with a quadratic failure rate is applied to describe the equipment degradation in the aging stage. Thus, the adjusted model has two phases:

- **Useful life**

Where the constant failure rate is applied.

- **Aging**

Where the quadratic failure rate is applied.

Phase 1: Useful life

For the useful life the failure rate is represented by:

$$\lambda = \lambda_u = \text{constant} \quad (4.6)$$

where:

λ_u is the useful life failure rate

For the next calculations, it is necessary to define the transition age t_e . It represents the age of transition from the useful life to the aging phase.

The average reform age for generators, without any failure, and with diagnostic indication, suggest the transition moment. It is assumed this moment as the transition age. It is a initial estimation for the transition moment. Further, the monitoring of the generator condition can be useful to adjust the transition stage.

Thus, the t_e obtained from CEMIG database is equal to 52,9 years. As a consequence, the calculation of the following parameters is possible:

- Failure Probability in the useful life;

The failure probability is a time function, and it is calculated using the Reliability Function. The Reliability Function represents the probability of a given component does not fail until a given instant t , that is, $P(T > t)$. It represents a specific area in the probability density function for values higher than the desired instant t . Thus, the failure probability is the complementary probability. It represents the probability of a component fail until a given instant t . Equation 4.7 represent the calculation of the failure probability.

$$F_p(t) = P(T < t) = 1 - R(t) \quad (4.7)$$

Using $t=t_e= 52,9$ years, it is possible to obtain the failure probability for the useful life.

$$F_p(t) = F_p(UL) = P(T < t_e) = 1 - R(t_e) = 1 - \exp^{-\lambda \cdot t_e} \quad (4.8)$$

Where:

$F_p(UL)$ is the failure probability in the useful life.

- MTTF

MTTF is equal to the expected life. It is possible to be calculated by the discrete equation 4.9:

$$E_l(T) = MTTF = \sum_{j=1}^N t_j \cdot P(j_i) \quad (4.9)$$

Δt equal to 1 year is applied for MTTF calculation.

Table 11 represents the useful life phase results.

Table 11 – Statistical result for useful life

t_e (years)	53
$F_p(UL)$	0,222332
λ (failures/year)	0,004744
MTTF (years)	25,8

Phase 2: Aging

The failure rate for used to model the aging phase is given by Equation 4.10.

$$\lambda(t) = \lambda_u + k_c(t - t_e)^2 \quad (4.10)$$

k_c is the quadratic term coefficient. The parameter has the initial estimation according to:

- k_c must be adjusted for t_{max} and the expected life E_l estimated by the model are compatible with the historical values.
- t_{max} is the maximum life with 99% of probability.

k_c can be adjusted by the condition monitoring of the hydro-generator. Given that each failure mode has a specific level of deterioration, the most suitable adjustment of k_c is according to the failure mode present in a given generator.

The calculation of the following statistics variables is executed for the aging phase:

- Failure Probability in the Aging Phase

$$F_P(A) = 1 - F_p(UL) \quad (4.11)$$

Where:

$F_P(A)$ is the failure probability in the aging phase.

- Maximum life with 99% of probability (t_{max})

t_{max} is the instant t which the area in the probability density function is equal to 99%, that is:

$$P(T \leq t_{99}) = 0,99 \quad (4.12)$$

- MTTF in the Aging Phase

Equation 4.9 is applied again with Δt is equal to 1 year. t starts from 53 years.

The results for the aging phase is present in table 12.

Table 12 – Statistical result for the Aging Phase

Coefficient K	0,0007
$F_P(A)$	0,777668
t_{max} (years)	80
MTTF (years)	66,8

Statistical Results

Here is present the result of the statistical method used to estimate the lifetime of generators. The result is the combination of useful life and aging phases. The expected value for a generator is equal to 57,7 years. Figures 51 present the Statistical Analysis Results.

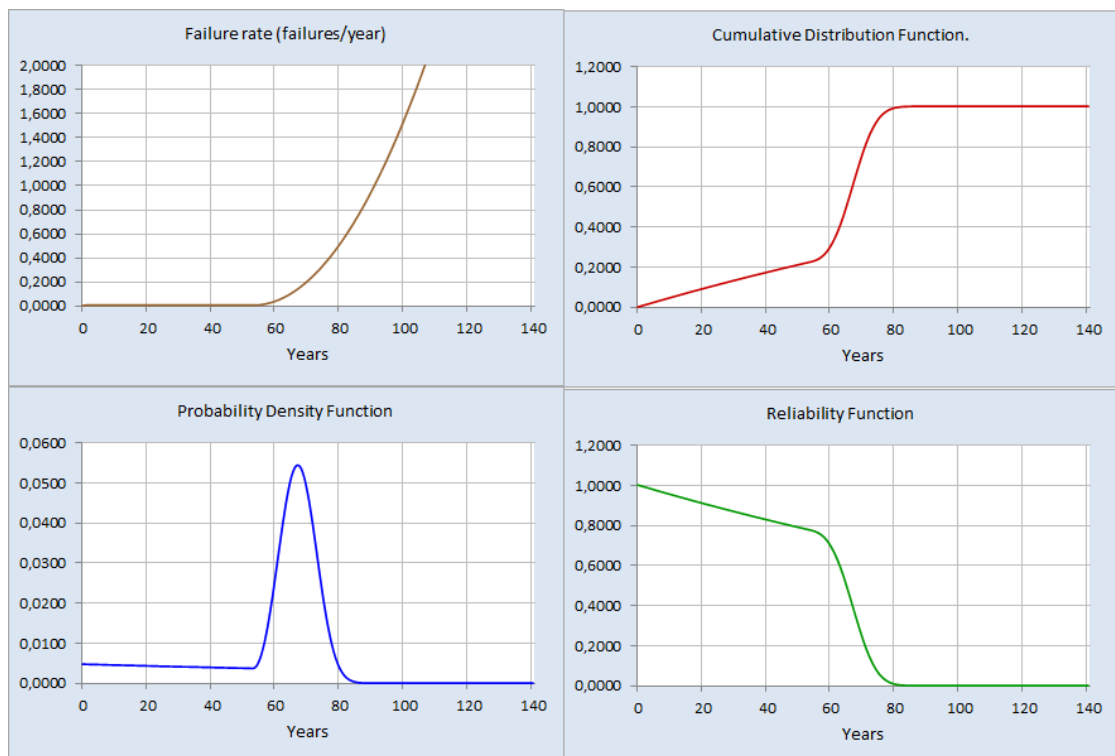


Figure 51 – Statistical Analysis Results

4.2 Accelerated Aging Tests

It is present here the part of the proposed methodology for estimating the remaining useful life of the hydro-generator. The analysis is based the insulation condition of the stator windings. Thus, it is necessary the monitoring of the insulation condition over aging time. The proposed methodology has a new method for the accelerated aging test. The new methodology involves basically:

- Perform the test in stator bars/coils with the aging stress above normal condition. If possible, the proposal test must be performed until insulation breakdown. Thus, the evaluation of the changes in the insulation properties over the entire life is observed.
- Use PD as the diagnostic test. The PD measures are continuously taken over the tests. Thus, it is possible to find out when a deterioration process starts instantly. Moreover, track the tendency of PD, detection of pre-failure conditions, among others, to estimate the insulation lifetime and improve the maintenance activities.
- Online monitoring of many variables. The sensors send all the information to the PI interface. Thus, all the data is stored at the PI server, constructing a considerable database. The temporal database facilitates the data analysis. The PI Visualization Tools provide many tools to manipulate the stored data quickly.

4.2.1 Tests

The central part of the insulation condition evaluation is the tests performed at LAT-UNIFEI.

The tests accelerate the degradation and aging in the insulation system, becoming possible to analyze these processes quickly.

The ideal scenario is to execute tests that combine the aging stress to simulate all the stator failure mechanisms presented in section 3.2. However, it would demand a lot of resources, equipment, and specimens.

Therefore, taking in account the available equipment and specimens the following tests were taken:

- **Voltage Applied:**

Accelerated aging tests were carried out by applying different voltage levels in the specimens.

- **Thermal cycling test:**

Intense thermal cycling was applied to the specimen under test.

Voltage Applied

The voltage applied test is the first in the series of aging tests. In the test, a stator coil specimen is positioned in the test cell and subjected to one thousand hours of voltage applied at industrial frequency. The test is applied in individual coils. Since the coil is outside the stator, a conductor layer (aluminum paper) involves the straight part of the coil. The layer is connected to the ground. In this way, the voltage applied is between the conductor (copper) and the grounded conductor layer, which represents the stator core electrically.

The test was applied until now at two phases voltages levels:

- 1 pu of phase-to-ground rated voltage, 7967 V.
- 2 pu of phase-to-ground rated voltage, 16 kV.

The voltage is on the solid insulation of the coil under test. Partial discharges measurements are continuously taken. Comparison between PD measurements is made at the end of the test.

Figure 52 shows the configuration of the voltage applied test at LAT. It is possible to visualize the specimen involved by the conductor layer over three insulating supports. The connection of the specimen with the coupling capacitor that leads the partial discharges signals to the register is by 50-ohm coaxial cable. The medium voltage cable with a termination connects the voltage source with the specimen.



Figure 52 – Voltage Applied - Test Configuration

Figure 53 shows an overview of the test configuration. It is possible to observe the voltage source (single-phase transformer 220 V/100000 V, 20 kVA, 60 Hz), and the coupling capacitor (80 pF).



Figure 53 – Voltage Applied - Overview of the Test Configuration

Test results

Here are present the results for the voltage applied test. It is essential to observe that the PDA instrument used is the HydroTrac II/Iris.

1 pu of phase-to-ground rated voltage, 7967 V

The first test has a goal to experiment with the proposed scheme. The test is performed under a regular voltage operation. Thus, it does not expect accelerated aging. The PD results work as a reference value for the subsequent tests. It is essential to point out that 475 hours of information was registered. There was a loss of information during the data acquisition. A suitable correction was made for future tests. Since this is the first experimental test, the data loss does not cause further problems.

Figures 54, 55 and 56 show the test results. The calculation of a moving average for Q_m values is used to track the PD tendency. The moving average takes in account the last 25 Q_m values.

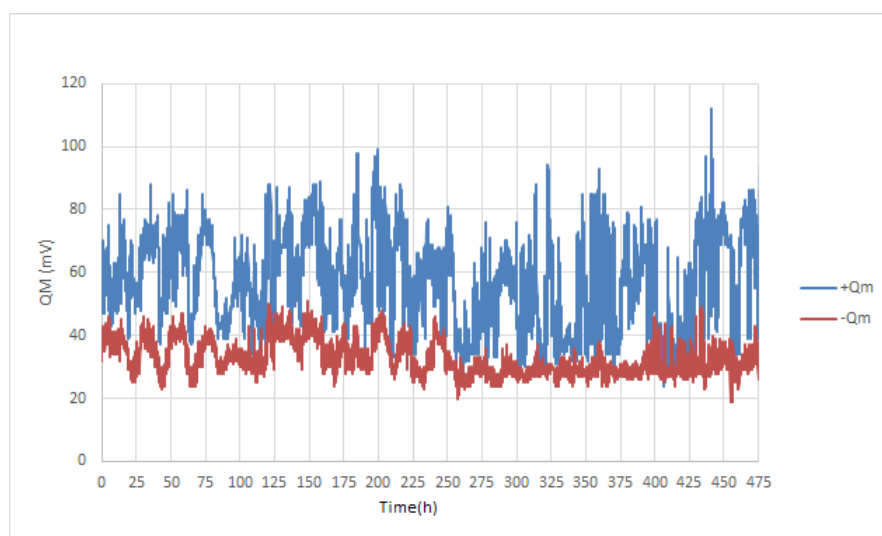
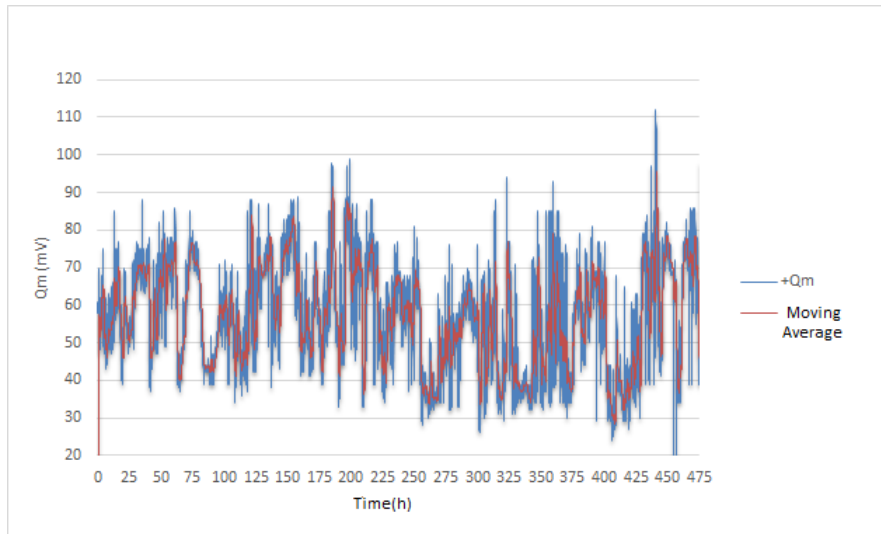
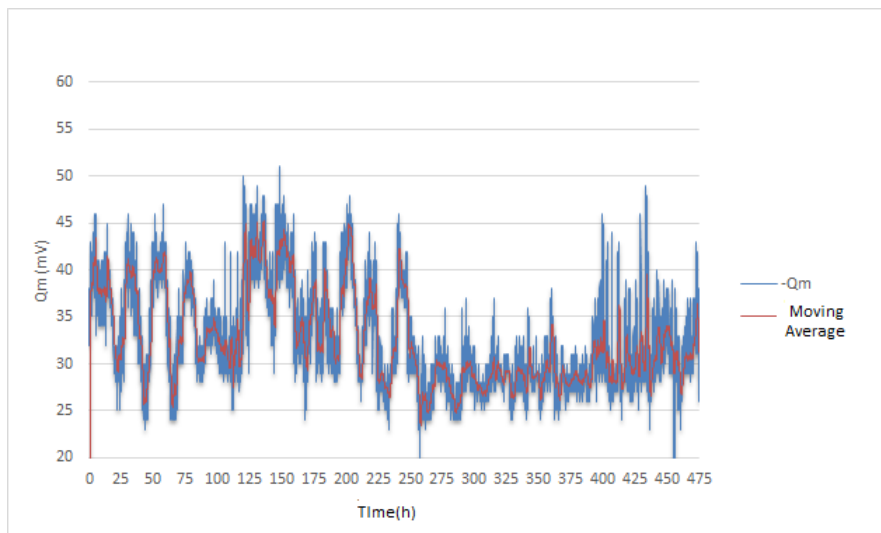


Figure 54 – 1pu voltage test - Partial discharges intensity (Q_m)

Figure 55 – 1pu voltage test - Trend analysis by moving average (Q_m+)Figure 56 – 1pu voltage test - Trend analysis by moving average (Q_m-)

2 pu of phase-to-ground rated voltage, 16 kV

Here is presented the result of the voltage applied test with 16 kV in the coil insulation. In this test, the accelerate aging factor is present. The intention is to verify the partial discharge evolution. In the case of insulation breakdown, it is also possible to analyze changes in the pattern before failure. Figures 57, 58, 59 show the Q_m values and the moving average over time.

Result Analysis of Voltage Applied Test

The voltage applied test did not show any changes in the PD trend or pattern during test performance. As a result, no alarm condition was detected, and no valid data for the prediction model was generated. The electrical stress alone hardly ever will impose intense deterioration or fast aging to the insulation even if the stress level is high above the

rated condition, as the second test with two times the machine rated voltage. It is essential to impose a fast deterioration/aging on the insulation to force an insulation breakdown. The electrical stress by itself will need a very long time to impose this condition on the insulation. These statements converge with the technical literature studied [2](#), and here was proven based on the PD measurements made continuously during the test, with the same equipment and cables (sizes and length). The electrical stress is essential in an insulation breakdown to be the last case of this event, but it only happens with aged and deteriorated insulation. Others stress are responsible for insulation deterioration/aging. These conclusions were applied in the test procedures on the second aging test developed in this work, the thermal cycle test.

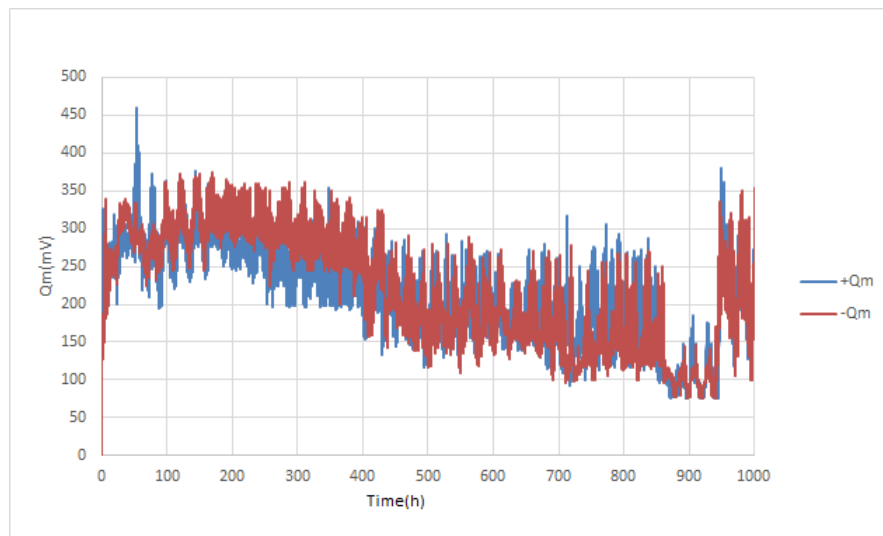


Figure 57 – 2pu voltage test - Trend analysis by moving average (Q_{m+})

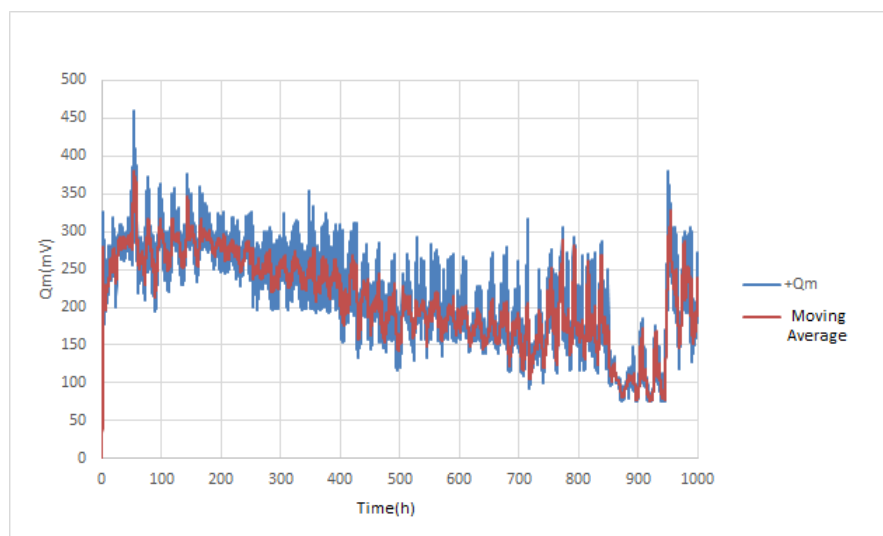


Figure 58 – 2pu voltage test - Trend analysis by moving average (Q_{m+})

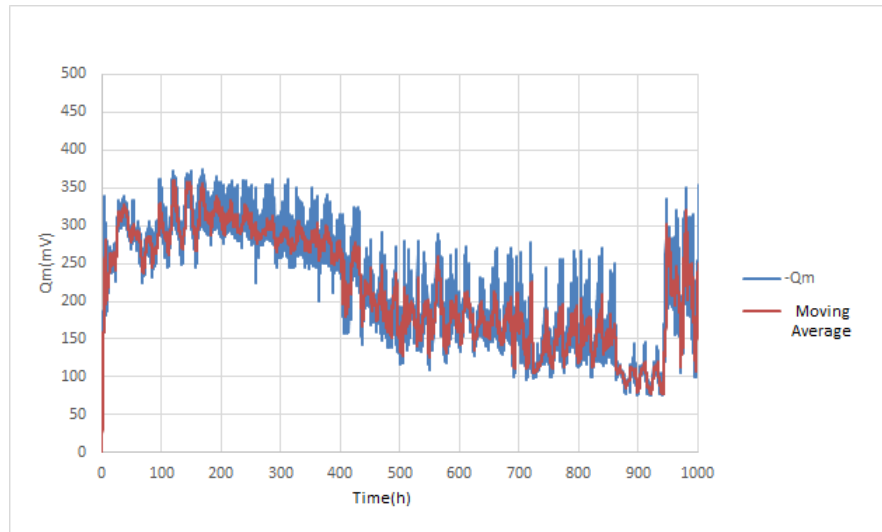


Figure 59 – 2pu voltage test - Trend analysis by moving average (Q_m)

Thermal Cycle

The thermal cycle test is an essential test for the insulation system approval in the manufacturing stage. Machine manufacturers widely apply the test to qualify a given insulation system for operation. The test simulates the thermal-mechanical stress present in the generator due to starts/stops and load variation. In this application, the thermal cycle test is applied as an accelerated aging test, and the goal is to evaluate the insulation aging until an insulation breakdown. The observation of its insulation properties by the PD measurements is fundamental.

Since the goals are different, new procedures were proposed to carry out the test, with some changes compared to the IEEE STD 1310 recommendations. [62]:

- The test is performed with voltage application to allow continuous PD measurements.
- Instead of 500 cycles, the criteria to finish the test is the insulation breakdown. The presence of electrical stress during test execution enables the test finish criteria.
- The measurement of the coil temperature in the test was performed by thermographic cameras [74]. The reference temperature is in the copper conductors, and the thermographic camera measures the surface temperature. Thus, a previous test was made in another coil sample to establish a correlation between the internal and external temperatures.

The reference [75] presents details about the test procedures and the automation applied for test execution. Excluding these differences, the procedures to carry out the test are according to the IEEE STD 1310 regarding the thermal cycle test in stator bars/coils



Figure 60 – Circuit with Inductors and Insulated Cable

of hydro generators. The test consists of the application of thermal cycles between 40 °C and the rated temperature of the insulation system, according to table 7. For example, for a insulation system class F, the cycles are between 40 °C and 155 °C.

For heating semi-cycle, electrical current is applied through the coils to generate heating by the joule effect. Thus, it necessary a specific circuit to the electrical current application. Figure 60 show the inductors and the insulated cable. These equipment are responsible for electrical current application through the coils. In this circuit, the current is induced in the coils by the inductors. The voltage in the inductors controls the current applied.

For the cooling semi-cycle, the current is turned off. The coils can naturally cool, or a refrigeration system can accelerate the process. It is essential to point out that the rate of temperature variation for both heating and cooling half cycle suggested is 2.5 °C (+/- 1.0 °C) per minute. In our application, the cooling system used is shown in figure 61. It is activated whenever the temperature reaches the peak of the thermal cycle.

Figure 62 is an overview of the test bench. The PDA instrument used in the test is Haefely Test AG: DDX 9121b. Its coupling capacitor has 10 nF. The equipment and procedures to apply voltage in the coil are the same as the voltage applied test.

Test Results

1) Thermal Cycle test 1 with coil rated voltage applied;

Figures 63 and 64 show the results for Thermal Cycle with rated voltage applied in the coil. The figures present the moving average for Q_m and the Q_m value for each temperature level, respectively. The Q_m values in the beginning of the test present high levels. During the test, Q_m drops and remains constant over time. This value represents the



Figure 61 – The Cooling System

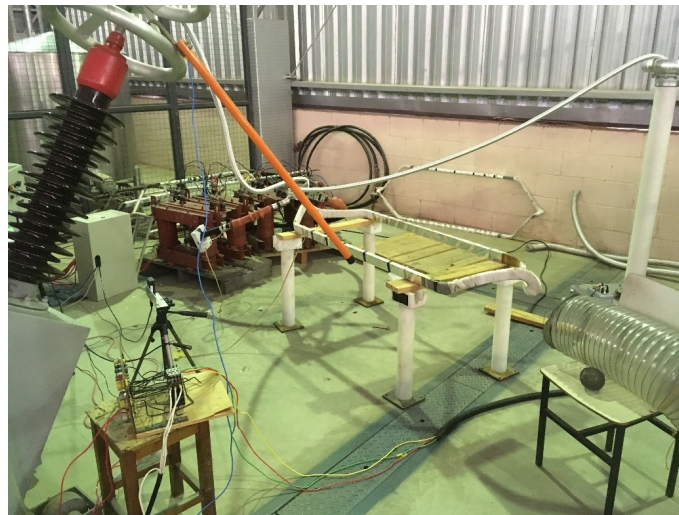


Figure 62 – Overview of the Test Bench

Q_m level during the normal operation condition (around 20 nC). The behavior described above on the PD trend is common in new winding and report in figure 72 in chapter 5. After 409 cycles, no trends to failure was detected. Thus, we decided to raise the thermomechanical stress by increasing the upper-temperature limit from 155 C to 170 C. Under these conditions, a mechanical failure was detected after 13 cycles, as depicted in figure 65. Moreover, no evidence of electrical failure was found after specimen examination. No PD trends to failure was detect because there was not electrical failure (insulation breakdown).

A strong correlation between Q_m and the winding copper temperature was found, as showed in figure 64. Q_m increases with the temperature rise. This statement is beneficial for diagnostic proposes. Aged insulation with strong thermal-mechanical deterioration usually presents this correlation between PD and temperature. Moreover, it is essential to point out the importance of PI system in this observation. Therefore, the proposed

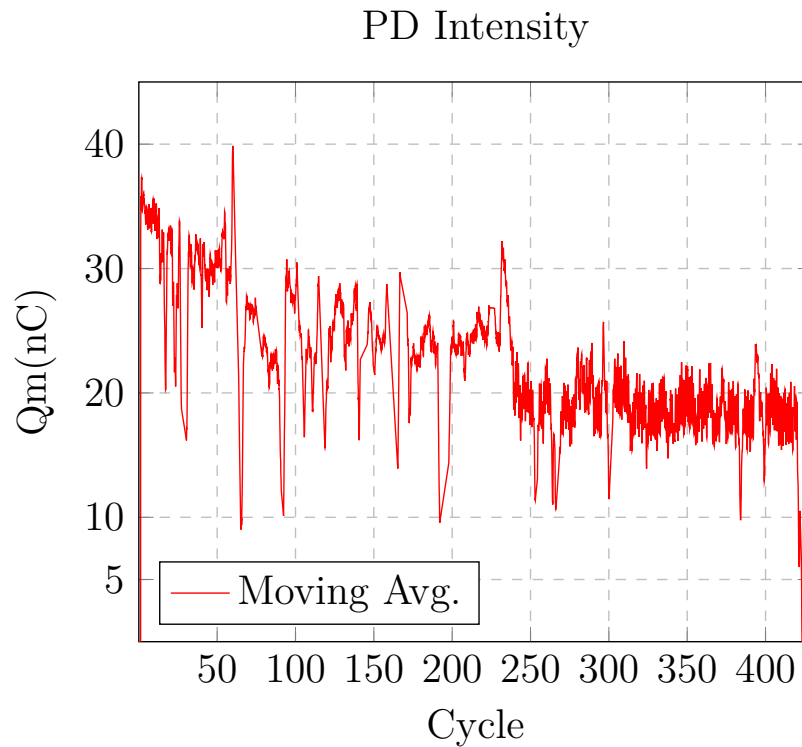


Figure 63 – Thermal cycle test 1 - PD intensity (moving average window = 25)

methodology that combines accelerated aging test, PI system, and widely observation of variables facilitates the identification of correlation. That is important to the condition-based maintenance in diagnostic execution.

2) Thermal Cycle 2 with 1,25 times the rated voltage (10 kV) applied.

Here the strategy was to submit the coil to stronger electrical stress (1.25 pu). Therefore, the tested coil was under electrical and thermal-mechanical stress above normal operating conditions. After 120 cycles, the insulation shows signals of electrical properties changing. These signals were observed in the heating current, heating duration, cooling duration, and Q_m , all by changing their pattern. As a result, at cycle number 180, the insulation could no longer hold the electrical stress, and an insulation breakdown was observed (figure 66). Here, it is essential to point out that the same thermal-mechanical stress was applied in test 1. The only difference is the higher electrical stress.

The heating current during the test was constant and equal to 600 A during around 120 cycles. After that, the current drop to 560 A, without any interference in the test. It may represent a variation on the insulation properties due to the insulation aging [15]. Moreover, the heating and cooling duration demonstrated changes in the pattern simultaneously, reinforcing that the insulation properties had changed due to degradation/aging. The heating duration in the 120 initial cycles has an average value of 45 min, varying most of the time between 40 to 50 min. After that, it drops to an average of 30 min until the insulation breakdown. On the other hand, the cooling duration varying more in the

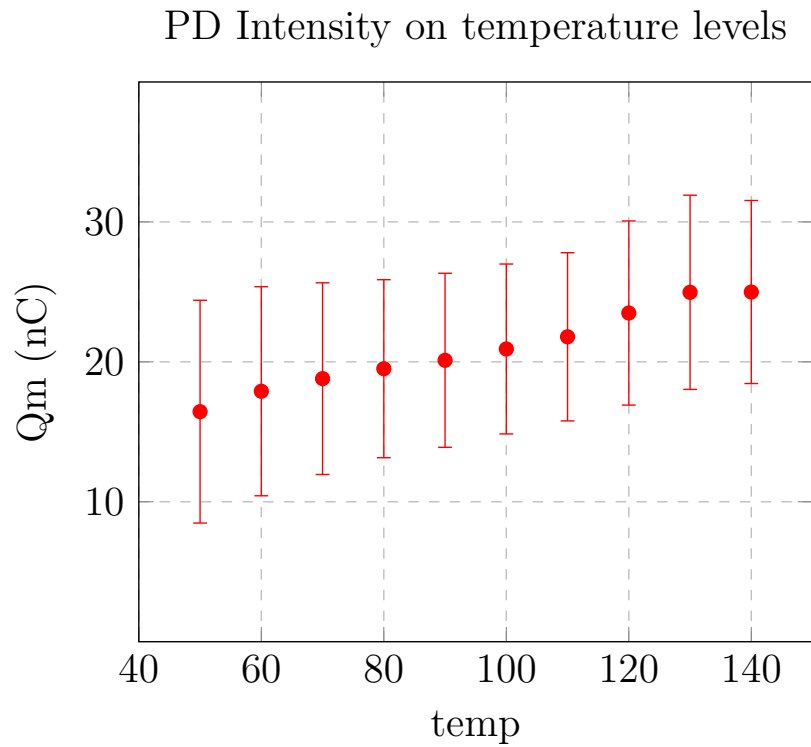


Figure 64 – Thermal cycle test 1 - Upper Limit = 140 C

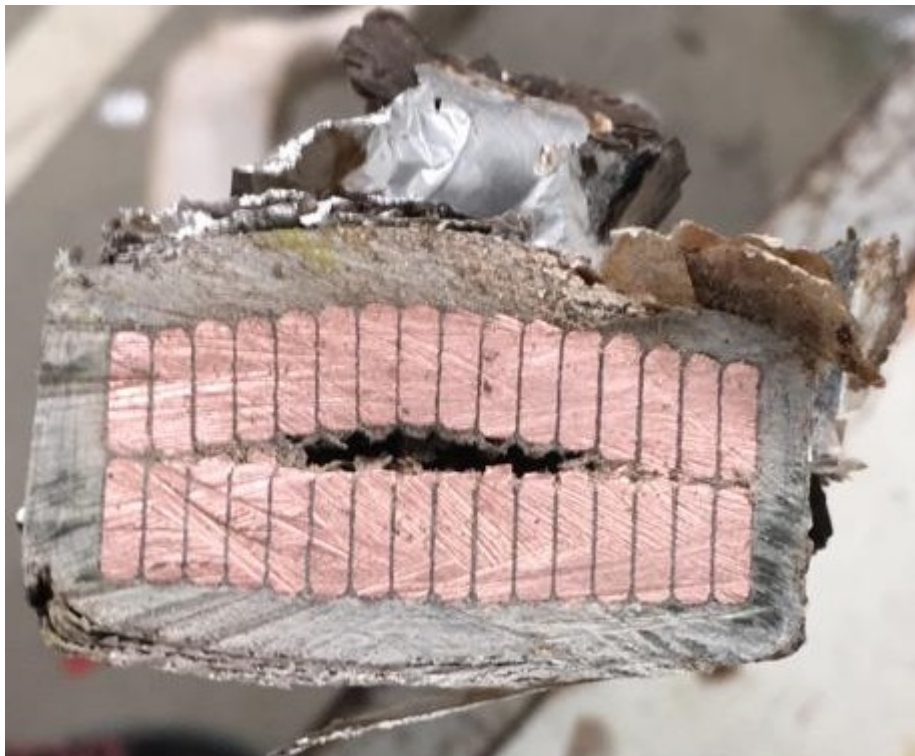


Figure 65 – Thermal cycle test 1- Coil Condition after failure

initial 120 cycles, probably because of the room temperature variation (as lower is the room temperature, as faster is the heating duration). However, after the 120 cycles, the cooling duration rises until the moment of the insulation breakdown. Figure 67 show all

these variables over time.

Finally, the Q_m demonstrated the behaviors represented in the figure 72. In the initials 120 cycles, Q_m has an average value of 22 nC. After that, the values go to 34 nC and increase until the insulation breakdown moment. Figure 69 shows the Q_m values for both haft cycles.

The same behavior is observed in the PD values over 90°C, 110°C, and 130°C (Figure 68). For 50°C, Q_m rises faster from 20 nC to the critical value of 30 nC, remaining this level until the failure moment.

Test conclusion

1. These trends to failure in the Q_m values are one of the main objectives of this thesis. This observation was possible by the proposed methodology of continuous measurement of PD in the accelerated aging test;
2. The algorithms to predict the remaining useful life of hydrogenerators in chapter 5 will explore the trends to failure observed in the thermal cycles test 2;
3. The pattern' changes over Q_m , heating current, heating duration, and cooling duration might represent a change in the electrical insulation properties. It is a typical signal of insulation systems in advanced stages of degradation/aging [76]. Here it was observed by measurement variables, monitored continuously.



Figure 66 – Thermal cycle test 2 - Insulation breakdown

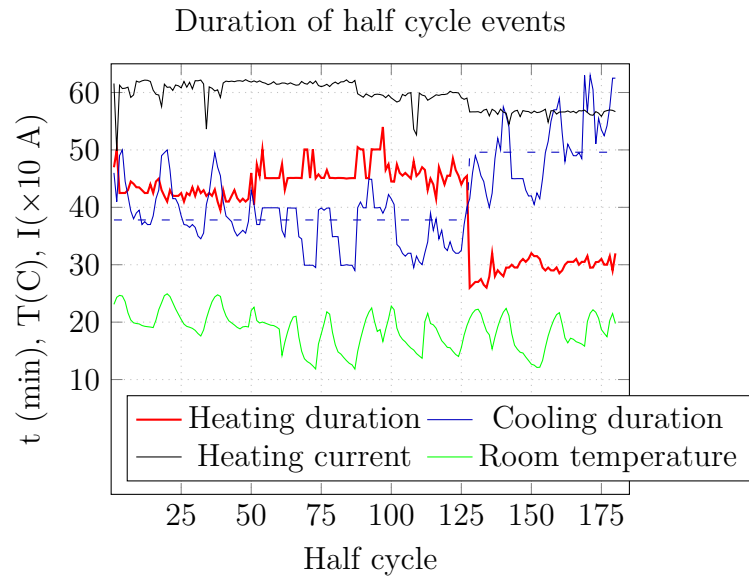


Figure 67 – Thermal cycle test 2 -Half cycle events analysis (Thermal Cycle experiment with 10 kV) - Duration in minutes (dashed lines are averages), Room Temperature and applied current.

PD Intensity on temperature levels over half cycle events

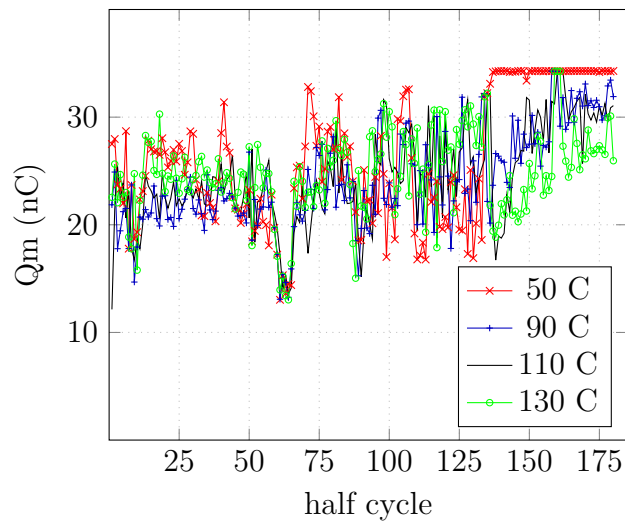


Figure 68 – Thermal cycle test 2 - Q_m on Temperature Levels over cycles

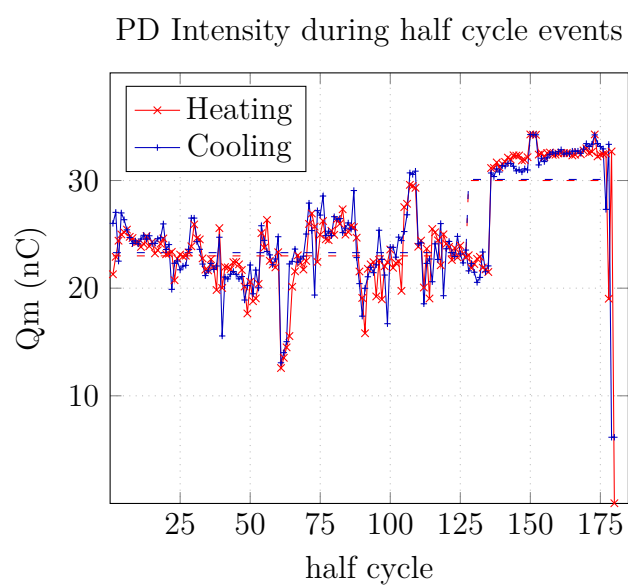


Figure 69 – Thermal cycle test 2 - Half-cycle events analysis - PD intensity averages in nC (Dashed lines are averages).

5 State Estimation

This chapter first introduces the fundamental concepts of **KF** and **EKF** and their basic equations. Both are further applied to estimate the actual state of the insulation system through partial discharge measurements. The application of KF and EKF in Simulation cases are performed in this chapter. The simulated cases are based on the partial discharge trends over aging reported by the experts. Finally, KF and EKF are applied in real accelerated aging tests results.

5.1 Kalman Filter

Rudolf Emil Kalman first introduced Kalman Filter in 1960 [77]. He presented a new recursive method to filter a given variable's measurements and provide a more accurate estimation of its state. Since then, this method is widely applied in engineering problems, such as self-drives cars, tracking objects (rockets), among others.

The KF is a tool that estimates the states of a given measurement contaminated by noise. It is essential to point out that KF is only applied for normal distribution measurements. To understand how KF works, let us start with the process and measurement model of a system. The process model defines the next state \hat{x}_k using the previous state $x(k-1)$ 5.2. On the other hand, the measurement model correlates the state vector with the measurement at step k .

$$x_k = F.X_{k-1} + B.u_{k-1} + w_{k-1} \quad (5.1)$$

where x_k is the predict value, F is the state u_{k-1} is the control vector and $w(k-1)$ is the Gaussian noise for the process model, also called process noise, with covariance Q

$$z_k = H.X_k + vk \quad (5.2)$$

where z_t is the measurement vector, H is the measurement matrix, and v is the measurement noise (Gaussian noise) with covariance R .

The KF algorithm is an iterative process based on two steps: Prediction and Update. The prediction step estimates the next state $x(k+1)$ and its uncertainty/error, equations 5.3 and 5.4, respectively. The uncertainty/error on the estimation is based on the process noise present in the system. That is, the error on the model. To understand better, taken as example a car moving at a constant speed. It is possible to predict the car's location by a simple linear system model. However, if the car goes through a hole or

mud during its way, its speed will inevitably change. The constant speed model does not predict this event. Therefore, using the constant speed linear system model to predict the car location will result in an error called process noise.

The update step is represented by four equations, including the Kalman Gain (KG) calculation. The Measurement residual 5.5 is computed first and represents the difference between the actual measurement and the predicted value. In the sequence, the KG is calculated (5.6). The KG is an essential parameter of the KF and is responsible for deciding how much weight is given to the measurement and predicted values. KG is range from 0 to 1 according to the measurement and predicts errors. If the KG value is close to 1, the prediction error is large, and the actual measurement is close to the actual values. On the other hand, if KG is close to 0, the measurement error is large, and the prediction value is close to the actual value. After the KG calculation, the state prediction and error covariance are updated, 5.7 and 5.8.

- Prediction

$$x'_k = F.X_{k-1} + B_u k - 1 \quad (5.3)$$

$$P_k = F.P_{k-1}.F^T + Q \quad (5.4)$$

Where P_k is the predict covariance, F^T is the transpose of the state transition matrix, and Q is noise. It is important to notice that the matrix Q is responsible for increasing the estimation uncertainty in each step. So the KF prediction step is responsible to calculated two predicted values, X_k , and P_K .

- Update

$$y = z - H.x'_k \quad (5.5)$$

$$KG = P_k.H^T.(H.P.H^T + R)^{-1} \quad (5.6)$$

$$\hat{x}_k = \hat{x}_k + KG.y \quad (5.7)$$

$$P = (I - KG.H).P \quad (5.8)$$

Where y is the measurement residual, z is the actual measurement, \hat{x}_k is the predicted value, KG is the Kalman Gain, and R is the measurement noise. All devices and measurement instruments present a measurement uncertainty, usually provided by the manufacturer, and the KF takes into account by the variable R .

5.2 Extended Kalman Filter

The KF is a powerful filter to estimate the state of a given variable, but only works properly in specific cases, here called as Kalman Filter assumptions:

- Linear functions
- Gaussian distribution

Most of the real-world applications involve non-linear function models, and KF does not work very well under this condition. Additionally, the addition of a Linear function with a Gaussian distribution results in a Gaussian distribution. On the other hand, the addition of a non-linear function with a Gaussian distribution results in a non-Gaussian distribution. Therefore, the non-linearity cancels both KF assumptions.

In this context, the EKF was developed to allow applications with non-linear functions. How EKF deals with non-linearity is very simple: In each time step, the non-linear function is linearized around the current estimation using the Taylor series. Thus, the KF equations can be applied in the linearized function. Let us first consider the process and measurements model of a non-linear system. 5.9 and 5.10:

$$x_k = f(x_{k-1}, u_{k-1}) + w_k - 1 \quad (5.9)$$

$$z_k = h(x_k) + v_k \quad (5.10)$$

Where f is function of the variables x_{k-1} and u_{k-1} , used to calculate the current state (x_k). h is the measurement function, that correlate the the variable x_k with the z_k . To apply the EKF is necessary to calculate the Jacobian matrix in each time step k , that is, the F_k and H_k as shown in 5.11 and 5.12.

$$F_k = \left. \frac{\partial f}{\partial x} \right|_{\hat{x}_k, u_k} \quad (5.11)$$

$$H_k = \left. \frac{\partial h}{\partial x} \right|_{\hat{x}_k} \quad (5.12)$$

Thus, the EKF equations can be calculated as shown in the equations 5.13, 5.14, 5.15, 5.16, 5.17 and 5.18.

- Prediction

$$\hat{x}_k = f(\hat{x}_{k-1}, u_{k-1}) \quad (5.13)$$

$$P_k = F_{k-1}.P_{k-1}.F_{k-1}^T + Q \quad (5.14)$$

- Update

$$y_k = z_k - h.(\hat{x}_k) \quad (5.15)$$

$$KG_k = P_k.H_k^T.(H_k.P_k.H_k^T + R)^{-1} \quad (5.16)$$

$$\hat{x}_k = \hat{x}_k + KG_k.y_k \quad (5.17)$$

$$P_k = (I - KG_k.H_k).P_k \quad (5.18)$$

5.3 State Estimators Apply to Partial Discharges Measurements

The PD measurements of the insulation system of hydrogenerators provide us valuable information about the actual insulation condition. On the other hand, KF and EKF are state estimators. They are used to provide better estimations about unknown variables using input measurements. Moreover, these state estimators have been applied to useful life estimation [78],[79],[80],[81], and [82].

Thus, The proposal is an online method to accurately predict the RUL of stator insulation systems tracking the PD by KF/EKF.

The degradation model of the stator insulation system is based on the PD. The KF/EFK estimate the coefficients of the degradation model and the RUL can be calculated. In this application, the degradation model coefficients are estimated online. Thus, the PD trend changes over agings will automatically be adjusted by the algorithms in each new measurement.

5.3.1 Algorithm for Hydrogenerators

The algorithm considered the PD trend depicted in Figure 70. The figure observation leads to four stages:

- Stage 1 - in new windings the PD trend drops over machine service. The insulation resin maturation might explain this behavior;
- Stage 2 - Q_m stays constant during the machine's useful life;
- Stage 3 - Q_m rise due to insulation aging/deterioration. In this stage, it is essential to perform the diagnostic and, if possible, the appropriated maintenance actions, as determined in the proposal methodology ??;

- Stage 4 - Q_m is constant and present high-levels of PD. In this stage, the insulation failure is imminent.

The algorithm takes into account the final three stages (2, 3, and 4) and is depicted in figure 71.

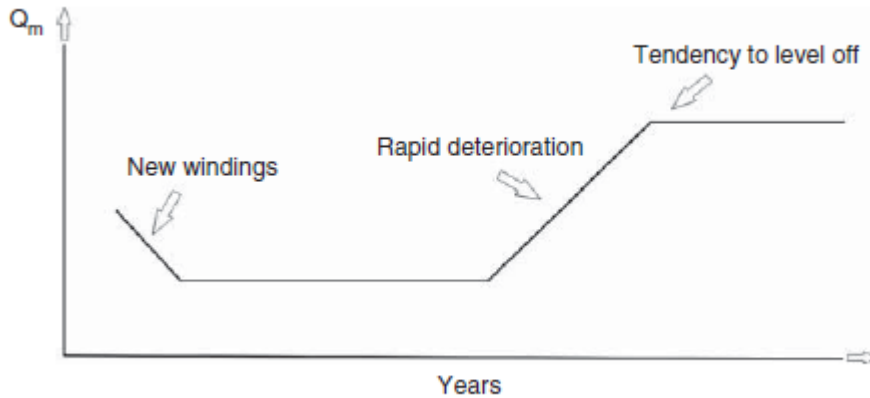


Figure 70 – Partial Discharges Trends [18]

The algorithm does three important tasks:

- Filter the data by KF during the useful life (stage 2)
- Detect aging/deterioration in the insulation system by Q_m rise. This task represents the identification of the transition moment from stages 2 to 3;
- Estimate the RUL. If the insulation is in stage 2, normal operation condition, the statical analysis provides the RUL estimation. On the other hand, when the insulation is in stage 3, the KF/EKF identifies the degradation model parameters and estimate the RUL by extrapolation to a Q_m threshold.

5.3.2 Partial Discharges Levels

It is important to define what is a critical values for PD to establish the Q_m threshold used to predict the RUL. The work [83] present comparative analysis for Q_m , based in over 225.000 tests. Table 13 present the result of this comparative analysis for hydrogenerators, according to voltage levels.

The PD level classified as critical present Q_m higher than 95% of registered data for similar machines (PD level > 95% of similar machines). For example, machines rated between 13-15 kV, Q_m values equal/above 560 mV are classified as critical, and this PD value is higher than 95% of the registered values for similar machines with this voltage level.

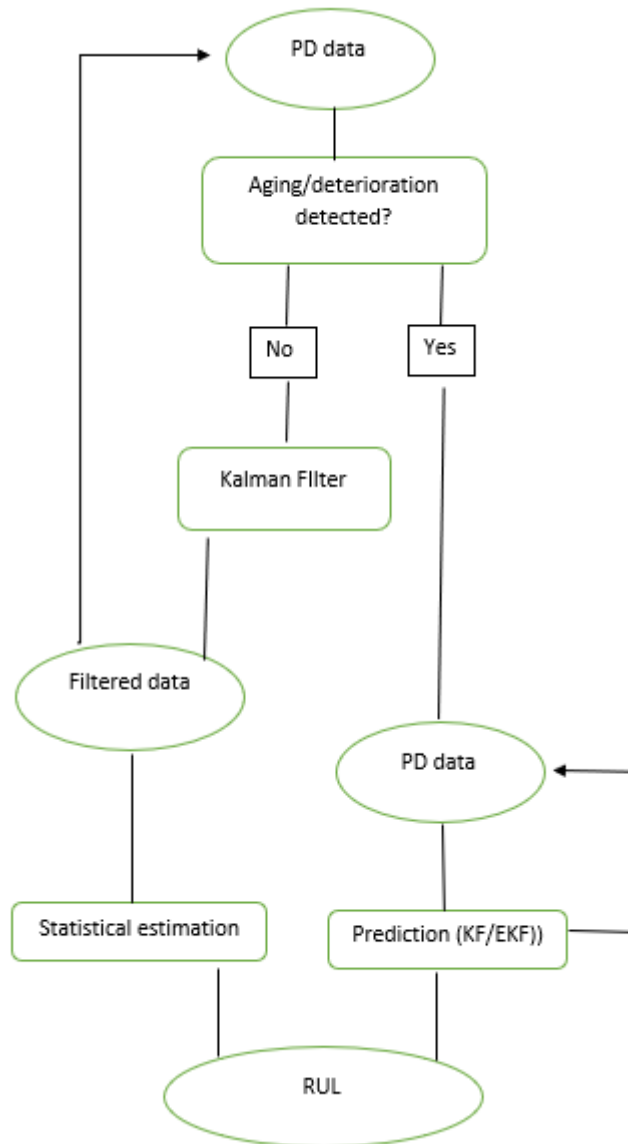


Figure 71 – Algorithm for Hydrogenerators

Thus, Q_m threshold for the proposed algorithm is defined in equation 5.19:

$$Q_{mL} = 1,5.Q_{mC} \quad (5.19)$$

Where Q_{mL} is the threshold considerate in the RUL estimation, and Q_{mC} is the critical value (critical classification for Q_m based in table 13).

5.3.3 Degradation model

The degradation model is defined based on life-working experience trends from [21], and [84]. It is important to note that this degradation model definition is an initial model. Based on the chapter 3.2, the better approach is to define a degradation model for each failure mode because they have different deterioration rates. This strategy leads to years or decades of accelerating agings tests and hydropower plant monitoring. Thus,

Table 13 – Hydrogenerators with coupling capacitor 80 pF - Qm values (mV)

PD Level	6-9 kV	10-12 kV	13-15 kV	16-18 kV	>19 kV
insignificant	13	19	35	36	76
Low	34	48	91	110	137
Normal	70	102	189	278	255
High	236	229	372	588	718
Critical	364	376	560	768	861

the solution is to propose an initial model and update it over time, as more results are available.

The degradation model is divided into 2 stages: the useful life stage, where Q_m is constant over time, and the Deterioration stage, where Q_m rises over time. In the useful life stage, a zero-order polynomial linear KF model is used, as show equations 5.20, 5.21, and 5.22. Here x_k is a state variable that represent Q_m .

- Useful Life Model

- State variables

$$x_k = \begin{bmatrix} x_k \\ 0 \end{bmatrix} \quad (5.20)$$

- State Transition matrix

$$F = \begin{bmatrix} 1 & 0 \\ 0 & 0 \end{bmatrix} \quad (5.21)$$

- Measurements Matrix

$$H_k = \begin{bmatrix} 1 & 0 \end{bmatrix} \quad (5.22)$$

To represent the deterioration stage, two models are tested: an exponential model of the form ae^{bt} to represent an intense degradation (5.23, 5.24 and 5.25); an inclined straight line model at to represent a slower degradation process (5.26, 5.29 and 5.28). In the exponential model functions f and h are locally linearized to produce F and H.

- Rapid Deterioration Model(Exponential Model)

- State Variables

$$x_k = \begin{bmatrix} a_k e^{b_k k} \\ a_k \\ b_k \end{bmatrix} \quad (5.23)$$

- State Transition matrix

$$F_k = \left. \frac{\partial f}{\partial x} \right|_{\hat{x}_k} = \begin{bmatrix} 0 & e^{b_k k} & k a_k e^{b_k k} \\ 0 & 1 & 0 \\ 0 & 0 & 1 \end{bmatrix} \quad (5.24)$$

- Measurement matrix

$$H_k = \left. \frac{\partial h}{\partial x} \right|_{\hat{x}_k} = [1 \ 0 \ 0] \quad (5.25)$$

- Slow Deterioration Model (Linear Model)

- State Variables

$$x_k = \begin{bmatrix} x_k \\ \dot{x}_k \end{bmatrix} \quad (5.26)$$

- State Transition Matrix

$$F_k = \begin{bmatrix} 1 & \Delta t \\ 0 & 0 \end{bmatrix} \quad (5.27)$$

- Measurement Matrix

$$H_k = [1 \ 0] \quad (5.28)$$

where \dot{x} is the rate of Qm variation and represent the coefficient a from the linear model.

5.3.3.1 Test results Simulation

The simulation of some PD trends over insulation aging was performed to validate the proposed algorithm (subsection 5.3.1). Thus, we considered different PD trends. Figure 72 shows PD trends for electrical stress and mechanical & thermal stress for different discharges: internal, corona, and slot discharges. Here the preference was the internal discharge trends. These trends were used to simulate test results to validate the proposed algorithm.

Simulation 1

Table 14, 15, 16, 17, 18, 19, 20 present details about the PD tendency simulated and the simulation parameters. In all the simulations the true useful life is calculated by:

$$TrueUL = L_{time} - t_{op}. \quad (5.29)$$

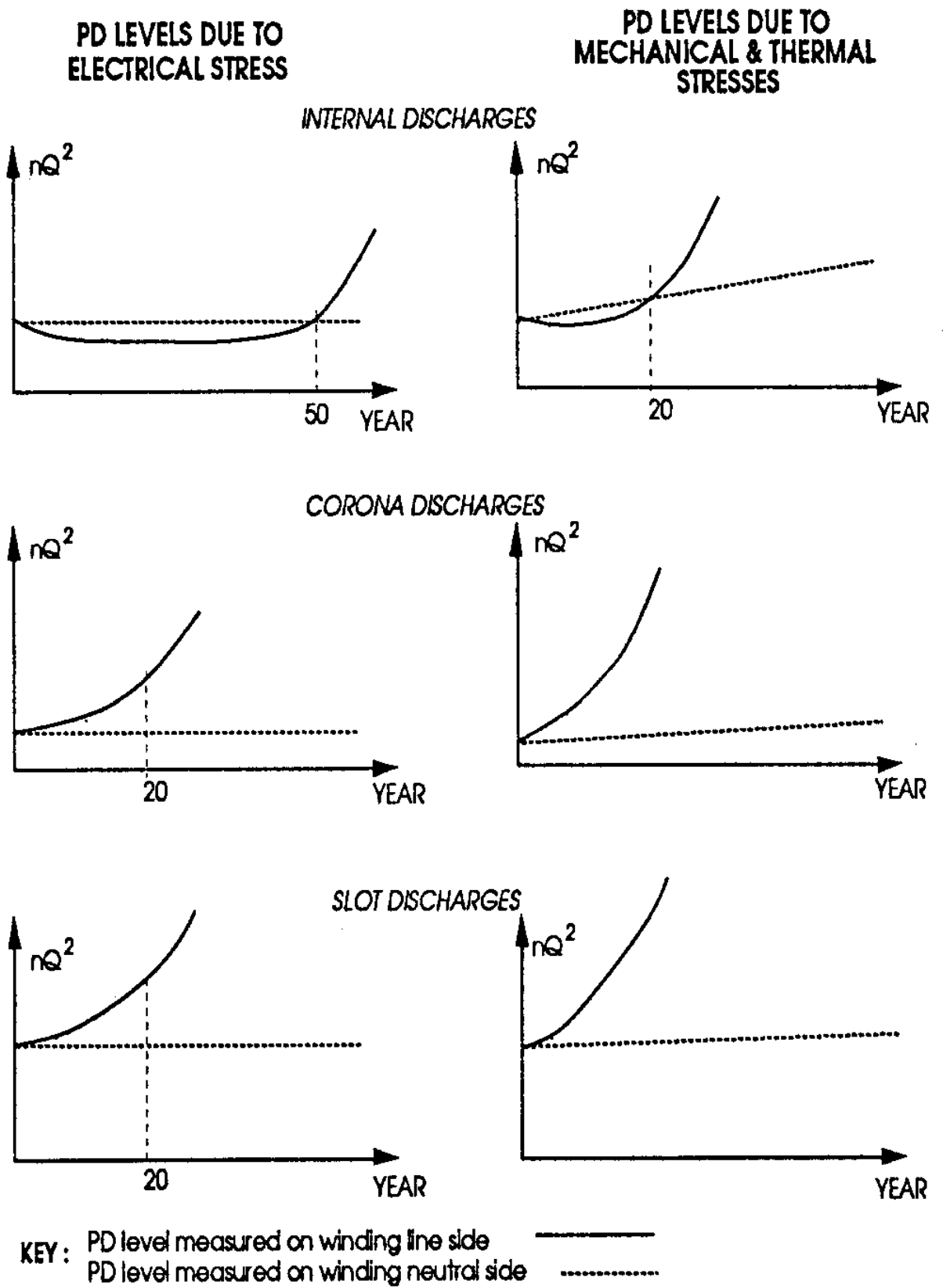


Figure 72 – Partial Discharges Trends [21]

L_{time} is the total operation time observed in years, and t_{op} is the actual operation time in years, represented in all graphics simulated in the horizontal axis. In the simulation 1 and

2, the true value by PD trend represents the RUL true estimation based on exponential model. This variable is important to observe the accuracy of the estimation by EKF.

In simulation 1, the PD values stay in the useful life stage for 20 years. After that, the exponential rise in for Q_m value is set. The mechanical and thermal stress simulated lead to an early end of life. Q_{mL} in the simulation is equal to 840 pC (generator voltage range 13,8-15 kV). Detail about PD evolution, KF, and EKF estimates for Q_m is present in figure 73. Figure 74 shows the RUL estimation over time. The statistical estimation is valid for about 20 years. After that, the EKF estimate the RUL. Detail about this transition moment is depicted in Figures 75. The statistical estimation presents a higher error (compare to the true RUL estimation red curve). The EKF adjust the estimation after aging/deterioration is detected. The estimation by EKF is very accurate from 21,4 years. At the time of 24,7 years, Q_m reach the limit value, and the RUL is equal to zero. Figure 76 shows the state variables estimations over time. The coefficient a and b are stabilized around 21 years (horizontal axis Time).

In simulation 2, the useful life stage lasts 50 years, simulated a slower aging process by electrical stress. After that, an exponential increase in Q_m is set. The Q_{mL} is 1054 nC (generator rated at 16-18 kV). Figure 77 shows the PD measurement, the KF estimation during the useful life, and the EKF estimation after aging/deterioration detection. The RUL estimation is showed in figure 78. In this simulation, the statistical estimation is more close to the true RUL. The EKF prediction starts at 50 years. This estimation is very accurate from the 52 to 58 years (79). Figure 80 represents the state variables estimation for simulation 2. The coefficients a and b became stable from 51 years. It is essential to point out that the coefficients a and b start to be estimated in both simulations after the algorithm detect aging/deterioration by a change in the PD pattern.

In simulation 3, the EKF was tested over a possible PD trend variation. The change in the exponential trend was set at 3,5 years. Figure 81 represents how the EKF adjust the estimation. Figure 82 represents the RUL estimation. Figure 83 shows the behavior of the state variables. At the 3,5 years, it is observed a degree in both coefficients a and b. That is how the EKF adjusts over a change in exponential trend.

In Simulation 4, a slower deterioration model is tested. Thus, after 65 years, a change in the PD pattern is set. Q_m rises according to a linear model and reach the threshold (1054 pC in this simulation) around 85 years (figure 84). In this simulation, the statistical estimation is lower than the true RUL (figure 85). When the algorithms detect aging/deterioration, the RUL estimation by KF adds more years to the previous statistical estimation. That is observed by a positive degree in the red dot line of figure 86. Figure 87 represents the state variables over time. In this model, just the coefficient a is present.

Table 14 – Simulation 1

Case 1 - PD Trend Due to Mechanical and Thermal Stress - Voltage Range 13-15 kV			
Partial Discharges	Qm (mV)	Equation	Time (years)
Normal Condition	Around 30	$Q_m = 30$	From 0 to 20
Rapid deterioration	From 30 to 840	$Q_m = 30 e^{0.7.t}$	From 20 to 25

Table 15 – Simulation 1 - Parameters

Useful Life Model	
Parameter	Values
Measurement Noise (R)	5
Process Noise (Q)	0.5
Initial State Covariance (P)	0.1
Rapid Deterioration Model	
Parameter	Values
Measurement Noise (R)	5
Process Noise of state variable 1	0.001
Process Noise of state variable 2	0.001
Process Noise of state variable 3	0.001
Initial State Covariance (P) for all states	0.1
Exponential parameters	
a	30
b	7

Table 16 – Simulation 2

Case 2 - PD Trend Due to Electrical Stress - Voltage Range 16-18 kV			
Partial Discharges	Qm	Equations	Time (years)
Normal Condition	Around 100	$Q_m = 100$	From 0 to 50
Rapid deterioration	From 100 to 1152	$Q_m = 100e^{0.3.t}$	From 50 to 60

Table 17 – Simulation 2 - Parameters

Useful Life Model	
Parameter	Values
Measurement Noise (R)	5
Process Noise (Q)	0.5
Initial State Covariance (P)	0.1
Rapid Deterioration Model	
Parameter	Values
Measurement Noise (R)	5
Process Noise of state variable 1	0.0001
Process Noise of state variable 2	0.001
Process Noise of state variable 3	0.001
Initial State Covariance (P) for all states	0.1
Exponential parameters	
a	100
b	0.3

Table 18 – Simulation 3

Rapid Deterioration Model	
Parameter	Values
Measurement Noise (R)	5
Process Noise of state variable 1	0.0001
Process Noise of state variable 2	0.001
Process Noise of state variable 3	0.001
Initial State Covariance (P) for all states	0.1
Exponential Parameters	
Initial	
a	30
b	0.2
Final	
a	70
b	0.2

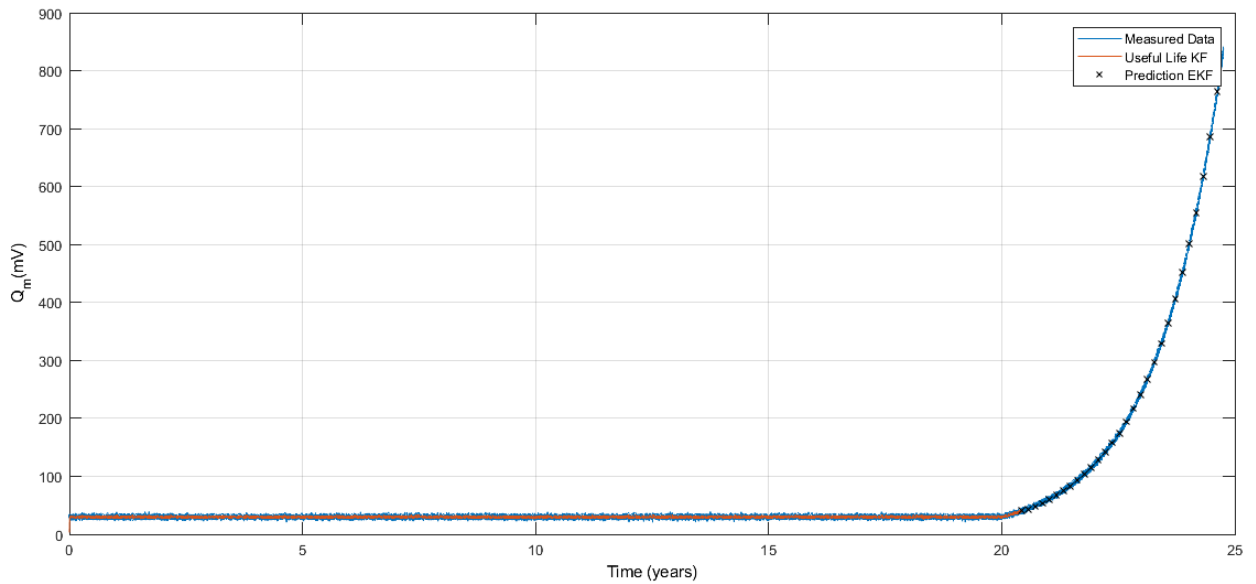
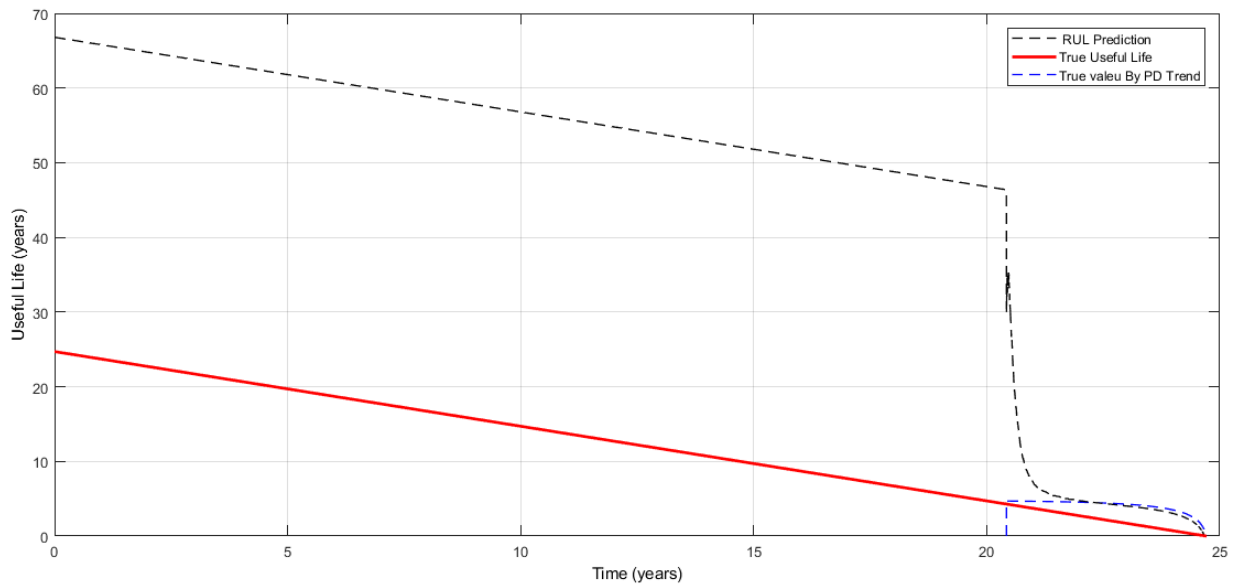
Figure 73 – Simulation 1 - Q_m over Time

Figure 74 – Simulation 1 - RUL over Time

5.4 Algorithm application in Thermal Cycle Test 2

Here the proposed algorithm to predict the RUL was used in the Thermal cycles Test 2 results. The following results represent an actual case application for the proposed algorithm to predict the RUL. Figure 88 presents the measurement results, the estimation values for the useful life stage, and the estimated values for the deterioration/aging stage for Q_m . The algorithm filters the data in the useful life and successfully detects the change in PD pattern around cycle 120. After that moment, the PD rises until the 180 cycles. The algorithm performs the prediction of the RUL by tracking the PD values from 120 to 180 cycles. Here the proposed algorithm to predict the RUL was used in the Thermal cycles

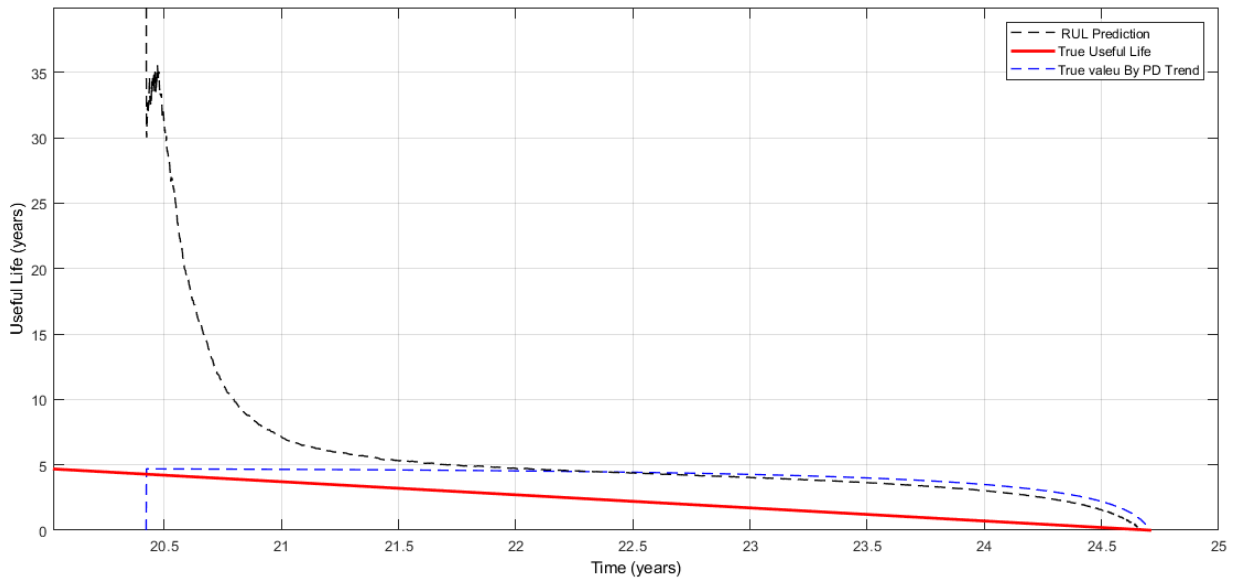


Figure 75 – Simulation 1 - RUL versus Time (zoom)

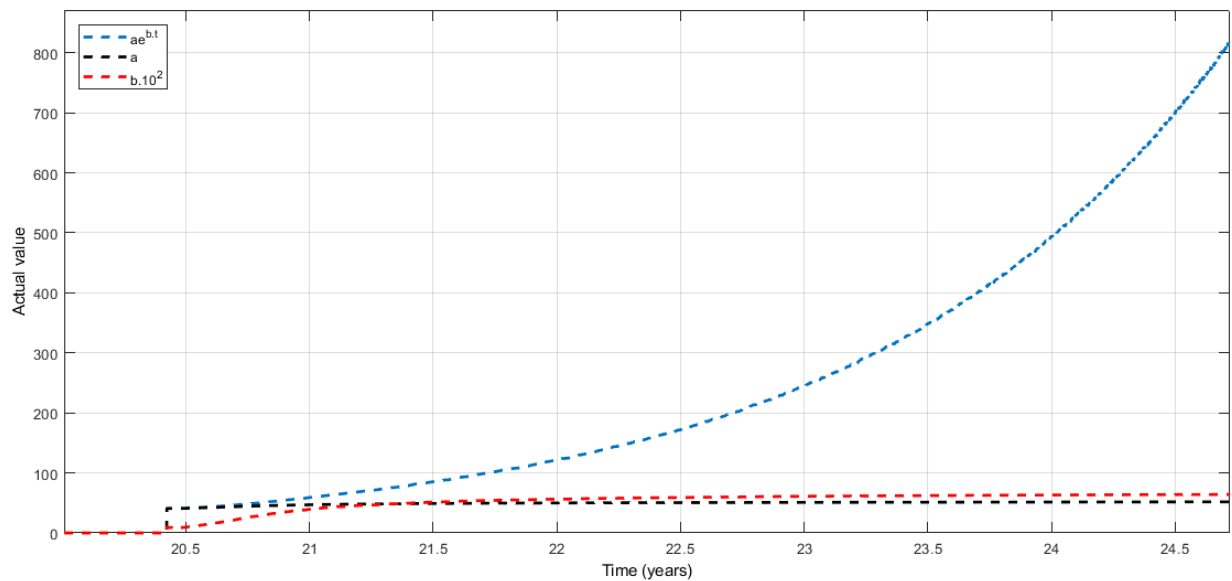


Figure 76 – Simulation 1 - State Variables over Time

Test 2 results. The following results represent an actual case application for the proposed algorithm to predict the RUL. Figure 88 presents the measurement results, the estimation values for the useful life stage, and the estimated values for the deterioration/aging stage for Q_m . The algorithm filters the data in the useful life and successfully detects the change in PD pattern around cycle 120. After that moment, the PD rises until the 180 cycles. The algorithm performs the prediction of the RUL by tracking the PD values from 120 to 180 cycles.

Figure 89 shows the RUL estimation for the insulation system under test. In this case, the time and the RUL estimation are in cycles. During the normal operation condition, the statistical estimation is replaced by the number of cycles recommended for

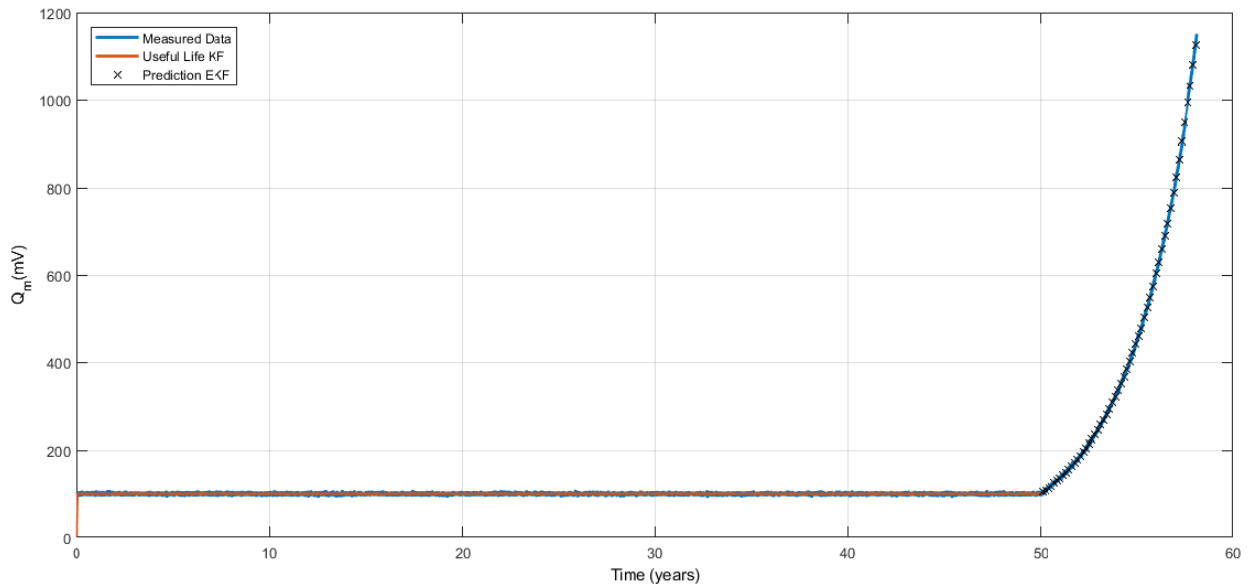
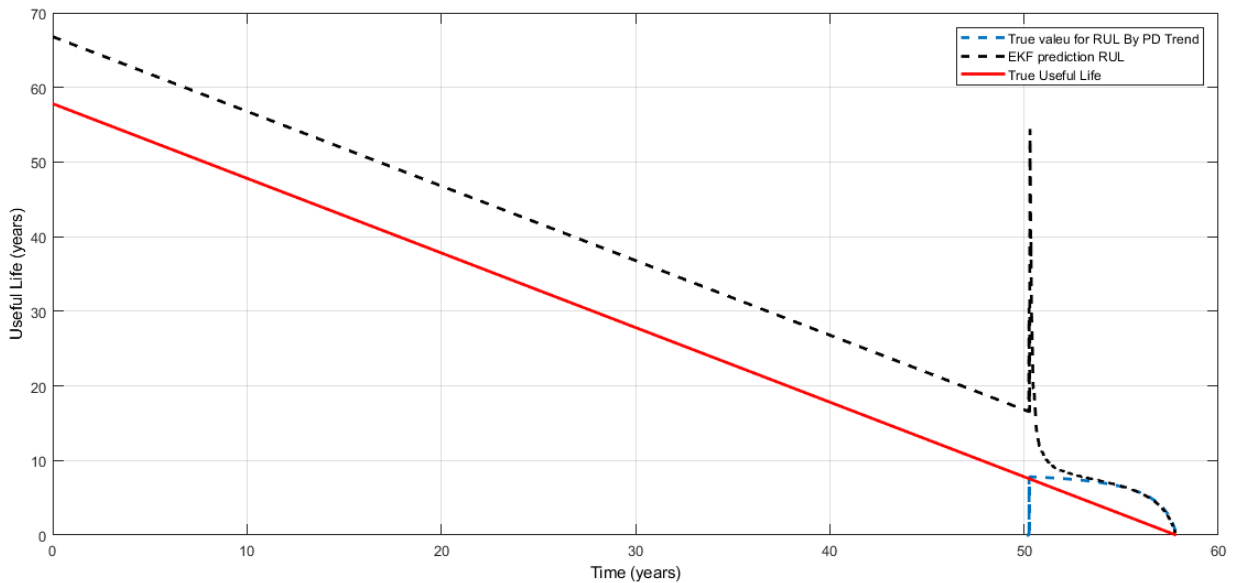
Figure 77 – Simulation 2 - Q_m over Time

Figure 78 – Simula 2 - RUL over Time

thermal cycle tests in stator winding [62](500 cycles). It is essential to point out the Q_{mL} used in the estimation. Q_m rises from 120 to 160 cycles (time instant), and its limit value is equal to 34 nC. After that, the Q_m value saturates. In this saturation stage, insulation failure is imminent. The proposal algorithm predicts the time instant Q_m reaches saturation. Thus, Q_m and true useful life used are 34 and 160 cycles, respectively. The algorithms accurately predict the RUL because of the prediction model based on the PD trend, as can be observed (90).

The useful life stage goes until cycle number 120. The algorithm detects the change in the PD pattern, and the RUL estimation based on the PD trend is set. After that, RUL prediction approximates very quickly to the useful true life (90). It shows that the

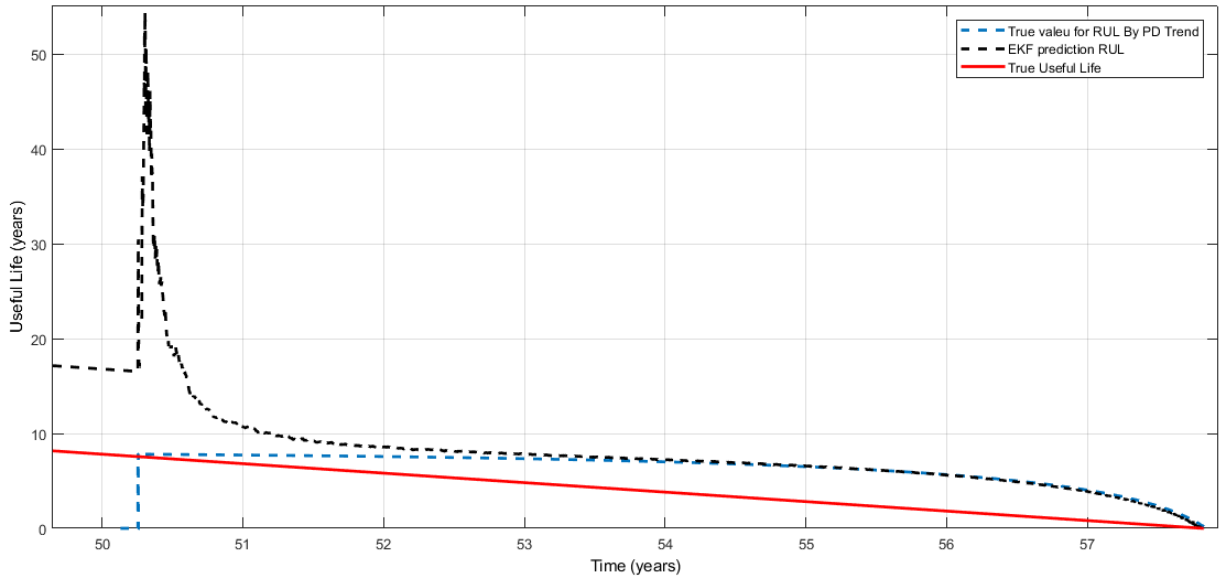


Figure 79 – Simulation 2 - RUL over time (zoom)

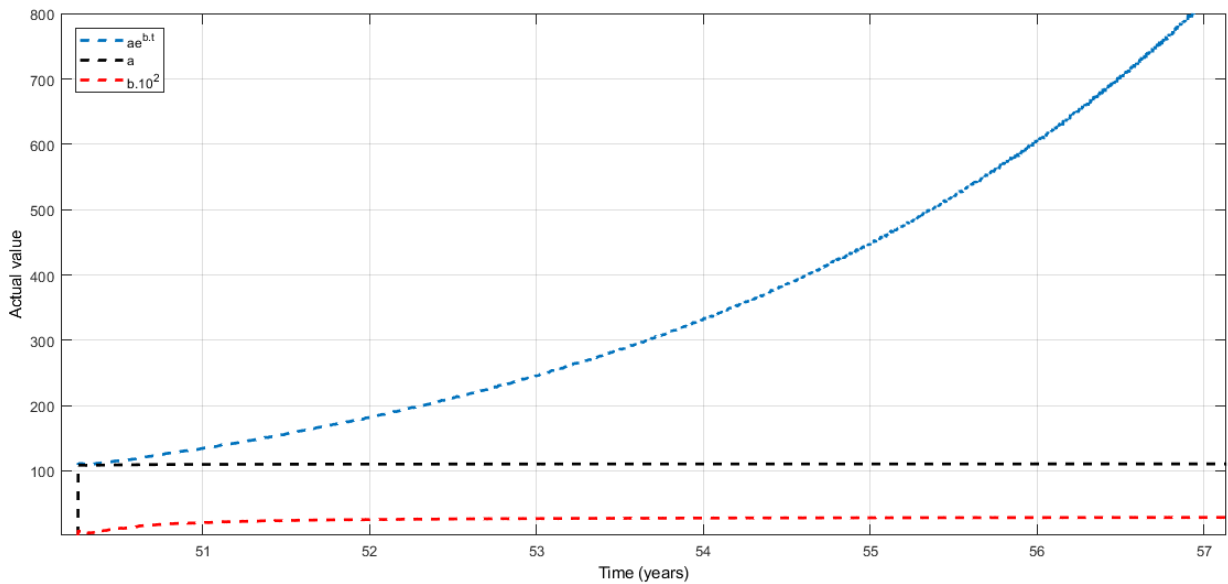


Figure 80 – Simulation 2 - State variables over Time

proposed model performs appropriately to estimate the RUL with real case data.

Finally, figures 91 and 92 show the predicted state variables for the KF prediction. The coefficient a is stable and presents a value around 0.135 after the algorithm detects the PD change in the pattern. The coefficient presents a little oscillation due to the high measurement noise.

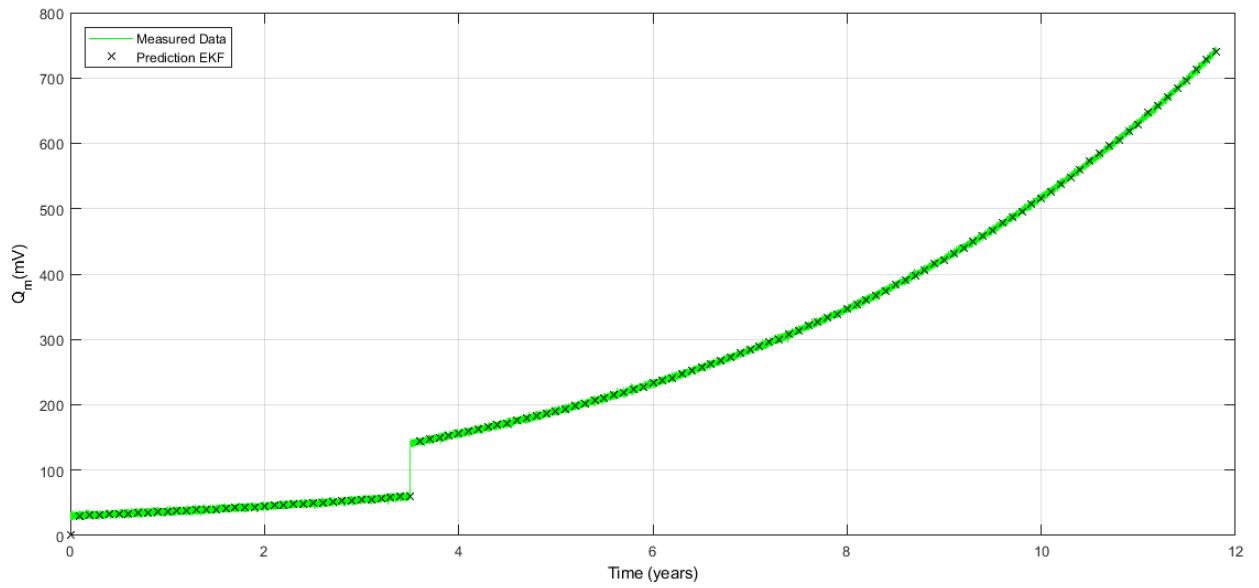


Figure 81 – Simulation 03 - Q_m over time

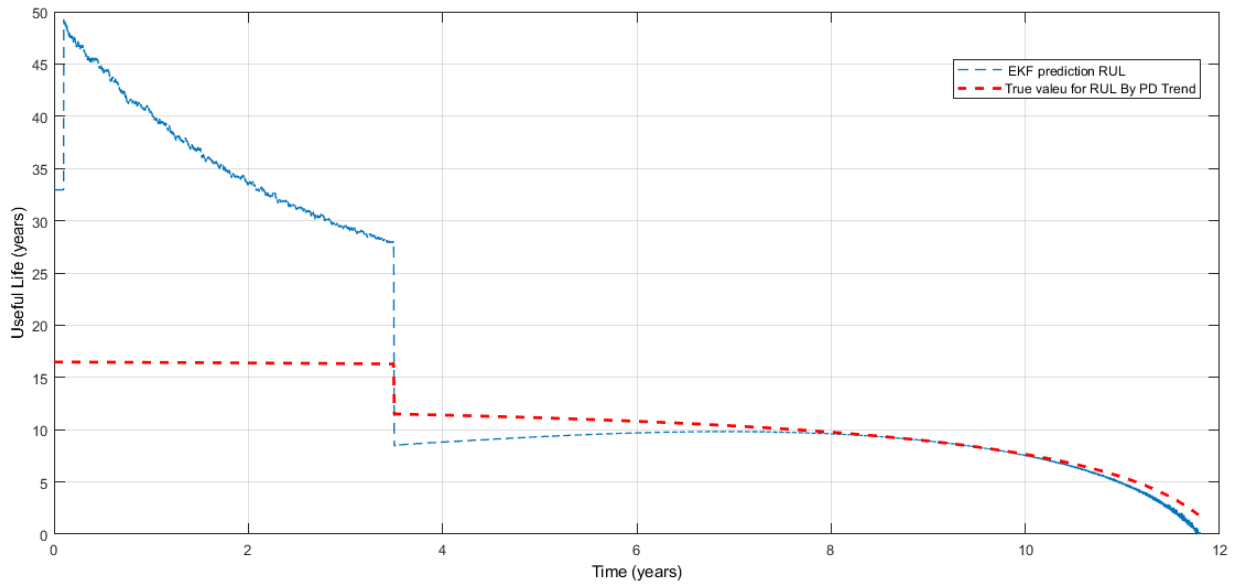


Figure 82 – Simulation 03 - Tendency Change Simulation

Table 19 – Simulation 4

Case 4 - PD Trend Due to Electrical Stress - Voltage Range 16-18 kV			
Partial Discharges	Q_m	Equations	Time (years)
Normal Condition	Around 100	$Q_m = 100$	From 0 to 65
Slow deterioration	From 100 to 1152	$Q_m = 50.t$	From 65 to 85

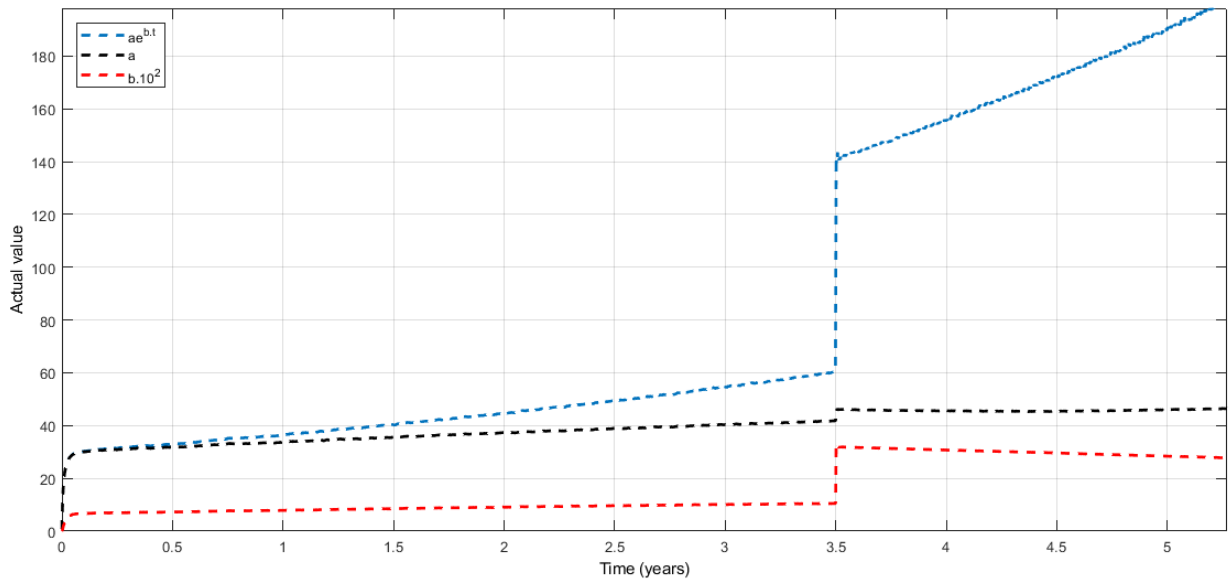


Figure 83 – Simulation 03 - State Variables over Time

Table 20 – Simulation 4 - Parameters

Useful Life Model	
Parameter	Values
Measurement Noise (R)	10
Process Noise (Q)	0.5
Initial State Covariance (P)	0.1
Slow Deterioration Model	
Parameter	Values
Measurement Noise (R)	10
Process Noise of state variable 1	0.1
Process Noise of state variable 2	0.1
Process Noise of state variable 3	0.001
Initial State Covariance (P) for all states	0.1
Linear parameter	
a	50

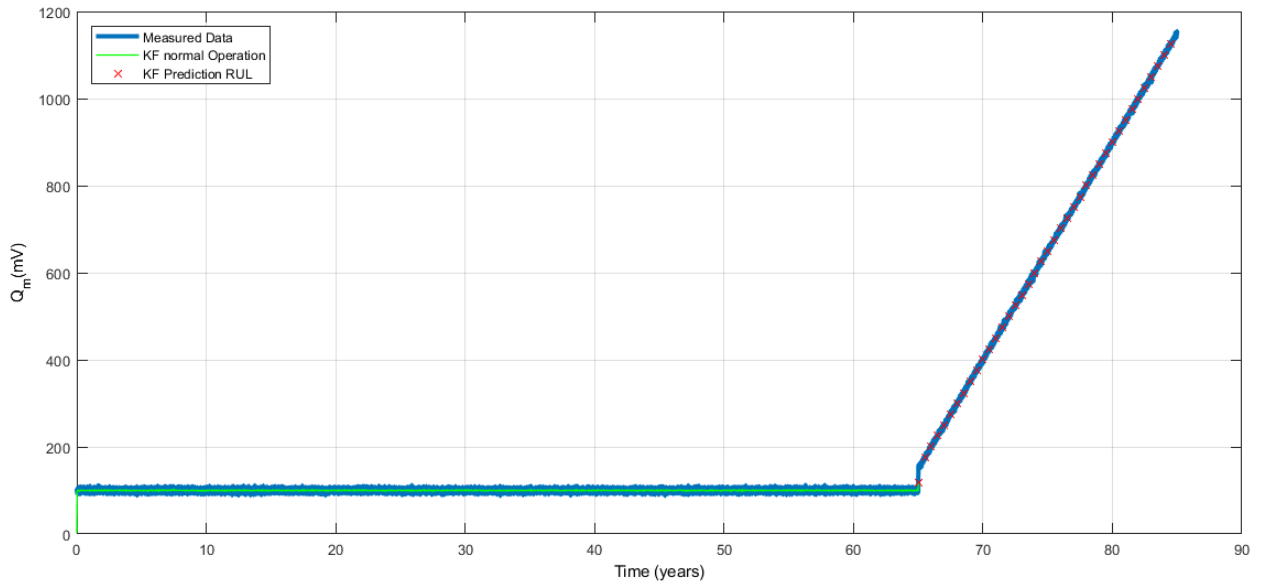


Figure 84 – Simulation 04 - Q_m x time

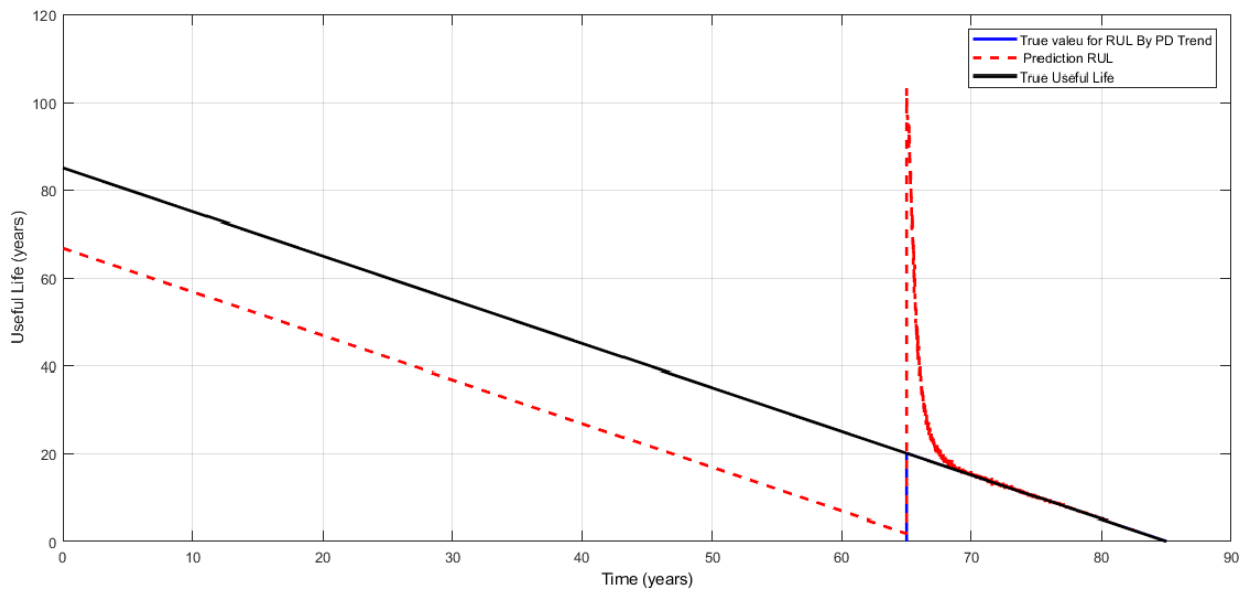


Figure 85 – Simulation 04 - RUL over Time

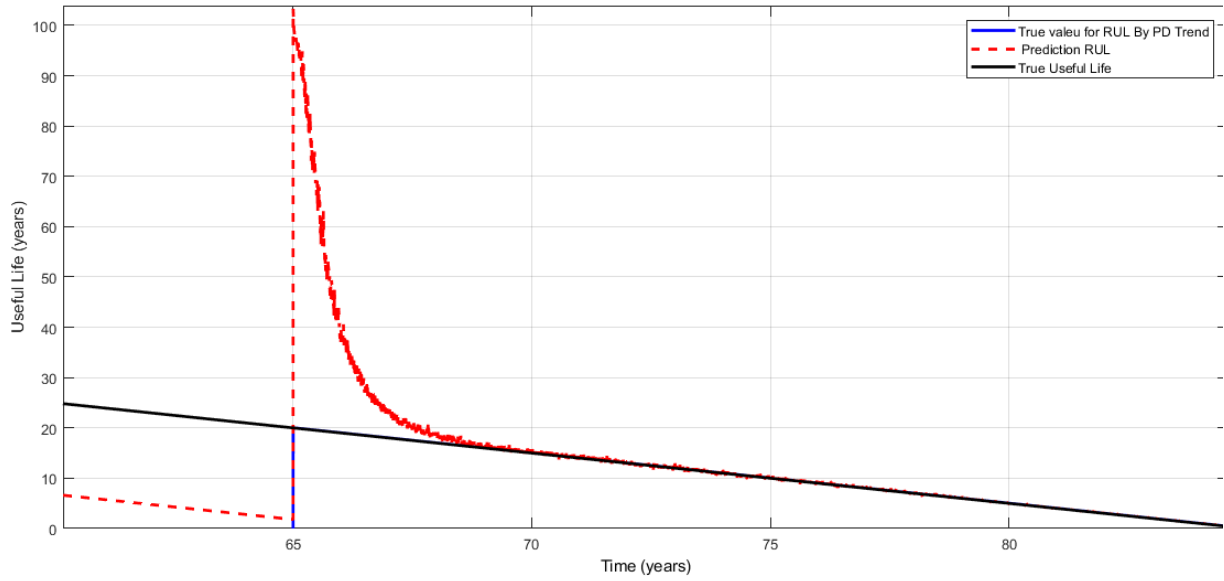


Figure 86 – Simulation 04 - RUL over Time (zoom)

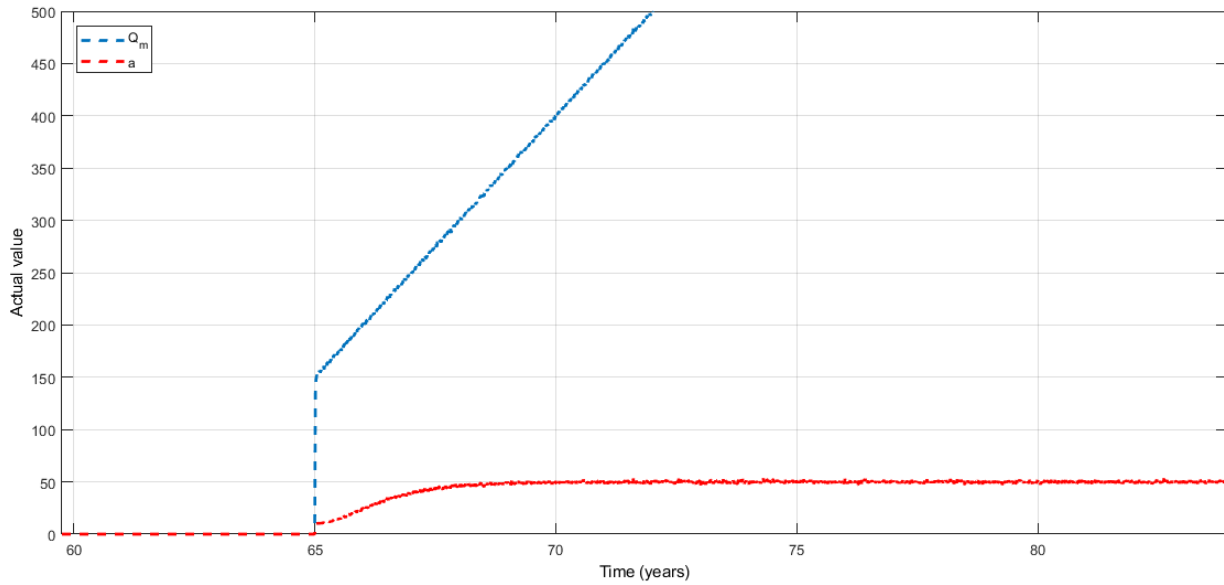


Figure 87 – Simulation 04 - State Variables over Time

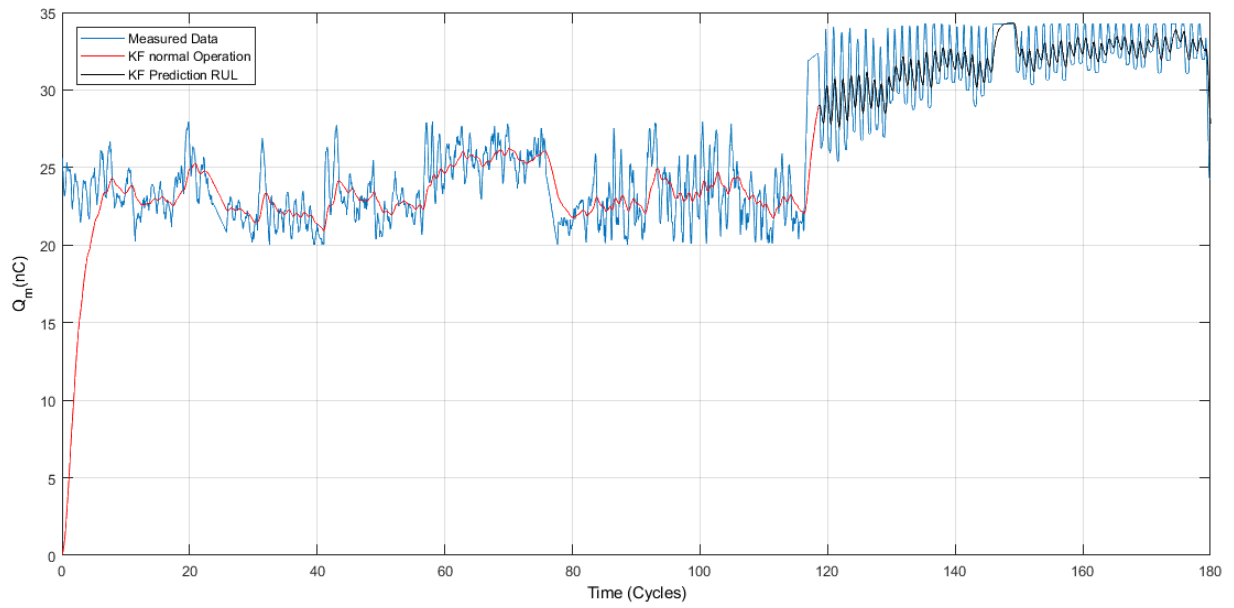


Figure 88 – Thermal Cycle Test 2 - Q_m over Cycle

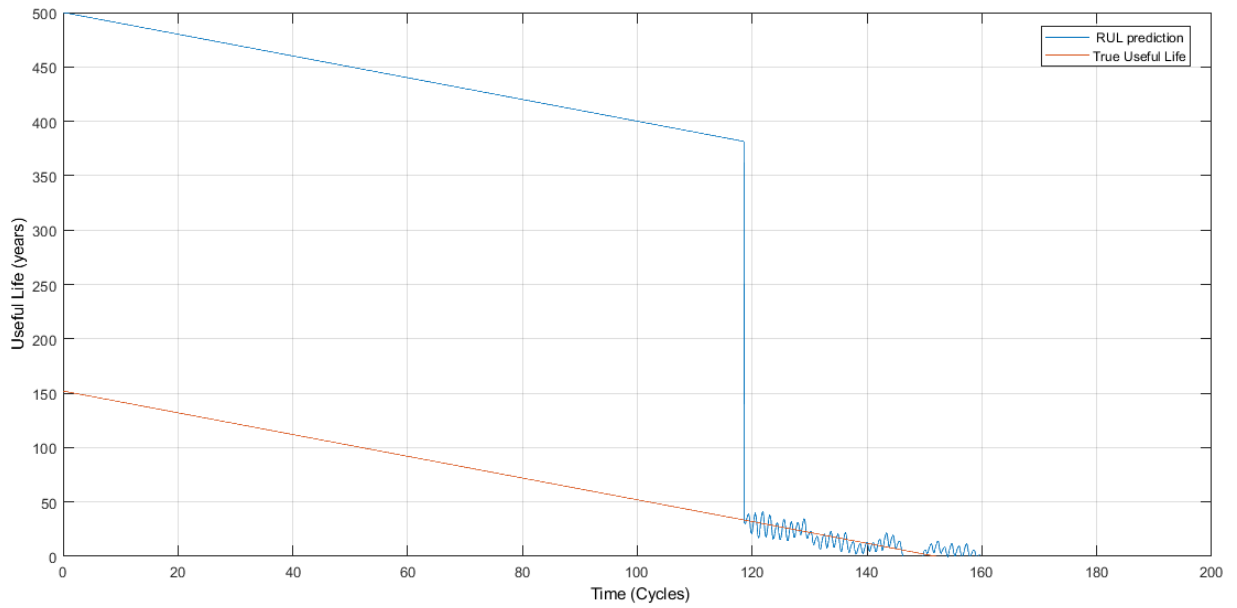


Figure 89 – Thermal Cycle Test 2 - RUL over Cycles

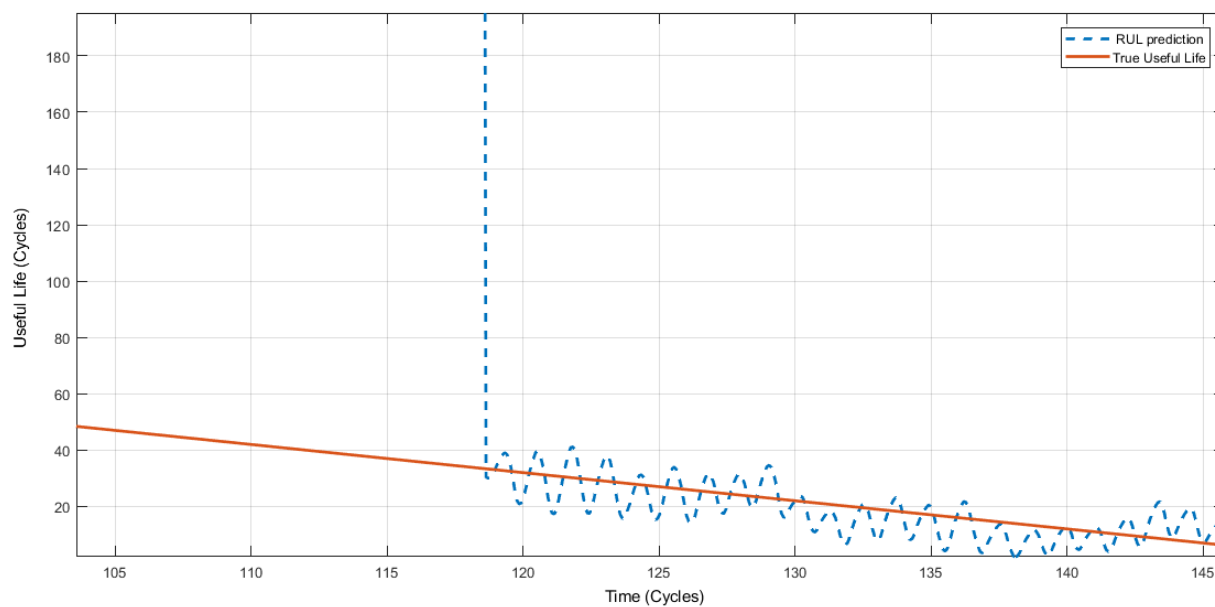
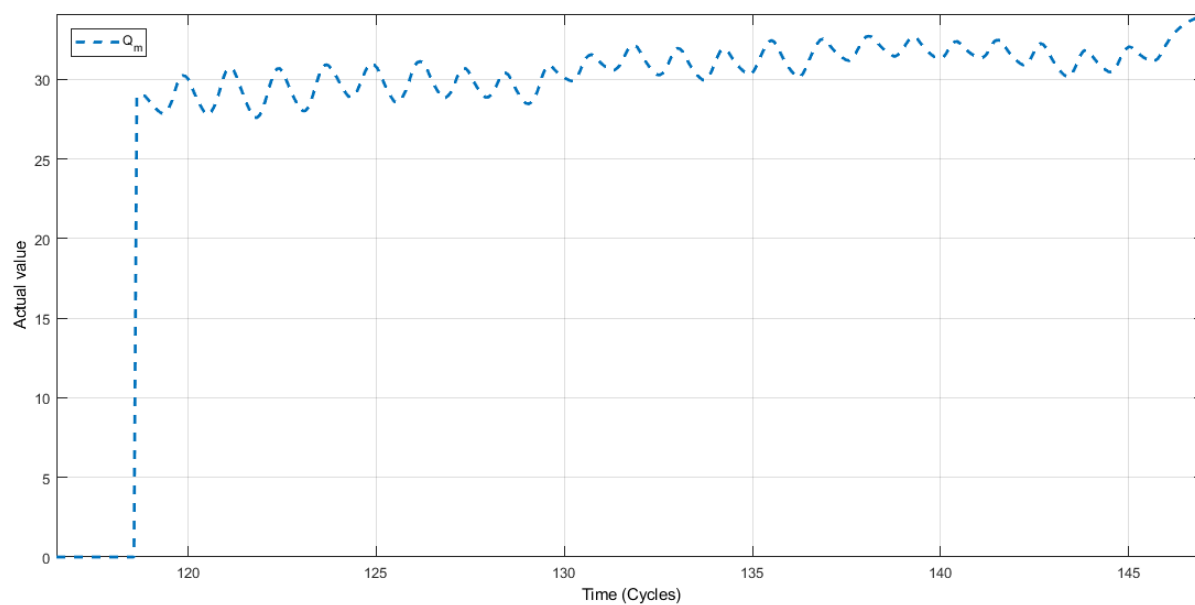


Figure 90 – Thermal Cycle Test 2 - RUL over Cycles

Figure 91 – Thermal Cycle Test 2 - State Variable (Q_m) over Cycles

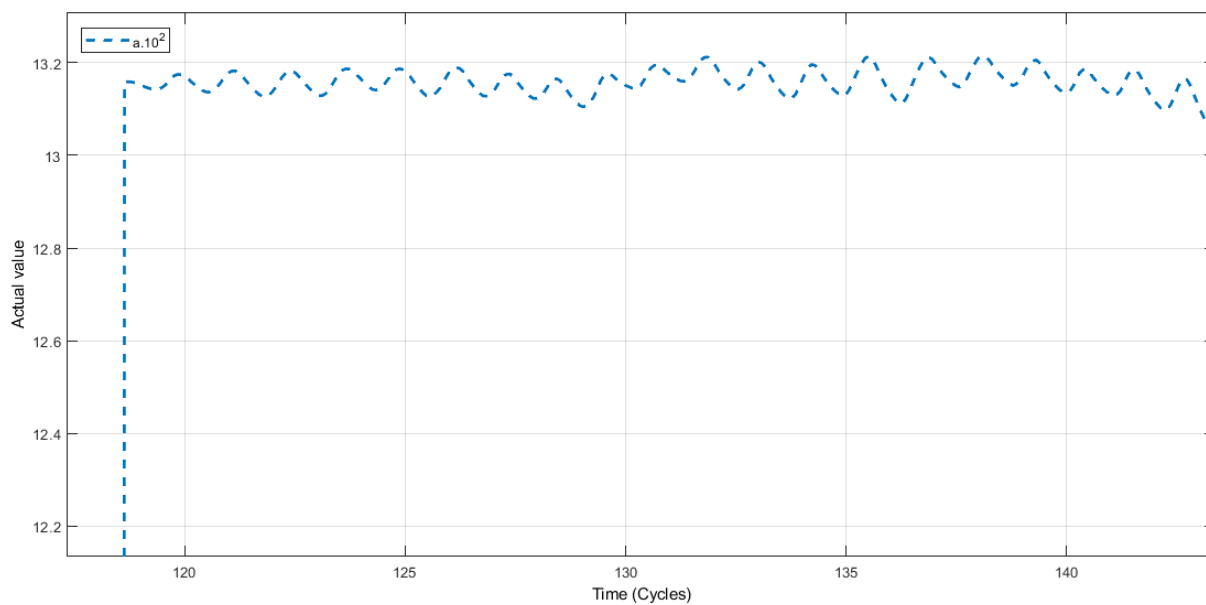


Figure 92 – Thermal Cycle Test 2 - State Variable (a) over Cycles

6 Conclusion

This thesis presents a proposed scheme to predict hydro generators' remaining useful life by combining statistical analyses of generators lifetime, PI System tools, accelerated aging test in stator windings specimens, hydropower plant monitoring, and estate estimators (KF and EKF). This proposed scheme can be integrated into hydropower plants' maintenance strategies as part of the condition-based maintenance. The main contribution of this work is a predictive model for the remaining useful life of the hydrogenerators.

The statistical analysis evaluate all hydro Generators' service life from Cemig Generation Complex, which has 6068 MW of installed power, being 96,6% hydraulic generation. The result is an average service life of 57,7 years, applying a constant failure rate for the useful life and a quadratic failure rate to represent the aging stage. This estimation is valid during the useful life stage, where the PD values are constants.

The PI system tools are employed to facilitate the analysis of the variables monitored. All data is stored in the PI server, and by using the Client Tools is easy to visualize, manage and access the data. The diagnostic of aging/intense deterioration and the identification of PD trends are remarkably facilitated through PI system application. The expanding use of the proposed method by monitoring more power plants and developing other aging tests have PI system utilization as the base.

The accelerated aging test scheme and procedures represent a secondary contribution of this work. The voltage applied test did not result in invalid data to the prediction model. However, essential details and conclusions were learned during the test. First, the electrical stress alone hardly leads a stator bar/coil specimens to fail. This statement converges with what is reported in the developed bibliographic review. The electrical stress is likely the final cause of an insulation breakdown, but not the root cause. Second, to track the tendency to fail in the PD measurements, the PD data acquisition must be continually taken. The accelerated aging test must have to be performed until an insulation breakdown if the objective is to predict the useful life.

These conclusions were applied in the thermal cycle test. Therefore, the proposed thermal cycle test present some modifications in the procedures, compared to the suggested in the [62]. The first modification was the voltage application over test development. This adjustment enables the continuous PD measurement over insulation aging, important to RUL prediction. Moreover, the final cause of an insulation breakdown, the electrical stress, is present during stator bar/coil aging. As a result, it enables the test performance until an insulation breakdown. The test results show that the proposal thermal cycle test presented significant data to predict the RUL. A clear tendency to failure was

observed in the results. Even though there are reports in the literature of PD trends over aging, usually observing during life experience, there is no work with continuous partial discharge measurements in the accelerated aging test, showing a tendency in PD values before an electrical failure.

The state estimators, KF and EKF, were applied to predict the RUL based on the actual insulation state. An algorithm filters the PD data during the normal condition operating, identifies changes in the PD pattern, and sets the RUL prediction based on the PD trend. The algorithm uses KF and EKF to filter and estimates the RUL. Exponential and linear deterioration models based on Q_m values were used to track PD tendency to fail and estimate the RUL. Both models were successfully applied. Moreover, the algorithm was applied in the Thermal cycle test 2. The good results validated the proposed algorithm in a real case application.

The application and widespread of this methodology will improve the accuracy of the prediction over time.

Since each failure mode has a specific deterioration rate, the ideal scenario for future works is to develop an accelerated aging test that emulates each failure mode affecting the hydro-generators stator insulation system. The diagnostic of the failure mode by PD is another possible work essential to the condition-based maintenance. The utilization of different features in the partial discharge pulse is not so much explored for diagnostic—mainly the PD frequency, which varies according to the PD location. Thus, investigate the correlation between PD frequency ranges and the failure modes is indicated for futures works.

Annex

ANNEX A – Data Base Cemig

Table 21 – Data Base Cemig 1

Hydroelectric Plant	Unit	Start of operation	Power (kW)	Voltage (V)	End of Operation	
					Failed	No failure
Aimorés	1	01/01/2005	110,000	14,400		
Aimorés	2	01/01/2005	110,000	14,400		
Aimorés	3	01/01/2005	110,000	14,400		
Amador Aguiar I	1	01/01/2006	80,000	13,800		
Amador Aguiar I	2	01/01/2006	80,000	13,800		
Amador Aguiar I	3	01/01/2006	80,000	13,800		
Amador Aguiar II	1	01/01/2007	70,000	13,800		
Amador Aguiar II	2	01/01/2007	70,000	13,800		
Amador Aguiar II	3	01/01/2007	70,000	13,800		
Baguari	1	01/01/2009	35,900	10,500		
Baguari	2	01/01/2009	35,900	10,500		
Baguari	3	01/01/2009	35,900	10,500		
Baguari	4	01/01/2009	35,900	10,500		
Camargos	1	01/01/1960	22,500	6,900		
Camargos	2	01/01/1960	22,500	6,900		
Emborcação	1	01/01/1982	297,920	16,500		
Emborcação	2	01/01/1982	297,920	16,500		
Emborcação	3	01/01/1982	297,920	16,500		
Emborcação	4	01/01/1982	297,920	16,500		
Funil	1	01/01/2002	60,000	10,000		
Funil	2	01/01/2002	60,000	10,000		
Funil	3	01/01/2002	60,000	10,000		
Igarapava	1	01/01/1999	41,990	6,900		
Igarapava	2	01/01/1999	41,990	6,900		
Igarapava	3	01/01/1999	41,990	6,900		
Igarapava	4	01/01/1999	41,990	6,900		
Igarapava	5	01/01/1999	41,990	6,900		
Irapé	1	01/01/2006	120,000	13,800		
Irapé	2	01/01/2006	120,000	13,800		
Irapé	3	01/01/2006	120,000	13,800		
Itutinga	1	01/01/1955	12,150	6,900		
Itutinga	2	01/01/1955	12,150	6,900		
Itutinga	3	01/01/1955	14,000	no info.		
Itutinga	4	01/01/1955	13,000	no info.		
Jaguara	1	01/01/1971	106,400	13,800		
Jaguara	2	01/01/1971	106,400	13,800		
Jaguara	3	01/01/1971	106,400	13,800		
Jaguara	4	01/01/1971	106,400	13,800		
Miranda	1	01/01/1998	130,150	16,500		
Miranda	2	01/01/1998	130,150	16,500	21/04/2005	
Miranda	2 ref	21/04/2007				
Miranda	3	01/01/1998	130,150	16,500		
Nova Ponte	1	01/01/1994	170,050	13,800		
Nova Ponte	2	01/01/1994	170,050	13,800		
Nova Ponte	3	01/01/1994	170,050	13,800		
Porto Estrela	1	01/01/2001	56,000	no info.		
Porto Estrela	2	01/01/2001	56,000	no info.		

Table 22 – Caption

Hydroelectric Plant	Unit	Start of operation	Power (kW)	Voltage (V)	End of Operation	
					Failed	No failure
Queimado	1	01/01/2004	35,000	no info.		
Queimado	2	01/01/2004	35,000	no info.		
Queimado	3	01/01/2004	35,000	no info.	05/07/2010	
Queimado	3 ref	05/07/2012				
Rosal	1	01/01/1999	27,500	6,900	30/04/2011	
Rosal	1 ref	30/10/2011				
Rosal	2	01/01/1999	27,500	6,900	08/05/2017	
Rosal	2 ref	08/05/2018				
Sá Carvalho	1	01/01/1951	14,737	13,800		
Sá Carvalho	2	01/01/1951	14,737	13,800		01/01/2009
Sá Carvalho	2 ref	01/11/2009				
Sá Carvalho	3	01/01/1951	16,947	13,800		
Sá Carvalho	4	01/01/1951	31,579	13,800		
Salto Grande	1	01/01/1956	27,000	13,800		01/01/2008
Salto Grande	1 ref	01/11/2008				
Salto Grande	2	01/01/1956	27,000	13,800		01/01/2009
Salto Grande	2 ref	01/11/2009				
Salto Grande	3	01/01/1956	25,000	13,800		
Salto Grande	4	01/01/1956	25,000	13,800		
São Simão	1	01/01/1978	268,850	16,500		
São Simão	2	01/01/1978	268,850	16,500		
São Simão	3	01/01/1978	268,850	16,500		
São Simão	4	01/01/1978	268,850	16,500		
São Simão	5	01/01/1978	268,850	16,500		
São Simão	6	01/01/1978	268,850	16,500		
Três Marias	1	01/01/1962	61,370	13,800		
Três Marias	2	01/01/1962	61,370	13,800		
Três Marias	3	01/01/1962	61,370	13,800		
Três Marias	4	01/01/1962	61,370	13,800		19/04/2010
Três Marias	4 ref	19/02/2011				
Três Marias	5	01/01/1962	61,370	13,800		
Três Marias	6	01/01/1962	61,370	13,800		
Volta Grande	1	01/01/1974	95,000	13,800	03/09/2005	
Volta Grande	1 ref	03/10/2005			02/10/2010	
Volta Grande	1 ref	02/11/2010			20/07/2014	
Volta Grande	1 ref	20/08/2014			20/09/2015	
Volta Grande	1 ref	20/10/2015			30/12/2015	
Volta Grande	1 ref	30/01/2016			07/05/2016	
Volta Grande	1 ref	07/06/2016			08/08/2016	
Volta Grande	1 ref	08/09/2016				
Volta Grande	2	01/01/1974	95,000	13,800	07/08/2017	
Volta Grande	2 ref	07/08/2019				
Volta Grande	3	01/01/1974	95,000	13,800		
Volta Grande	4	01/01/1974	95,000	13,800		

Table 23 – Useful information Data base Cemig 1

Hydroelectric	Unit	Generator age (yers)		
		At fault	At Operating output	Current
Aimorés	1			13.0
Aimorés	2			13.0
Aimorés	3			13.0
Amador Aguiar I	1			12.0
Amador Aguiar I	2			12.0
Amador Aguiar I	3			12.0
Amador Aguiar II	1			11.0
Amador Aguiar II	2			11.0
Amador Aguiar II	3			11.0
Baguari	1			9.0
Baguari	2			9.0
Baguari	3			9.0
Baguari	4			9.0
Camargos	1			58.0
Camargos	2			58.0
Emborcação	1			36.0
Emborcação	2			36.0
Emborcação	3			36.0
Emborcação	4			36.0
Funil	1			16.0
Funil	2			16.0
Funil	3			16.0
Igarapava	1			19.0
Igarapava	2			19.0
Igarapava	3			19.0
Igarapava	4			19.0
Igarapava	5			19.0
Irapé	1			12.0
Irapé	2			12.0
Irapé	3			12.0
Itutinga	1			63.0
Itutinga	2			63.0
Itutinga	3			63.0
Itutinga	4			63.0
Jaguara	1			47.0
Jaguara	2			47.0
Jaguara	3			47.0
Jaguara	4			47.0
Miranda	1			20.0
Miranda	2	7.3		
Miranda	2 ref			10.7
Miranda	3			20.0
Nova Ponte	1			24.0
Nova Ponte	2			24.0
Nova Ponte	3			24.0
Porto Estrela	1			17.0
Porto Estrela	2			17.0

Table 24 – Useful information Data base Cemig 2

Hydroelectric	Unit	Generator age (yers)		
		At fault	At Operating output	Current
Queimado	1			14.0
Queimado	2			14.0
Queimado	3	6.5		
Queimado	3 ref			5.5
Rosal	1	12.3		
Rosal	1 ref			6.2
Rosal	2	18.4		
Rosal	2 ref			0.0
Sá Carvalho	1			67.0
Sá Carvalho	2		58.0	
Sá Carvalho	2 ref			8.2
Sá Carvalho	3			67.0
Sá Carvalho	4			67.0
Salto Grande	1		52.0	
Salto Grande	1 ref			9.2
Salto Grande	2		53.0	
Salto Grande	2 ref			8.2
Salto Grande	3			62.0
Salto Grande	4			62.0
São Simão	1			40.0
São Simão	2			40.0
São Simão	3			40.0
São Simão	4			40.0
São Simão	5			40.0
São Simão	6			40.0
Três Marias	1			56.0
Três Marias	2			56.0
Três Marias	3			56.0
Três Marias	4		48.3	
Três Marias	4 ref			6.9
Três Marias	5			56.0
Três Marias	6			56.0
Volta Grande	1	31.7		
Volta Grande	1 ref	5.0		
Volta Grande	1 ref	3.7		
Volta Grande	1 ref	1.1		
Volta Grande	1 ref	0.2		
Volta Grande	1 ref	0.3		
Volta Grande	1 ref	0.2		
Volta Grande	1 ref			1.3
Volta Grande	2	43.6		
Volta Grande	2 ref			0.0
Volta Grande	3			44.0
Volta Grande	4			44.0

Bibliography

- 1 BRUTSCH, R. et al. Insulation failure mechanisms of power generators [feature article]. *IEEE Electrical Insulation Magazine*, v. 24, n. 4, p. 17–25, July 2008. ISSN 1558-4402. [8](#), [18](#), [44](#), [45](#), [47](#), [52](#)
- 2 GEMANT, A.; PHILIPPOFF, W. Die funkenstrecke mit vorkondensator, zeitschfür tekn-physik, vol. 13. 1932. [8](#), [23](#)
- 3 ENDRENYI, J.; ANDERS, G. J. Aging, maintenance, and reliability-approaches to preserving equipment health and extending equipment life. *IEEE Power and Energy Magazine*, IEEE, v. 4, n. 3, p. 59–67, 2006. [8](#), [29](#), [30](#)
- 4 SILVA, A. M. L. da et al. Probabilistic method for optimizing the number and timing of substation spare transformers. *IEEE Transactions on Power Systems*, v. 30, n. 4, p. 2004–2012, July 2015. ISSN 1558-0679. [8](#), [33](#), [34](#), [37](#), [38](#)
- 5 ENDRENYI, J.; ANDERS, G. J.; SILVA, A. M. L. da. Probabilistic evaluation of the effect of maintenance on reliability. an application [to power systems]. *IEEE Transactions on Power Systems*, v. 13, n. 2, p. 576–583, May 1998. ISSN 1558-0679. [8](#), [36](#)
- 6 ENDRENYI, J. et al. The present status of maintenance strategies and the impact of maintenance on reliability. *IEEE Transactions on Power Systems*, v. 16, n. 4, p. 638–646, Nov 2001. ISSN 1558-0679. [8](#), [39](#), [42](#), [43](#)
- 7 CIGRE Study Committee. Hydrogenerator failures-Results of the Survey. 2003. [8](#), [44](#)
- 8 FOTHERGILL, J. C. Ageing, space charge and nanodielectrics: Ten things we don't know about dielectrics. In: *2007 IEEE International Conference on Solid Dielectrics*. [S.l.: s.n.], 2007. p. 1–10. ISSN 2159-1687. [8](#), [11](#), [45](#), [46](#), [47](#)
- 9 ISTAD, M.; RUNDE, M.; NYSVEEN, A. A review of results from thermal cycling tests of hydrogenerator stator windings. *IEEE Transactions on Energy Conversion*, IEEE, v. 26, n. 3, p. 890–903, 2011. [8](#), [49](#), [54](#), [56](#)
- 10 BARTNIKAS, R.; MORIN, R. Multi-stress aging of stator bars with electrical, thermal, and mechanical stresses as simultaneous acceleration factors. *IEEE transactions on energy conversion*, IEEE, v. 19, n. 4, p. 702–714, 2004. [8](#), [49](#), [50](#)
- 11 FARAHANI, M. et al. Behavior of machine insulation systems subjected to accelerated thermal aging test. *IEEE Transactions on Dielectrics and Electrical Insulation*, v. 17, n. 5, p. 1364–1372, October 2010. ISSN 1558-4135. [8](#), [49](#), [51](#)
- 12 KOKKO, V. I. Electrical ageing in lifetime estimation of hydroelectric generator stator windings. In: IEEE. *The XIX International Conference on Electrical Machines-ICEM 2010*. [S.l.], 2010. p. 1–5. [8](#), [51](#), [52](#), [53](#)
- 13 KIELMANN, F.; KAUFHOLD, M. Evaluation analysis of thermal ageing in insulation systems of electrical machines-a historical review. *IEEE Transactions on Dielectrics and Electrical Insulation*, IEEE, v. 17, n. 5, p. 1373–1377, 2010. [8](#), [48](#), [54](#)

- 14 SUMEREDER, C.; WOSCHITZ, R.; MUHR, M. Condition evaluation of generator bars. In: IEEE. *2005 5th IEEE International Symposium on Diagnostics for Electric Machines, Power Electronics and Drives*. [S.l.], 2005. p. 1–4. [8](#), [55](#)
- 15 SUMEREDER, C. Statistical lifetime of hydro generators and failure analysis. *IEEE Transactions on Dielectrics and Electrical Insulation*, IEEE, v. 15, n. 3, p. 678–685, 2008. [8](#), [55](#), [56](#), [118](#)
- 16 IEEE Recommended Practice for Testing Insulation Resistance of Rotating Machinery. *ANSI/IEEE Std 43-1974*, p. 1–16, Nov 1974. [8](#), [65](#), [66](#)
- 17 IEEE Recommended Practice for Measurement of Power Factor Tip-Up of Electric Machinery Stator Coil Insulation. *IEEE Std 286-2000*, p. 1–29, March 2000. [9](#), [67](#), [68](#)
- 18 STONE, G. C. et al. Rotating machine insulation systems. In: _____. *Electrical Insulation for Rotating Machines: Design, Evaluation, Aging, Testing, and Repair*. [S.l.]: IEEE, 2014. p. 1–46. ISBN null. [9](#), [79](#), [81](#), [82](#), [83](#), [84](#), [85](#), [127](#)
- 19 HUDON, C.; BELEC, M. Partial discharge signal interpretation for generator diagnostics. *IEEE Transactions on Dielectrics and Electrical Insulation*, v. 12, n. 2, p. 297–319, April 2005. ISSN 1558-4135. [9](#), [93](#), [96](#), [97](#), [98](#)
- 20 OSISOFT. Historian. 2016. [9](#), [99](#)
- 21 AUDOLI, A.; DROMMI, J.-L. Analysis of partial discharges measurements and generator technology evolution. In: IEEE. *[1991] Proceedings of the 3rd International Conference on Properties and Applications of Dielectric Materials*. [S.l.], 1991. p. 687–690. [10](#), [128](#), [131](#)
- 22 ENDRENYI, J. et al. The present status of maintenance strategies and the impact of maintenance on reliability. *IEEE Transactions on Power Systems*, v. 16, n. 4, p. 638–646, Nov 2001. ISSN 1558-0679. [29](#)
- 23 LI, W.; VAAHEDI, E.; Choudhury, P. Power system equipment aging. *IEEE Power and Energy Magazine*, v. 4, n. 3, p. 52–58, May 2006. ISSN 1558-4216. [31](#)
- 24 LI, W.; VAAHEDI, E.; CHOUDHURY, P. Power system equipment aging. *IEEE Power and Energy Magazine*, v. 4, n. 3, p. 52–58, May 2006. ISSN 1558-4216. [32](#)
- 25 GUARDIA, E. C. Desenvolvimento de metodologia para cálculo da vida útil de ativos da distribuição de energia focando a revisão tarifária. 2014. [32](#)
- 26 BRAULIO, G. A. Avaliação de vida útil remanescente de hidrogeradores. Itajubá, 2018. [32](#)
- 27 ANDERS, G. J. et al. A probabilistic model for evaluating the remaining life of evaluating the remaining life of electrical insulation in rotating machines. *IEEE Transactions on Energy Conversion*, v. 5, n. 4, p. 761–767, Dec 1990. ISSN 1558-0059. [34](#), [35](#)
- 28 LI, W. et al. *Reliability assessment of electric power systems using Monte Carlo methods*. [S.l.]: Springer Science & Business Media, 2013. [36](#)
- 29 RUBINSTEIN, R. Y.; KROESE, D. P. *Simulation and the Monte Carlo method*. [S.l.]: John Wiley & Sons, 2016. v. 10. [36](#)

- 30 ALLAN, R. N. et al. *Reliability evaluation of power systems*. [S.l.]: Springer Science & Business Media, 2013. 42
- 31 AGARWAL, V. K. et al. The mysteries of multifactor ageing. *IEEE Electrical Insulation Magazine*, v. 11, n. 3, p. 37–43, May 1995. ISSN 1558-4402. 43
- 32 STONE, G. C. et al. General principles of testing and monitoring. In: _____. *Electrical Insulation for Rotating Machines: Design, Evaluation, Aging, Testing, and Repair*. [S.l.]: IEEE, 2014. p. 311–316. ISBN null. 44
- 33 RUSU-ZAGAR, C.; NOTINGHER, P. V.; STANCU, C. Ageing and degradation of electrical machines insulation. *J. Int. Sci. Publ. Mater. Methods Technol*, v. 8, p. 526–546, 2014. 45
- 34 NOTINGHER, P. “*Materials for Electrotechnics. Structure. Properties*.” [S.l.]: POLITEHNICA PRESS, Bucharest. v. 1. 45
- 35 NOTHINGER, P. Accelerated development of electrical trees. part i: Initiation of trees. *Electr. Eng. Electron. Autom*, v. 57, p. 1–19, 2009. 45
- 36 NOTINGHER, P. *Insulation Systems, PRINTECH House Ltd, Bucharest*. [S.l.: s.n.]. 46
- 37 CRINE, J.-P.; VIJH, A. A molecular approach to the physico-chemical factors in the electric breakdown of polymers. *Applied physics communications*, v. 5, n. 3, p. 139–163, 1985. 46
- 38 LEWIS, T. Ageing-a perspective. *IEEE Electrical Insulation Magazine*, IEEE, v. 17, n. 4, p. 6–16, 2001. 46
- 39 GJAERDE, A. C. Multi-factor ageing models-origin and similarities. In: IEEE. *Proceedings of 1995 Conference on Electrical Insulation and Dielectric Phenomena*. [S.l.], 1995. p. 199–204. 46
- 40 TANAKA, T. Internal partial discharge and material degradation. *IEEE Transactions on Electrical Insulation*, IEEE, n. 6, p. 899–905, 1986. 48
- 41 PALONIEMI, P.; LINDSTROM, P. Theory of equalization of thermal ageing processes of electrical insulating materials in thermal endurance teste i. review of theoretical basis of test methods and chemical and physical aspects of ageing. *IEEE transactions on electrical insulation*, IEEE, n. 1, p. 1–6, 1981. 48
- 42 PALONIEMI, P. Theory of equalization of thermal ageing processes of electrical insulating materials in thermal endurance tests ii: The theory with practical approximations and application principles. *IEEE Transactions on Electrical Insulation*, IEEE, n. 1, p. 7–17, 1981. 48
- 43 PALONIEMI, P.; LINDSTROM, P. Theory of equalization of thermal ageing processes of electrical insulating materials in thermal endurance teste iii. tests results on an enamelled wire, a polyester glass laminate and an epoxy casting resin. *IEEE transactions on electrical insulation*, IEEE, n. 1, p. 18–30, 1981. 48
- 44 MONTSINGER, V. Loading transformers by temperature. *Transactions of the American Institute of Electrical Engineers*, IEEE, v. 49, n. 2, p. 776–790, 1930. 48

- 45 BÜSSING, W. Beiträge zum lebensdauergesetz elektrischer maschinen. *Archiv für Elektrotechnik*, Springer, v. 36, n. 12, p. 735–742, 1942. [48](#)
- 46 DAKIN, T. W. Electrical insulation deterioration treated as a chemical rate phenomenon. *Transactions of the American Institute of Electrical Engineers*, IEEE, v. 67, n. 1, p. 113–122, 1948. [48](#)
- 47 BRANCATO, E. Insulation aging a historical and critical review. *IEEE Transactions on electrical Insulation*, IEEE, n. 4, p. 308–317, 1978. [48](#)
- 48 SIMONI, L. A general approach to the endurance of electrical insulation under temperature and voltage. *IEEE Transactions on Electrical Insulation*, EI-16, n. 4, p. 277–289, Aug 1981. ISSN 1557-962X. [48](#)
- 49 BOTTS, J. C. Corona in high voltage rotating machine windings. *IEEE Electrical Insulation Magazine*, v. 4, n. 4, p. 29–34, July 1988. ISSN 1558-4402. [49](#)
- 50 CIMBALA, R.; KURIMSKÝ, J.; KOLCUNOVÁ, I. Determination of thermal ageing influence on rotating machine insulation system using dielectric spectroscopy. *Przegląd Elektrotechniczny*, v. 87, n. 8, p. 176–179, 2011. [50](#)
- 51 BÉLEC, M.; GUDDIMI, C.; MILLET, C. Effect of long-term aging test under dc voltage on roebel bars. In: IEEE. *2012 IEEE International Conference on Condition Monitoring and Diagnosis*. [S.l.], 2012. p. 412–416. [50](#)
- 52 JIA, Z. et al. Evaluation of the degradation of generator stator ground wall insulation under multistresses aging. *IEEE Transactions on Energy Conversion*, IEEE, v. 23, n. 2, p. 474–483, 2008. [51](#)
- 53 SUMEREDER, C.; WEIERS, T. Significance of defects inside in-service aged winding insulations. *IEEE Transactions on Energy Conversion*, v. 23, n. 1, p. 9–14, March 2008. ISSN 1558-0059. [53](#), [54](#)
- 54 FRUTH, B.; FUHR, J. Partial discharge pattern recognition—a tool for diagnosis and monitoring of ageing. in *Proc. CIGR 'E Conf., 1990*, p. 15–32, 1990. [53](#)
- 55 KELEN, A.; DANIKAS, M. Evidence and presumption in pd diagnostics. *IEEE Transactions on Dielectrics and Electrical Insulation*, IEEE, v. 2, n. 5, p. 780–795, 1995. [53](#)
- 56 Weiers, T. Symptoms of winding insulation aging after 37 years of service life in a hydrogenerator. *IEEE Transactions on Energy Conversion*, v. 25, n. 1, p. 20–24, March 2010. ISSN 1558-0059. [54](#)
- 57 EVALUATING Insulation Materials and Systems. In: ELECTRICAL Insulation for Rotating Machines. [S.l.]: John Wiley Sons, Ltd, 2014. cap. 2, p. 47–81. ISBN 9781118886663. [57](#), [60](#), [71](#)
- 58 IEEE STD 1043, IEEE Recommended Practice for Voltage-Endurance Testing of Form-Wound Bars and Coils. 2003. [58](#)
- 59 IEEE Trial-Use Standard for Voltage-Endurance Testing of Form-Wound Coils and Bars for Hydrogenerators. *IEEE Std 1553-2002*, p. 0₁ — —, 2003. [58](#), [59](#)

- 60 (REPLACED) IEEE Guide for the Statistical Analysis of Electrical Insulation Breakdown Data. *IEEE Std 930-2004 (Revision of IEEE Std 930-1987)*, p. 1–41, April 2005. [58](#), [59](#)
- 61 JOHNSTON, D. R. et al. Frequency acceleration of voltage endurance. In: *1978 IEEE International Conference on Electrical Insulation*. [S.l.: s.n.], 1978. p. 9–12. [59](#)
- 62 IEEE Recommended Practice for Thermal Cycle Testing of Form-Wound Stator Bars and Coils for Large Rotating Machines. *IEEE Std 1310-2012 (Revision of IEEE Std 1310-1996)*, p. 1–30, May 2012. ISSN null. [60](#), [115](#), [137](#), [146](#)
- 63 IEEE Recommended Practice for the Preparation of Test Procedures for the Thermal Evaluation of Insulation Systems for Electrical Equipment. *IEEE Std 99-2007 (Revision of IEEE Std 99-1980)*, p. 1–16, Feb 2008. [61](#)
- 64 IEEE Guide for the Statistical Analysis of Thermal Life Test Data. *ANSI/IEEE Std 101-1987(R2010) (Revision of IEEE Std 101-1972)*, p. 1–34, Dec 1988. [62](#), [72](#)
- 65 IEEE Guide for the Measurement of Partial Discharges in AC Electric Machinery. *IEEE Std 1434-2014 (Revision of IEEE Std 1434-2000)*, p. 1–89, Dec 2014. [69](#), [92](#)
- 66 STANDARD, I. Evaluation and qualification of electrical insulation systems. *IEC*, v. 60505, p. 2011, 2011. [71](#), [72](#)
- 67 ISTAD, M. R. M.; NYSVEEN, A. *A Review of Results From Thermal Cycling Tests of Hydrogenerator Stator Windings*. 2011. [73](#)
- 68 STONE, G. et al. Evaluating insulation materials and systems. In: _____. *Electrical Insulation for Rotating Machines: Design, Evaluation, Aging, Testing, and Repair*. [S.l.]: IEEE, 2004. p. 43–71. ISBN null. [73](#)
- 69 D.L.EVANS. *IEEE Working Group report of problems with hydrogenerator thermoset stator windings part I-Analysis of survey*. 1981. [74](#)
- 70 IEEE Guide for the Measurement of Partial Discharges in AC Electric Machinery. *IEEE Std 1434-2014 (Revision of IEEE Std 1434-2000)*, p. 1–89, Dec 2014. ISSN null. [86](#), [87](#)
- 71 IEEE Guide to the Measurement of Partial Discharges in Rotating Machinery. *IEEE Std 1434-2000*, p. 1–64, Aug 2000. ISSN null. [90](#)
- 72 FARD, M. A. et al. Partial discharge defects classification using neuro-fuzzy inference system. In: IEEE. *2010 10th IEEE International Conference on Solid Dielectrics*. [S.l.], 2010. p. 1–4. [93](#)
- 73 YOUN, Y. W. et al. A synthetic noise suppressing algorithm for partial discharge signals of generators. In: *2009 Transmission Distribution Conference Exposition: Asia and Pacific*. [S.l.: s.n.], 2009. p. 1–5. ISSN 2160-8644. [93](#)
- 74 SANTOS, M. G. *Automação de bancada para ensaios de descargas parciais em estatores de hidrogenadores*. Itajubá: [s.n.], 2018. 121 p. [115](#)
- 75 SANTOS, M. G. et al. Test bench automation for aging and partial discharge experiments in hydrogenerator stators. *Anais da Sociedade Brasileira de Automática*, v. 1, n. 1, 2019. [115](#)

- 76 CIMINO, A.; STAUBACH, C.; JENAU, F. Analysis of accelerated multi-factor aging tests on the winding insulation system of generator stator bars used in large rotating machines. In: IEEE. *2018 IEEE Electrical Insulation Conference (EIC)*. [S.l.], 2018. p. 110–113. [120](#)
- 77 KALMAN, R. E. A new approach to linear filtering and prediction problems. [123](#)
- 78 SINGLETON, R. K.; STRANGAS, E. G.; AVIYENTE, S. Extended kalman filtering for remaining-useful-life estimation of bearings. *IEEE Transactions on Industrial Electronics*, IEEE, v. 62, n. 3, p. 1781–1790, 2014. [126](#)
- 79 JENSEN, W. R.; STRANGAS, E. G.; FOSTER, S. N. Online estimation of remaining useful life of stator insulation. In: *2017 IEEE 11th International Symposium on Diagnostics for Electrical Machines, Power Electronics and Drives (SDEMPED)*. [S.l.: s.n.], 2017. p. 635–641. [126](#)
- 80 BABEL, A. S.; STRANGAS, E. G. Condition-based monitoring and prognostic health management of electric machine stator winding insulation. In: IEEE. *2014 International Conference on Electrical Machines (ICEM)*. [S.l.], 2014. p. 1855–1861. [126](#)
- 81 WASSILIADIS, N. et al. Revisiting the dual extended kalman filter for battery state-of-charge and state-of-health estimation: A use-case life cycle analysis. *Journal of Energy Storage*, Elsevier, v. 19, p. 73–87, 2018. [126](#)
- 82 CUI, L. et al. A novel switching unscented kalman filter method for remaining useful life prediction of rolling bearing. *Measurement*, Elsevier, v. 135, p. 678–684, 2019. [126](#)
- 83 WARREN, V. Partial discharge testing—a progress report. In: *Iris Rotating Machinery Conference, USA, Santa Monica*. [S.l.: s.n.], 2010. p. 1–13. [127](#)
- 84 STONE E. A. BOULTER, I. C. G.; DHIRANI, H. *Electrical Insulation for Rotating Machines Design, Evaluation, Aging, Testing, and Repair*. [128](#)